



UNIVERSITÀ  
DEGLI STUDI  
DI PADOVA

UNIVERSITÀ DEGLI STUDI DI PADOVA

DIPARTIMENTO DI INGEGNERIA INDUSTRIALE

CORSO DI LAUREA MAGISTRALE IN CHEMICAL AND PROCESS ENGINEERING

**Tesi di Laurea Magistrale in  
Chemical and Process Engineering**

# **Synthesis and optimization of novel polyols from renewable lignin waste**

*Relatrice: Prof.ssa Alessandra Lorenzetti*

*Laureando: RICCARDO LA TORRE*

ANNO ACCADEMICO 2023-2024



# Abstract

The objective of this dissertation is the production of flexible polyurethane foams through the synthesis of new polyols derived from the liquefaction of lignin, a waste of the paper industry. Lignin was depolymerized using microwave heating, employing polyols from renewable sources as liquefaction solvents. The operational conditions, such as time, temperature, type of solvent and amount of catalyst were studied to obtain polyols with optimal characteristics for the production of flexible polyurethane foams. In particular, a design of experiment (DoE) has been used to assess the most significant processing parameters on the final quality of the lignin polyol. By using the optimized polyol, several polyurethane flexible foams were produced. The physical-mechanical characterization of the foams was carried out through measurements of density, thermal conductivity, and compression strength, while the foam morphology was analyzed using scanning electron microscopy. This was followed by thermogravimetric analysis (TGA), dynamic mechanical analysis (DMA) and fire behavior characterization (limiting oxygen index and cone calorimeter test).

The properties of the foams obtained using lignin-based polyols were compared with those of foams made with commercial polyol, obtained from fossil source. The results show that, by optimizing both the operational conditions of the liquefaction process and the formulation of the foams, it is possible to obtain foams with comparable properties to those of foams made from fossil-based polyols, using up to 30% of lignin based polyol.

This, therefore, offers the possibility of reusing lignin, paving the way for the introduction of polyols synthesized from renewable sources into the market for the production of foams with good performance.

# Table of Contents

|  |           |
|--|-----------|
| Introduction.....                              | 1         |
| <b>Chapter 1</b> .....                         | <b>3</b>  |
| Polyurethane .....                             | 3         |
| 1.2.1 Polyols .....                            | 5         |
| 1.2.2 Isocyanates .....                        | 7         |
| 1.2.3 Catalysts .....                          | 8         |
| 1.2.4 Blowing Agents .....                     | 9         |
| 1.2.5 Surfactants .....                        | 9         |
| 1.2.6 Additives.....                           | 9         |
| <b>Chapter 2</b> .....                         | <b>15</b> |
| Renewable raw materials .....                  | 15        |
| 2.1.1 Lignin molecular structure.....          | 15        |
| 2.1.2 Methods of lignin extraction.....        | 18        |
| 2.1.2.1 Kraft extraction process .....         | 18        |
| 2.1.2.2 Sulfite extraction process.....        | 18        |
| 2.1.2.3 Soda extraction process .....          | 18        |
| 2.1.2.4 Organosolv extraction process.....     | 18        |
| 2.1.2.5 Steam extraction process.....          | 19        |
| 2.1.2.6 Diluted acids extraction process ..... | 19        |
| <b>Chapter 3</b> .....                         | <b>21</b> |
| Microwave heating.....                         | 21        |
| 3.5.1 Thermal effect (kinetic).....            | 26        |
| 3.5.2 Specific microwave effect .....          | 26        |
| 3.5.3 Non thermal microwave effect .....       | 27        |
| <b>Chapter 4</b> .....                         | <b>29</b> |
| Lignin liquefaction process.....               | 29        |
| 4.1.1 Reaction mechanism.....                  | 30        |
| 4.1.1.1 Phenol process .....                   | 30        |
| 4.1.2 Ethyl glycol process .....               | 32        |
| 4.1.3 Reaction kinetics .....                  | 33        |
| 4.2.1 Effect of liquefaction solvent .....     | 33        |
| 4.2.2 Catalyst effect.....                     | 34        |
| 4.2.2.1 Acid catalyst .....                    | 34        |

---

|  |   |           |
|--|---|-----------|
| 4.2.2.2  | Basic catalyst .....                                      | 34        |
| 4.2.3  | Temperature effect.....                                   | 35        |
| 4.2.4  | Time effect.....  | 35        |
| 4.2.5  | Lignin-solvent ratio effect .....                         | 35        |
| <b>Chapter 5</b>                                       | .....   | <b>37</b> |
| Liquefaction materials and methods                     | .....   | 37        |
| 5.1.1  | Lignin type.....  | 37        |
| 5.1.2  | Liquefaction solvents.....                                | 38        |
| 5.1.3  | Catalysts .....   | 39        |
| 5.1.4  | Extraction solvent.....                                   | 39        |
| 5.4.1  | Hydroxyl value .....                                      | 41        |
| 5.4.2  | Gel permeation chromatography .....                       | 44        |
| <b>Chapter 6</b>                                       | .....   | <b>49</b> |
| Methods for the characterization of polyurethane foams | .....   | 49        |
| 6.1.1  | Apparent density.....                                     | 49        |
| 6.1.2  | Thermal conductivity.....                                 | 49        |
| 6.1.3  | Compression stress/strain .....                           | 51        |
| 6.1.4  | Compression set.....                                      | 52        |
| 6.1.5  | Dynamic mechanical analysis (DMA) .....                   | 53        |
| 6.3.1  | Polymers combustion processes.....                        | 56        |
| 6.3.2  | Fire reaction characterization of polyurethane foams..... | 57        |
| 6.3.2.1  | Limiting Oxygen index .....                               | 58        |
| 6.3.2.2  | Cone calorimetry.....                                     | 59        |
| 6.4.1  | Thermogravimetric analysis (TGA) .....                    | 60        |
| <b>Chapter 7</b>                                       | .....   | <b>63</b> |
| Lignin Liquefaction                                    | .....   | 63        |
| 7.5.1  | Acid Catalysis.....                                       | 68        |
| 7.5.2  | Basic catalyst.....                                       | 70        |
| 7.6.1  | Hydroxyl number optimization .....                        | 76        |
| <b>Chapter 8</b>                                       | .....   | <b>83</b> |
| Foam synthesis and characterization                    | .....   | 83        |
| 8.1.1  | Polyols from liquefaction .....                           | 83        |
| 8.5.1  | Compression stress .....                                  | 90        |
| 8.5.2  | Compression set.....                                      | 91        |
| 8.5.3  | Dynamic mechanical analysis (DMA) .....                   | 92        |

|                    |   |     |
|--------------------|---|-----|
| 8.5.4              | Thermogravimetric analysis (TGA) .....            | 95  |
| 8.5.5              | Limiting Oxygen Index (LOI) analysis .....        | 99  |
| 8.5.6              | Calorimetry analysis.....                         | 100 |
| 8.5.7              | Morphological characterization, SEM analysis..... | 101 |
| 8.5.8              | FT-IR analysis .....                              | 104 |
| Conclusion .....   |   | 107 |
| Bibliography ..... |   | 110 |

# Introduction

The depletion of fossil fuel resources and the ensuing environmental issues have made alternate and renewable sources more important, not just for energy production but also for obtaining chemicals needed for chemical synthesis.

Lignocellulosic biomass, the most prevalent vegetal product on the earth, is renewable and is obtained from agricultural waste, and it has played a major role in this field of study.

Cellulose, hemicellulose, and lignin make up biomass. About 20–30% of the biomass is composed of lignin, which may be removed using a variety of techniques that determine its qualities. The most popular method is the Kraft process, which yields lignin as a byproduct that is utilized in the paper industry.

Lignin is regarded as a platform element in the synthesis of polymers, chemical compounds, and biofuels because it is the largest renewable deposit of aromatic compounds. However, currently, only 5% of the lignin produced is used for this purpose; the remaining lignin is burned to produce energy.

Lignin bio-based polyols can be obtained via liquefaction, which involves a depolymerization process carried out at high temperatures of 150–170°C, in the presence of an organic solvent, and with the aid of a catalyst. Since microwaves provide a uniform and efficient heating source, they can have several advantages over the traditional heating methods in the liquefaction of lignin.

Polyurethanes, a broad class of polymers distinguished by the urethane group. Isocyanate and polyols, which are raw materials, often produced from petroleum, react to produce polyurethanes. Foams are a significant category of polyurethane goods, which are further divided into three categories: rigid, semi-rigid, and flexible. There are several uses for them, like cushioning, insulation, support and impact resistance, that's why they are employed in different work field like packaging, medical, sport and automotive.

The present thesis work consisted of two main parts: the improvement of the liquefaction process to obtain lignin-based polyols and the preparation and characterization of polyurethane foams obtained by using those biobased polyols..

In order to produce polyols with qualities appropriate for the creation of polyurethane foams, the liquefaction process was examined. Particular attention was paid to the impact of the liquefaction solvent and catalysis on the features of the polyols. Flexible polyurethane foams have been created using lignin-based polyols, derived from azelaic acid (EMEROX®).

As a result, the following thesis is broken up into eight chapters:

The fundamental chemistry of polyurethanes is covered in Chapter 1 along with a discussion of the key reactions and source ingredients.

Information on the renewable raw materials utilized in the production of polyols is provided in Chapter 2. After providing the structure and extraction techniques for lignin, the synthesis of EMEROX® polyols, which serve as liquefaction solvents, is explained.

Chapter 3 examines microwaves, their nature and their principal impact on heating. Chemical reactions using microwave reactors are also described.

The state of the art for the lignin liquefaction method is covered in Chapter 4. Particular attention was paid to the bonds involved, the reactions that occur and the reaction mechanism. The main factors of the liquefaction process were also studied.

The materials and procedures utilized in the synthesis and characterization of the polyols obtained from the liquefaction of lignin are fully covered in Chapter 5.

The characterization methods of polyurethane foams are covered in Chapter 6. Additionally, the fundamental ideas of polymer combustion are given to them.

The experimental portion of the thesis starts with Chapter 7, when the liquefaction process's outcomes are presented. Special attention was paid to the solvents of liquefaction; the effect of catalyst, reaction time and type of lignin are also investigated.

Finally, Chapter 8 describes the raw materials used in the production of the polyurethane flexible foams and their formulations. The main characteristics from the point of view of physical, morphological, thermal and fire behaviour of the foams are discussed.



# Chapter 1

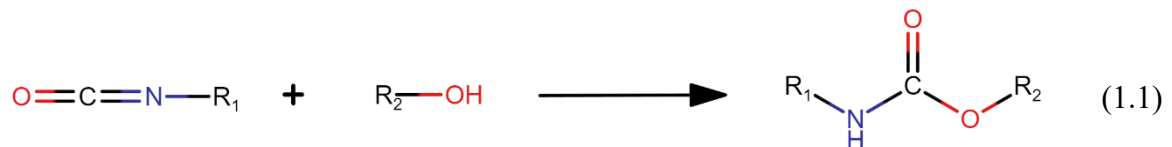
## Polyurethane

Polyurethanes (PUs) represent a broad class of polymers that can be obtained by reaction between diisocyanates or polyisocyanates with diols or polyols through an addition mechanism. Depending on the proportions of reactants, structure of polyols or isocyanates, catalysts, reaction conditions, and so on, foams (rigid or flexible), rubbers, elastomers, coatings, or adhesives can be obtained. More generally, PUs are available in the market as both thermoplastic and thermosetting polymers. The subject of this thesis work is the production of flexible polyurethanes (PUs) foams characterized by an open-cell morphological structure. Flexible polyurethane foams are becoming more and more popular in fields like biomedicine, intelligent materials, and nanocomposites<sup>1-3</sup>. Currently they are also widely used in a variety of applications, including mattresses, seating, and the automobile industry. Environmental concerns related to material synthesis are becoming more and more prevalent these days. This factor, together with changes in the price of crude oil, has pushed scientists to create materials based on renewable resources, such as polyurethanes.

Below, in Chapter 1, the raw materials and the basic chemistry of them will be given.

### 1.1 General information e chemical reactions<sup>4-6</sup>

The formation of the polyurethanes happens when an alcohol (characteristic functional group -OH) and an isocyanate (characteristic functional group -NCO) react according to the reaction (1.1):



Thus the urethane bond is obtained (also known as carbamate), showed in Figure 1.1, which is representative of the polymeric chain of polyurethanes.

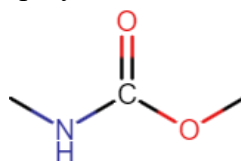
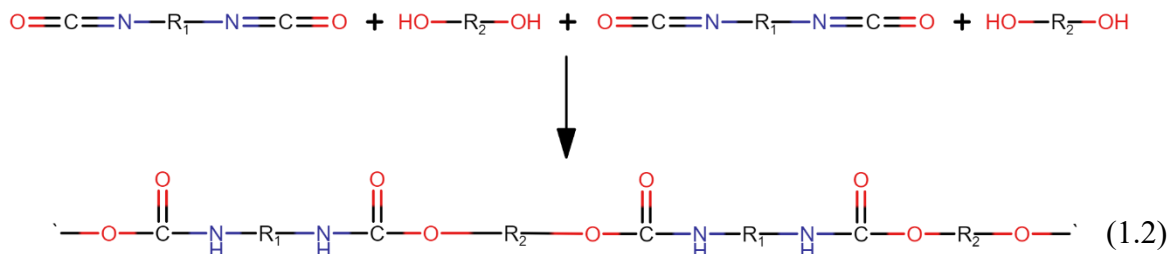


Figure 1.1 Urethane bond

Reaction (1.1) occurs exothermically, releasing 24 [kCal/mol] at room temperature and with a reaction rate which is correlated to the reactants, catalysts and other factors.

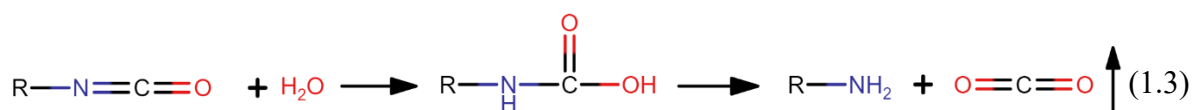
It is known that the reaction mechanism is the polyaddition, so the polymeric chains will be obtained as shown below in the equation (1.2):



Structure and characteristics of polyurethane foams are determined by the functionality ( $f$ ) of the reagents, that is the number of functional groups of each molecule. If both the reactants have functionality equal to 2, linear polymeric chains are formed, while factor  $f$  greater than 2 will create branched and reticulated structures.

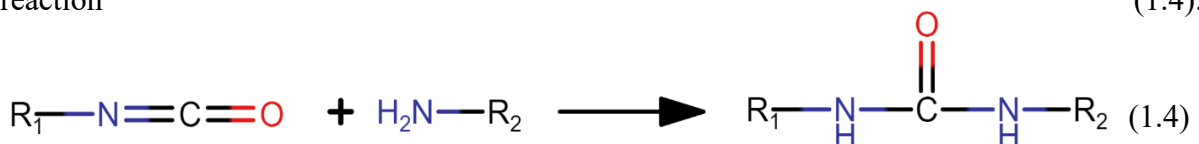
Secondary reactions are involved in the making of polyurethane foams, determined by the ability of isocyanates to react with other functional groups, particularly active hydrogens, that is, groups containing a hydrogen bonded to strongly electronegative atoms such as oxygen and nitrogen.

The -NCO group reacts with water (1.3) leading to the formation of an amine group and releasing CO<sub>2</sub>, via the formation of an unstable intermediate called carbamic acid:



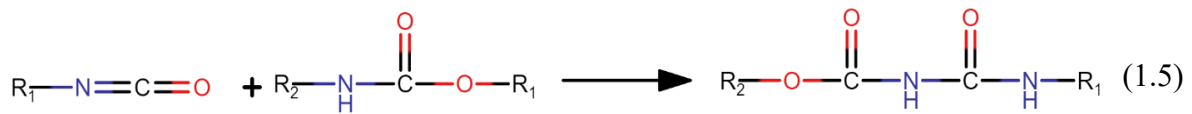
This reaction is also known as the *blow* reaction and it is more exothermic than equation (1.1), producing 42 [kCal/mol]. The CO<sub>2</sub> released in equation (1.3) is the reason of the foam expansion, this is why the water is assessed as chemical blowing agent.

The reaction between isocyanate and an amine yields to disubstituted urea according to the reaction (1.4):

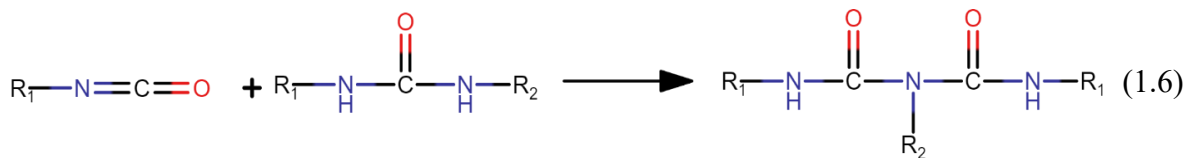


Different secondary reactions take place between the isocyanate group and others, for example:

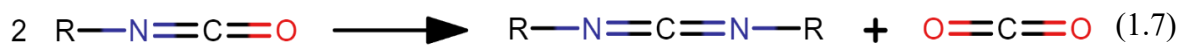
- Reaction between isocyanate and urethane to produce allophanate



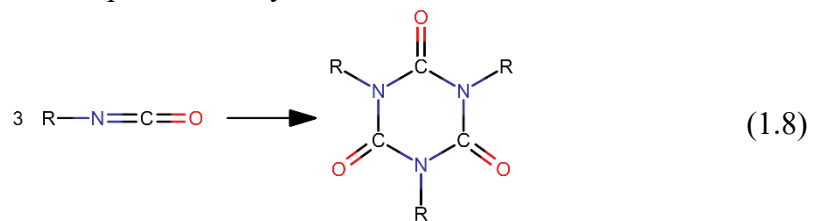
- Reaction between isocyanate and disubstituted urea to produce biuret:



- Dimerization reaction to form carbodiimide:



- Cyclotrimerization reaction to produce isocyanurate:



All these reactions produce molecules that have different resistance to the thermo-degradation; specifically, allophanates and biurets decompose at 106°C and 135°C, while the urethane bond degrades at higher temperature, namely 200°C<sup>5</sup>.

Usually, one way to improve the thermal stability of the polyurethane foams is favor the production of the isocyanurate because of its higher decomposition temperature of 270°C.

## 1.2 Raw material for the production of polyurethane foams

This section contains the description and function of the main raw materials used in the synthesis of rigid polyurethane foams. The raw materials, usually, are mainly derived from light petroleum components, while only to a small extent are materials from renewable sources used.

### 1.2.1 Polyols

Since the end product's qualities are determined by its molecular weight and chemical composition, polyols are the primary raw material used in the creation of polyurethane foams.

The hydroxyl number ( $nOH$ ) determines the concentration of the reactive hydroxyl group (-OH) in each polyol per unit weight. Using the relationship (1.9), one may determine the hydroxyl number based on the polyol's functionality and molecular weight<sup>6</sup>.

$$nOH = \frac{56100 \cdot \text{Functionality}}{\text{Molecular Weight}} \quad (1.9)$$

The majority of polyols fall into two categories:

- *Polyethers*, which are created by polyadding epoxides, typically ethylene or propylene, to polyfunctional initiators, including amines or glycols. Since they behave well at low temperatures and have a low viscosity (40–15,000 [mPa·s]), they are the most commonly employed in the manufacture of foam. The primary issue is that they degrade thermo-oxidatively when exposed to oxygen and UV light. There are two types of polyethers that may be identified: those with long chains, which are often utilized in the creation of flexible foams, and those with short chains, which are utilized in the creation of rigid foams.
- *Polyesters*, which are made by polycondensation of dicarboxylic acids and glycols. They are fair UV stable and have a greater viscosity than polyethers. Since they can now be generated from some recovered diacids, such as PET, their cost, which formerly rendered them less competitive than polyethers, has been reevaluated.

For the production of flexible polyurethane foams, two polyols were used. One was an industrial-grade polyol, specifically PM6000, which is commercially utilized for the synthesis of flexible foams, and the polyols produced in the present study, which are derived from renewable sources such as Emerox® 14511, whose precursor is azelaic acid. The foams obtained from these two types of polyols were compared to evaluate the impact of lignin on them. The Table 1.1 summarizes the main physical characteristics for the pure polyols.

Table 1.1 Polyol physical characteristics

| Polyol               | Hydroxyl value<br>[mgKOH/g] | Viscosity @ 25°C | Functionality | Molecular weight<br>[g/mol] |
|----------------------|-----------------------------|------------------|---------------|-----------------------------|
| <b>Emerox® 14511</b> | 104-116                     | 1500             | 2             | 1000                        |
| <b>PM6000</b>        | 30                          | 1500             | 3             | 6000                        |

PM6000 was used for the reference foam, which is utilized for commercial purpose and is 100% fossil-based, while Emerox® 14511 cannot be used alone due to its low functionality, which does not allow for proper cross-linking of the foam. This issue will later introduce a limitation during the formulation phase.

### 1.2.2 Isocyanates

Since aromatic isocyanates are more reactive with hydroxyl-containing compounds than aliphatic or cycloaliphatic isocyanates, they are used to make the majority of polyurethane foams.

For this purpose, the most widely used isocyanate is toluene diisocyanate (TDI), specifically a mixture of two isomers: 80% Of 2,4-TDI and 20% of 2,6-TDI.

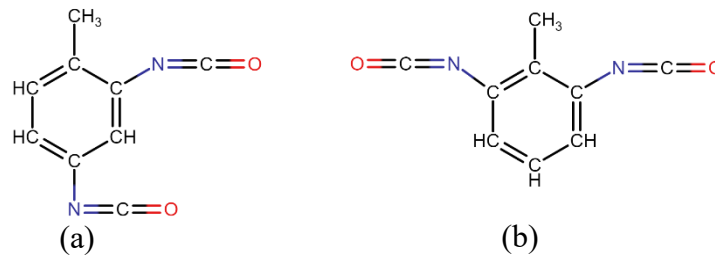


Figure 1.2 (a) 2,4-TDI and 2,6-TDI chemical structure

Equation (1.10) may be used to calculate the isocyanate index for isocyanates, which is the concentration of reactive -NCO groups per unit weight<sup>6</sup>.

$$\% - NCO = \frac{42 \cdot \text{Functionality}}{\text{Molecular Weight}} \cdot 100 \quad (1.10)$$

The stoichiometric quantity in grams of isocyanate required for the polymerization reaction (1.11) may be determined using the isocyanate index, the hydroxyl numbers of the polyols employed, and the amount of water to be added to the formulation.

$$g_{NCO} = \left( \frac{gp_{ol_1}}{100} \cdot nOH_1 + \frac{gp_{ol_2}}{100} \cdot nOH_2 + \dots + \frac{gp_{ol_n}}{100} \cdot nOH_n + \frac{g_{H_2O}}{100} \cdot nOH_{H_2O} \right) \cdot \frac{7.5}{\% - NCO} \quad (1.11)$$

Flexible foams require a different approach unlike the rigid ones, since flexibility and elasticity are important qualities of the final product the isocyanate index is often kept close to 100 percent, indicating that the amount of isocyanate utilized is nearly stoichiometric. This is done to avoid the formation of molecules like the isocyanurates which stiffens the polymeric chains.

To calculate the grams of isocyanate to be added to the formulation, multiply (1.11) by the isocyanate index ( $I$ ), shown in equation (1.12), which takes into account the difference between stoichiometric and real amount.

$$I = \frac{\text{quantity of experimental isocyanate}}{\text{quantity of stichiometric isocyanate}} \quad (1.12)$$

The isocyanate used for the production of flexible polyurethane foams is the ISOTECH TCC105 provided by Technochem, which is a polyether-based prepolymer. The main chemical-physical characteristics are shown in the table below:

Table 1.2 ISOTECH TCC105 physical properties

|                                       |           |
|---------------------------------------|-----------|
| % NCO [%]                             | 27±0.5    |
| Viscosity [cP]                        | 150±50    |
| Specific weight [kg/dm <sup>3</sup> ] | 1.21±0.02 |

### 1.2.3 Catalysts

Catalysts are employed to control the timing and completeness of the many reactions that occur during the production of polyurethane foams.

There are various types of catalysts that act on the different characteristic times of the foams (*cream time, gel time, and tack free time*), thereby affecting the rate of reaction between isocyanate and water and isocyanate and polyol. Often tertiary amines, like 1,4-diazobicyclo[2,2,2]octane, promotes the blowing reactions, while the gelling phase are favored from tin octoate.

Thus, the following sorts of catalysts can be differentiated:

- *Blow catalyst*, promotes the reaction between water and isocyanate releasing carbon dioxide which affects creaming time.
- *Gel catalysts*, which minimize gel and tack free time by acting on the reaction between isocyanate and polyol, promoting cross-linking during the foaming phase; they also have a little impact on cream time.

It is evident that the correct ratio between these two catalysts is crucial for optimally managing the characteristic times of a polyurethane foam: cream, blow, and tack-free time. The catalysts used are listed below:

- JEFFCAT Z110, chemically known as N,N,N'-trimethylaminoethyl ethanolamine
- NIAX A1, a blow catalyst composed of 70% bis(2-dimethylaminoethyl) ether diluted with 30% by weight dipropylene glycol
- DABCO 33LV, a strong gel catalyst consisting of 33% tertiary amine (triethylenediamine) and 67% dipropylene glycol
- DBTDL, chemically known as dibutyltin dilaurate, a strong tin-based gel catalyst.

### 1.2.4 Blowing Agents

Blowing agents define the foam's specific cellular structure by generating gas bubbles during polymerization, which expand the mixture and cause cells to form.

Bubble formation happens through two distinct methods, resulting in two kinds of blowing agents:

- Physical expanders are chemicals that evaporate due to the heat produced during polymerization. They are volatile chemicals, low-boiling liquids, or liquefiable gases with low temperature and/or pressure. Hydrofluorocarbons (HFCs) and hydrocarbons (HCs) are now used as physical blowing agents due to the ozone depletion (ODP) impact of chlorofluorocarbons (CFCs) and hydrochlorofluorocarbons (HCFCs).
- Chemical expanders are substances that react with a compound in a mixture to produce a gas. Water is the most often utilized chemical expander (reaction (1.3)), followed by carboxylic acids such as formic acid.

Several critical characteristics are considered while selecting the blowing agent<sup>6</sup>. The first is its conductivity, which is very important for expanders used as insulators; the second is ease of application; some expanders are flammable and require certain safety standards, while others require certain temperature and pressure conditions because they are low-boiling; and the third factor is the solubility of the expanding agent in the matrix, which should be low to allow sufficiently high gas pressure in the cells and moderate plasticization of the matrix.

As a blowing agent, a chemical blowing agent was chosen for this study, specifically water, which reacts with isocyanate to release carbon dioxide.

### 1.2.5 Surfactants

Surfactants are added to the formulation to reduce the surface tension of the liquid so as to regulate emulsification and compatibility between reactants and to promote cell formation; they are also used to prevent collapse of the foam, thereby they improve the stability and uniformity of the cellular structure. Silicone surfactants are usually used so as not to affect the fire behavior of the foam; in this specific case TEGOSTAB B8629 was used.

### 1.2.6 Additives

In addition to the main reagents listed in the previous sub-paragraph, other substances can be added to enhance or introduce new physical/chemical properties within the polyurethane foam. In this specific case, a cell opener was introduced, which is useful for flexible foams which require an open-cell structure. For this purpose the Rokopol M1170 was used. It is a polyether polyol, a block/statistical copolymer of ethylene oxide and propylene oxide based on glycerol. Its hydroxyl number ranges between 31-36 mgKOH/g, and its viscosity ranges from 1250-1550

mPas at 25°C. In addition to the cell opener, three different biochar were used, derived from rice husk, *Arundo donax*, and waste tetrapak. The purpose of these additives is to improve the thermal stability and mechanical strength of the foams.

### 1.3 Polyurethane preparation

The synthesis of polyurethane foams begins with defining the mixture formulation, which follows precise stoichiometric ratios. It is known that a hydroxyl group (-OH) reacts with an isocyanate group (-NCO). It is therefore evident that, to determine the quantity of each reagent, the functional group content per unit weight of the polyol and isocyanate must be known. These values can be found in the literature, in technical datasheets, or obtained through titration. There is a correlation that relates the hydroxyl number ( $nOH$ ), functionality ( $f$ ), and molecular weight ( $MW$ ):

$$nOH = \frac{56000 \cdot f}{MW} \quad (1.13)$$

The constant 56100 represents the molecular weight of KOH multiplied by 1000 since the number of hydroxyl groups is calculated in milligrams. The equivalent weight,  $P_{eq}$ , is defined as:

$$P_{eq} = \frac{MW}{f} \quad (1.14)$$

By combining the two equations, it is obtained:

$$P_{eq,OH} = \frac{56100}{nOH} \quad (1.15)$$

Similarly, the equivalent weight of isocyanate groups is:

$$P_{eq,NCO} = \frac{42}{\%NCO} \quad (1.16)$$

Where  $\%NCO$  represents the isocyanate percentage index.

The number of equivalents is in turn defined as the ratio between the weight in grams and the equivalent weight:

$$n_{eq} = \frac{g}{P_{eq}} \quad (1.17)$$



Thus, the grams of isocyanate are equal to:

$$g_{TCC} = n_{eq} \cdot P_{eq,NCO} \quad (1.18)$$

As stated at the beginning of this section, it is necessary to ensure that the isocyanate groups react in a one-to-one ratio with the hydroxyl groups. Therefore, taking a reference weight of 100 grams:

$$g_{TCC} = \frac{100 \text{ gOH}}{P_{eq,OH}} \cdot \frac{42}{\%NCO} \quad (1.19)$$

Re writing  $\%NCO$  like:

$$\%NCO = \frac{NCO}{100} \quad (1.20)$$

By substituting into the previous equation and considering that the  $NCO$  value in this case is 27, it is gotten:

$$g_{TCC} = 7.486 \cdot \frac{n_{OH}}{NCO} = \frac{7.486}{27} \cdot n_{OH} \quad (1.21)$$

In the formula above,  $n_{OH}$  indicates the average of all hydroxyl numbers of the reactants, including the expanding agent, weighted by their respective fractions. Thus, expanding this term, it would be obtained:

$$g_{TCC} = \frac{7.486}{27} \cdot \left( \frac{g_1}{100} \cdot n_{OH,1} + \frac{g_2}{100} \cdot n_{OH,2} + \dots + \frac{g_n}{100} \cdot n_{OH,n} + \frac{g_{H_2O}}{100} \cdot n_{OH,H_2O} \right) \cdot I \quad (1.22)$$

$$I = \frac{\text{quantity of experimental isocyanate}}{\text{quantity of stichiometric isocyanate}} \quad (1.23)$$

The terms  $n_{OH,i}$  represent the hydroxyl number of all the reagents, while that of water is known a priori and equal to 6220 mg KOH/g. The term  $I$  represents the isocyanate index and indicates the excess of this substance to ensure the completeness of the reaction. In this specific case, a value of 100 was used. An excess of isocyanate would introduce a percentage of unreacted

isocyanate groups into the system, and additionally, it would result in more rigid foams due to cross-linking induced by interactions between isocyanate groups, urea, and urethanes. The amount of blowing agent to be added is calculated based on the density  $\rho$  of the foam, defined as the ratio between the total mass  $m_{TOT}$  and the volume  $V$ .

Considering that the total mass is given by the sum of the mass of the blowing agent plus that derived from the polyurethane, we can write:

$$\rho = \frac{m_{TOT}}{V} = \frac{m_{PU} + m_{H_2O}}{V} \quad (1.24)$$

Given that the degree of expansion is about 97%, the volume can be approximated to that of the blowing agent, which is carbon dioxide. From the ideal gas law, we know that:

$$V = \frac{n \cdot R \cdot T}{P} \quad (1.25)$$

where  $n$  represents the number of moles,  $R$  is the universal gas constant,  $T$  is the temperature, and  $P$  is the pressure. Considering the molar volume  $V_0$  of a gas under standard conditions, with a temperature  $T_0$  of 0°C and a pressure  $P_0$  of 1 atm, we know it is equal to:

$$V_0 = R \cdot T_0 = 22.414 \text{ L} \cdot \text{mol} \quad (1.26)$$

By combining the last two equations, we obtain:

$$V = V_0 \cdot \frac{n \cdot T}{T_0} \quad (1.27)$$

In this case,  $n$  represents the number of moles of the blowing agents, including both physical and chemical ones.

Substituting further into the equation found previously, we get:

$$\rho = \frac{m_{TOT}}{V} = \frac{m_{PU} + m_{H_2O}}{\left( V_0 \cdot \frac{m_{H_2O}}{MW_{H_2O}} * \frac{T}{T_0} \right)} \quad (1.28)$$

Note that in the present work, only water was used as the blowing agent, which is why there is only one term in the denominator; otherwise, the sum of the number of moles of each blowing agent would have to be considered.

Rearranging the above equation to solve for the mass of the blowing agent ( $m_{H_2O}$ ) we get:

$$m_{H_2O} = \frac{m_{PU}}{\left(\frac{V_0}{MW_{H_2O}} \cdot \frac{T}{T_0} \cdot \rho - 1\right)} \quad (1.29)$$

Where  $MW_{H_2O}$  is equal to 18 g/mol, and the ratio  $T/T_0$  is chosen within a range between 1.1 and 1.5; in this specific case, 1.2 was chosen. If the foam does not reach the required density, then the ratio  $T/T_0$  is recalculated as:

$$\frac{T}{T_0} = \frac{m_{PU} + m_{H_2O}}{\rho_{exp} \cdot V_0 \cdot \left(\frac{m_{H_2O}}{MW_{H_2O}}\right)} \quad (1.30)$$

Where  $\rho_{exp}$  represents the real and undesired density value.

It is important to note that the calculation of the quantities of isocyanate and blowing agent mass is performed using iterative methods.

## 1.4 Foaming methodology

The foams described in this study were prepared using the one-shot technique, named because the isocyanate is added at the final stage into a container where all the other reagents are already present. The specific steps to follow are as follows:

1. Weigh all the reagents that make up the initial mixture (i.e., polyols, surfactants, catalysts, additives, and water) into a pitcher. Mix them with a high-speed radial mechanical stirrer until a homogeneous mixture is obtained.
2. Add the previously calculated amount of isocyanate and mix rapidly for 10-15 seconds, depending on the volume of the reagents. It is necessary to mix for a short time to prevent the foam from starting to react inside the container.
3. After 10-15 seconds of stirring, pour the content of the pitcher into an open mold. In this specific case, two molds were available, with dimensions of 20x20x20 cm and 25x25x25 cm.
4. Remove the foam from the mold and let it cure in an oven at 70°C for at least 24 hours to ensure that the reaction between the isocyanate and polyol is complete.

After pouring the contents of the container into the mold, it is important to take note of three characteristic times: cream time, gel time, and tack-free time.

- Cream time: it is the time at which the first perpendicular growth of the foam occurs. It is called "cream" time because it sometimes corresponds to a colour change, such as a yellowish cream colour.
- Gel time: also known as "string time", it refers to when the polymer begins to gel and a polymeric network is formed due to the formation of urethane and urea bonds, along with the branching of allophanate and biuret. Visually, when inserting an object a few centimetres into the foam and removing it, polymer strands will be visible.
- Tack-free time: The time at which the reaction has reached about 70-80% completion. At this point, the foam has hardened sufficiently so that pressing a finger on it does not leave an imprint.

It is important to take note these times because they allow for preliminary considerations regarding foam catalysis. The formation of foam should occur within a time range of 60 to 90 seconds.

# Chapter 2

## Renewable raw materials

Nowadays the need to use renewable sources in polymer production has led to focusing attention on lignin due to its properties, availability, and the fact that it does not compete with the food sector.

Chapter 2 therefore presents the chemical structure and extraction methods of lignin, along with a description of the main characteristics and production method of EMEROX® bio-based polyols. These polyols will be used as solvents in the lignin liquefaction process to obtain new polyols.

### 2.1 Lignin

Lignocellulosic biomass is the most abundant plant product on Earth and consists mainly of three main elements in order of quantity: cellulose, lignin and hemicellulose. Lignin represents the largest renewable reservoir of aromatic compounds, especially phenolics, and therefore, with its wide availability, is considered a platform element in the production of polymers, chemicals and biofuels.

The production of biosynthesized lignin is estimated at  $6 * 10^{14}$  tons, of which pulp and paper mills produce 50-70 million tons of lignin per year and by 2030, it is estimated that the production of lignin may increase by 225 million tons per year<sup>7</sup>. Currently lignin is mainly used for energy production through combustion, where only 5% of the lignin produced is sold commercially, due to its complex structure that makes it difficult to understand and use.

According to the physical and chemical treatments applied to the lignin, modifications can be obtained in terms of structure and molecular weight distribution. In addition, the presence of impurities in the raw material and the method of lignin isolation from the biomass affect the characteristics of the final products. However, despite the increase in wood processing, the efficient use of waste, especially lignin, has not yet been achieved.

#### 2.1.1 Lignin molecular structure

Several studies<sup>8</sup> have been conducted to determine the chemical structure of lignin, identifying it as a racemic, aromatic complex of heterogeneous biopolymers with branching and cross-linking, whose content depends on the origin of the lignin and the extraction method. Chemically, lignin is composed of three primary phenylpropanoid monomers: p-coumaryl alcohol, coniferyl alcohol and sinapyl. These monomers are linked together by different types

of ether and carbon-carbon bonds, forming a highly branched and irregular network<sup>9</sup>. The exact composition and structure of lignin can vary according to plant species, tissue types and even environmental conditions. Lignin is also very resistant to hydrolysis, which contributes to its role in protecting plants against microbial attack and mechanical stress<sup>10</sup>. The complexity of lignin's structure results from its random polymerization gives to lignin its hardness and resistance to biodegradation<sup>11</sup>.

The chemical structure of lignin is one of the most challenging problems in the field of natural polymers. Lignin molecules and their breakdown products have many asymmetric centers, but without optical activity<sup>12</sup>. Natural lignin is not a simple connection of monomers, but is formed by the union or irregular addition in p-coumaryl alcohol, coniferyl alcohol and sinapyl alcohol, also known as respectively H, G and S units<sup>13</sup>. Therefore, lignin is a complex molecular structure class of polymers that cannot be described by a structural formula, and the properties of lignin can only be expressed by the elements, functional groups and the combination of the shape of each unit.

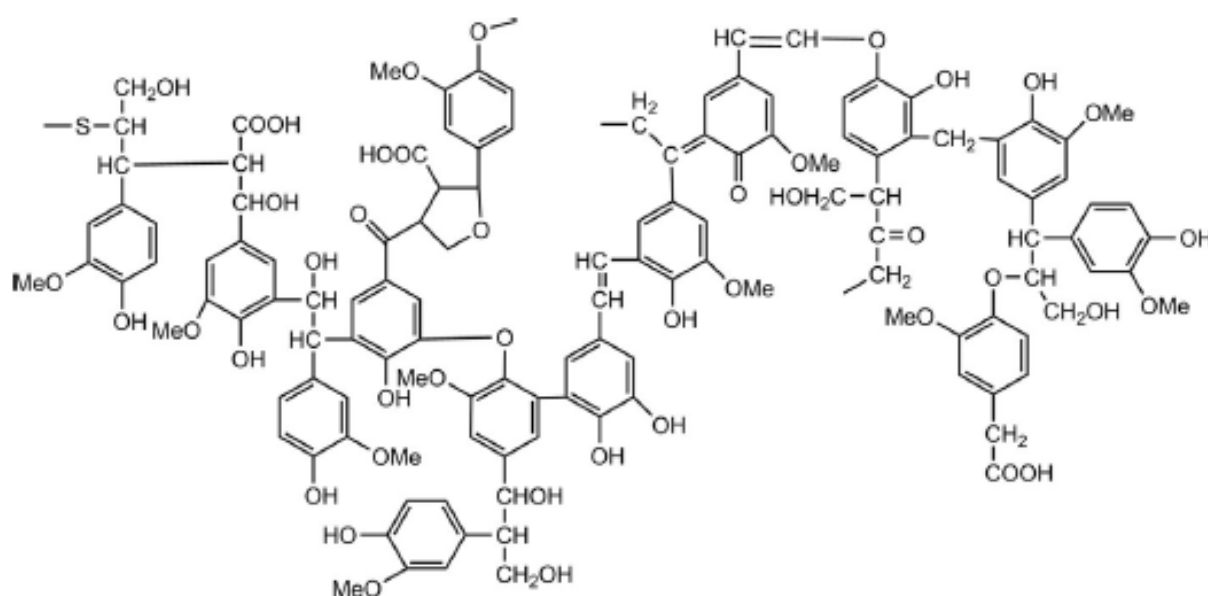


Figure 2.1 The structure of the softwood kraft lignin model.<sup>57</sup>

The structural units of lignin's complex backbone are linked by C-O bonds such as  $\beta$ -O-4,  $\alpha$ -O-4 and 4-O-5 and by C-C bonds such as  $\beta$ -5, 5-5,  $\beta$ -1 e  $\beta$ - $\beta$ , as shown Figure 2.2.

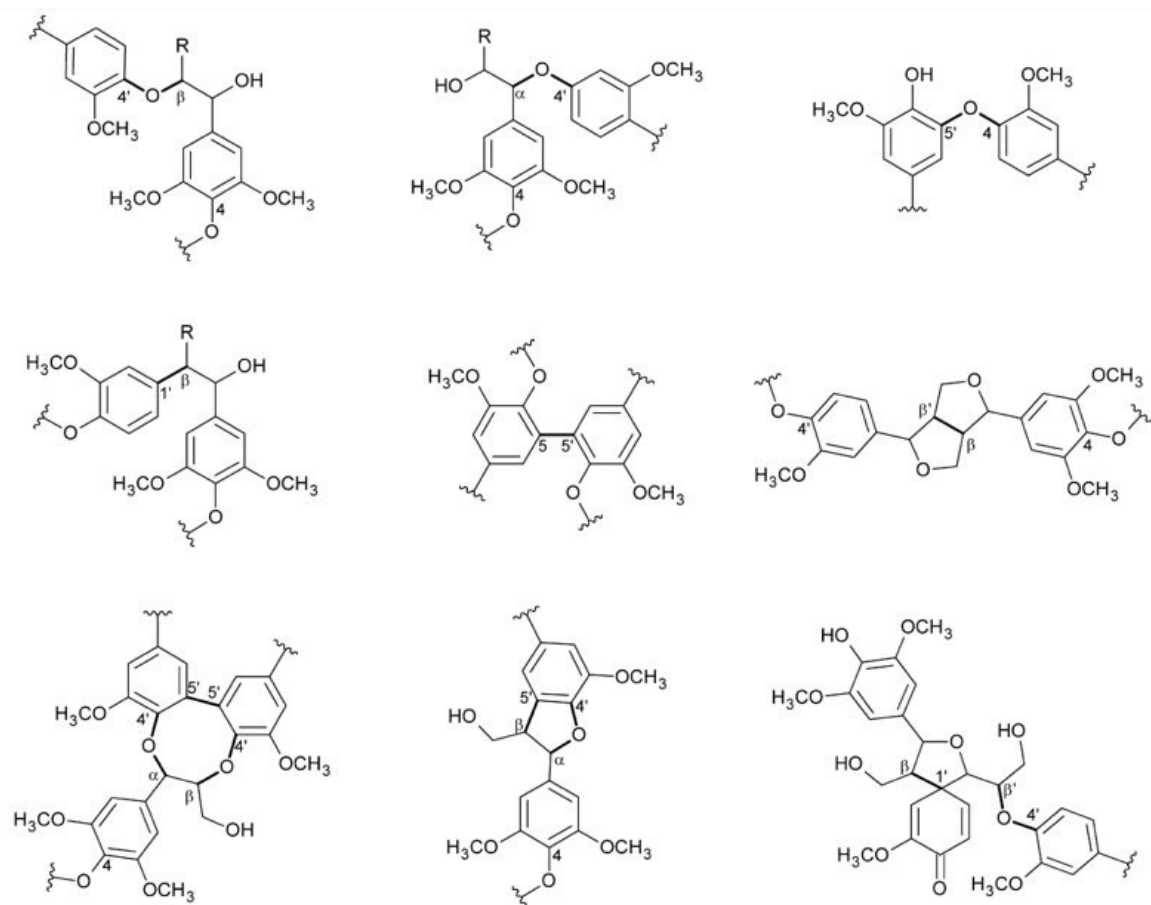


Figure 2.2 Characteristic bonds of lignin between the different structural units

While in Table 2.1 will be shown the frequency percentages of C-O and C-C bonds in lignin derived from gymnosperms and angiosperms

Table 2.1 Frequency of linkages between lignin structural units from gymnosperms and angiosperms<sup>14</sup>

| Linkage type      | Substructure                                  | % C <sub>6</sub> -C <sub>3</sub> units for lignin from |                  |
|-------------------|---|--|------------------|
|                   |   | Spruce (softwood)                                      | Birch (hardwood) |
| $\beta$ -O-4      | Phenylpropane $\beta$ -aryl ether             | 45-51  | 60-65            |
| $\beta$ -5        | Phenylcurmaran                                | 9-15   | 6                |
| 5-5               | Biphenyl                                      | 9.5-11   | 2.3-4.5          |
| $\alpha$ -O-4     | Phenylpropane $\alpha$ -aryl ether            | 6-8  | 6-8              |
| $\beta$ -1        | 1,2-diarylpropane                             | 7-10   | 7-10             |
| 4-O-5             | Diphenyl ether                                | 3.5-8  | 6.5              |
| $\beta$ -O-4      | Glyceryl aldehyde-2-aryl ether                | 2  | 2                |
| $\beta$ - $\beta$ | Resinol ( $\beta$ - $\beta$ linked structure) | 3  | 2-5.5            |

## 2.1.2 Methods of lignin extraction

Lignin can be extracted from lignocellulosic biomass using a variety of extraction techniques. The lignin's qualities, functionality and chemical structure are all impacted by the extraction process. The most popular techniques are listed and explained below<sup>14</sup>.

### 2.1.2.1 Kraft extraction process

During the Kraft process, sodium hydroxide transforms phenolic groups into quinonemide groups. Then, the hydrogen sulfide ion targets the  $\alpha$ -carbon atoms in the lignin's ether linkages, causing benzylthiolate anions to develop. The latter occur because of the sodium sulfate, which releases  $\beta$ -phenolate anions to form free phenolic groups. Lastly, the same procedure is used again to the produced phenolic groups in order to break the bonds and lower the molecular weight. Carbon-carbon bonds have the potential to form at the last phase of the process. Kraft lignin is hydrophobic and contains thiol-aliphatic groups.

The majority of lignin is obtained from the Kraft process as a by-product of the papermaking.

### 2.1.2.2 Sulfite extraction process

Sulfite extraction takes place between 125 and 150 °C for three to seven hours. Acids, calcium or magnesium sulfates, or both, are used as catalysts to break down  $\alpha$ -carbon and  $\beta$ -carbon bonds. After that, the resulting lignin can be dissolved and separated in an aqueous solution. As a consequence, the lignin produced has phenolic and aliphatic hydroxyl groups along with lignosulfonic acids and lignosulfonates. Lignin's high sulfur concentration makes it suitable for the use as fuel.

### 2.1.2.3 Soda extraction process

The primary purpose of the soda extraction method is to extract the lignin that is not derived from wood. High temperatures and pressures are used during extraction to cause a reaction between biomass and sodium hydroxide, which breaks  $\alpha$ -carbon bonds. The use of anthrahydroquinone or anthraquinone as a catalyst allows the  $\beta$ -O-4 ether linkages to be broken. This is an excellent chemical precursor lignin since it doesn't include sulfur.

### 2.1.2.4 Organosolv extraction process

In the Organosolv process, lignin is extracted through the use of organic solvents, such as ethanol, methanol, formic acid and acetic acid, and acid or basic catalysts. The cost and environmental impact of the process are increased by the use of organic solvents, but a sulfur-free lignin with a low molecular weight is obtained.



### 2.1.2.5 Steam extraction process

High temperatures and pressures are applied during the brief (1–20 minute) steam extraction process, which permits homolytic breakdown, aryl ether group rupture, and hydrolysis. It yields lignin with a low molecular weight and strong water solubility. This method, which is the initial stage in the manufacturing of biofuel, has a lot of promise.

### 2.1.2.6 Diluted acids extraction process

Lignin can be isolated by using dilute sulfuric acid (0.5-1.4 percent) and letting the reaction for 3 to 12 minutes; this is followed by washing with water. The obtained lignin has high solubility in water but the yield is rather low and the it contains impurities derived from sugar.

## 2.2 Azelaic acid and EMEROX® polyols

As seen in Figure 2.3, azelaic acid is a dicarboxylic acid with nine carbon atoms (C<sub>9</sub>). It is produced by ozonolysis of oleic acid, which is acquired from vegetable fats and oils<sup>15</sup>. Although azelaic acid is mostly utilized in medicines, it may also be esterified to produce bio-based polyols that are useful in a variety of industries, including the synthesis of polymers.

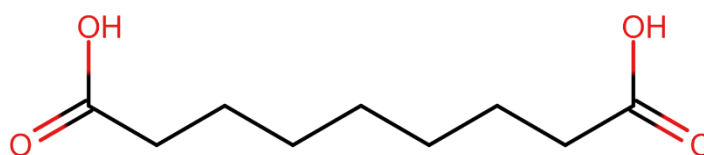


Figure 2.3 Azelaic acid chemical structure

These reactions and procedures serve as the foundation for EMEROX® technologies, which synthesize renewable source polyols commercially available on an industrial scale. The method employed by EMEROX®<sup>16</sup> is depicted in Figure 2.4 and consists of two steps: the first is the esterification process, which yields polyols from azelaic acid, and is represented by Emery Oleochemicals' ozonolysis technology, which has been used to produce azelaic acid from natural oils since the 1950s.

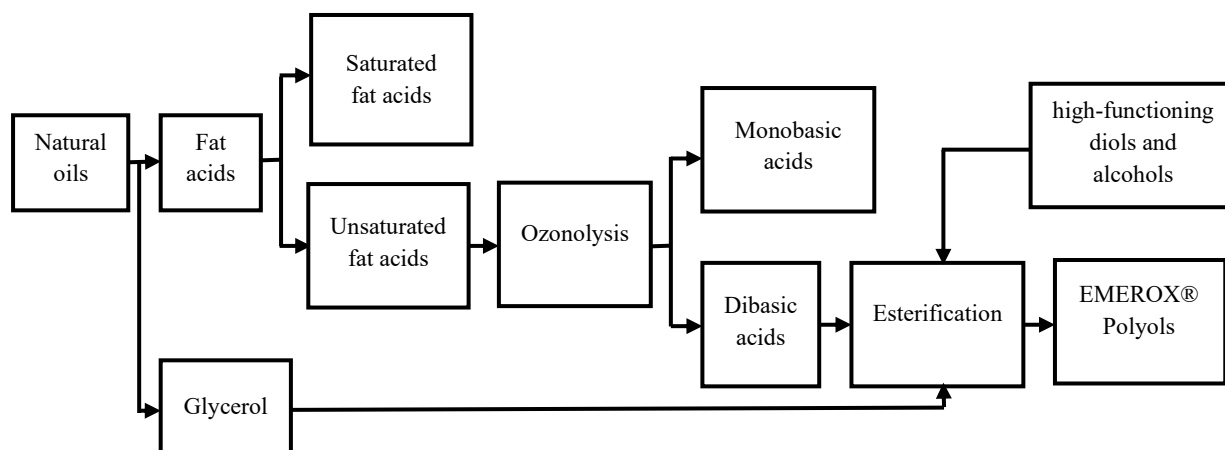


Figure 2.4 Block diagram of the EMEROX® process for the production of polyols from azelaic acid<sup>16</sup>

As observed in Figure 2.4, the starting material, vegetable oil, is hydrolyzed and split into glycerin and fatty acids. These are further divided into unsaturated and saturated fatty acids, such as oleic and steric, respectively. Monofunctional C18s have unsaturation at carbon 9 and carbon 10, which by ozonolysis are divided into monobasic and dibasic acids; separation and purification will be applied at the end. By esterification (performed in the same manner as that done in the petrochemical industry) of dibasic acids with glycerin, with diols and with high-functioning alcohols, we obtain n EMEROX® polyols, which have a high content from renewable sources.

# Chapter 3

## Microwave heating

Von Hippel discovered the macroscopic interactions between matter and microwaves in the 1950s. Microwaves offer a substitute energy source for traditional heating, which has significant benefits but is not yet extensively employed in the chemical sector.

The characteristic of microwaves, their interactions with materials, their main effects, and their benefits are all covered in Chapter 3. The instruments used in chemical synthesis are also provided.

### 3.1 Microwave radiation

Microwaves are electromagnetic radiations with a wavelength of between  $10^{-2}$  and 1 m. They are classified as part of the electromagnetic spectrum. In Figure 3.1 can be seen the locations of the microwave-related wavelengths within the electromagnetic spectrum.

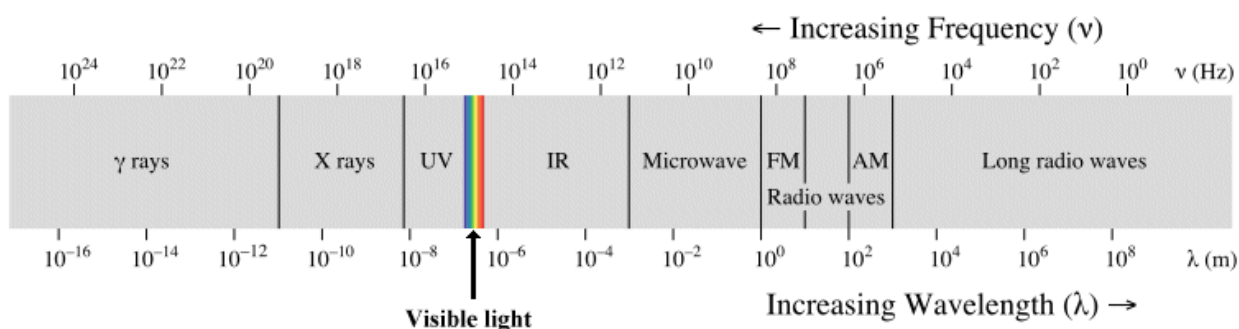


Figure 3.1 Electromagnetic spectrum

From equation (3.1) it is possible to retrieve the relation between the wavelength  $\lambda$  [m] and the frequency  $\nu$  [ $\text{sec}^{-1}$ ], given that  $c$  is the light velocity equal to  $3 \cdot 10^8$  [ $\text{m} \cdot \text{sec}^{-1}$ ]:

$$\lambda = \frac{c}{\nu} \quad (3.1)$$

As a result, the microwave frequency range that we have is 0.3 GHz to 300 GHz. In industrial and residential applications, only specific frequencies, typically 2.45 GHz and 915 MHz, are permitted to prevent interference with radar and telecommunications devices.

The frequencies that are allowed for use in residential, commercial, and medical settings are listed in Table 3.1.

Table 3.1 ISM frequencies allowed for industrial, scientific and medical use according to international agreements.<sup>17</sup>

| Frequency [MHz]     | Wavelength [cm] |
|---------------------|-----------------|
| 433.92±0.2%         | 69.14           |
| 915±13 <sup>a</sup> | 32.75           |
| 2450±50             | 12.24           |
| 5800±75             | 5.17            |
| 34135±125           | 1.36            |

The energy transmitted by the radiation is calculated by the equation (3.2):

$$E = h \cdot \nu \quad (3.2)$$

In which energy,  $E$ , is expressed in Joules and  $h$  is Planck's constant equal to  $6.626 \cdot 10^{-34}$  [J·sec]. It can be seen from Table 3.2 that the energy provided by microwaves is too low to allow the breaking of bonds, and therefore the microwaves do not directly activate the reaction by absorption of electromagnetic energy.

Table 3.2 Comparison of binding energies and energies of some electromagnetic radiation in the microwave range.<sup>17</sup>

|                | Energy [eV]         | Energy [kJ mol <sup>-1</sup> ] |
|----------------|---------------------|--------------------------------|
| Single bond CC | 3.61                | 347                            |
| Double bond CC | 6.35                | 613                            |
| Single bond CO | 3.74                | 361                            |
| Double bond CO | 7.71                | 744                            |
| CH bond        | 4.28                | 413                            |
| OH bond        | 4.80                | 463                            |
| Hydrogen bond  | 0.04-0.44           | 4-42                           |
| MW 0.3 GHz     | $1.2 \cdot 10^{-6}$ | 0.00011                        |
| MW 2.45 GHz    | $1.0 \cdot 10^{-5}$ | 0.00096                        |
| MW 30 GHz      | $1.2 \cdot 10^{-3}$ | 0.11                           |

### 3.2 Microwave dielectric heating

Electromagnetic waves, or microwaves, contain two components, as shown in Figure 3.2, an electrical component that is typically the most significant in matter-wave interaction, and a

<sup>a</sup> Not allowed in Germany

magnetic component that is only significant in certain applications, such those involving transition metal oxides.<sup>18</sup>

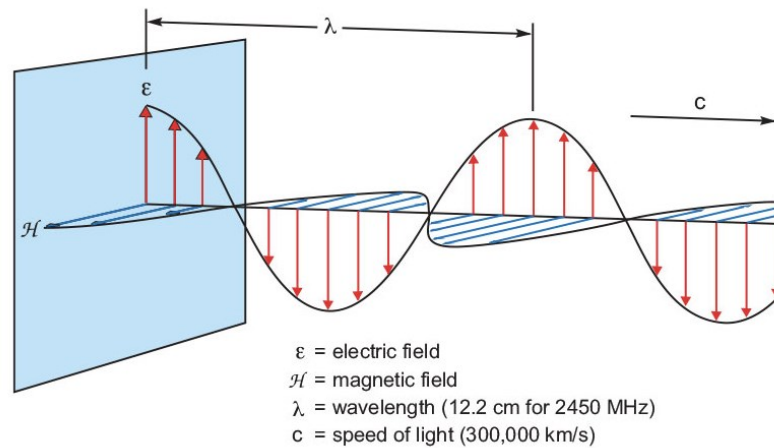


Figure 3.2 Electrical and magnetic components of the microwaves

The process of dielectric heating causes matter exposed to microwaves to warm up because of the material's capacity to absorb and transform microwave energy into heat. The electromagnetic field's electric component and the dipoles found in polar molecules are what cause the dielectric heating.<sup>19</sup>

Ion conduction and dipolar polarization are the two fundamental processes behind dielectric heating. The primary process is polarization, which results from heating caused by molecular friction and the material's dielectric losses.

When exposed to microwave radiation, the dipole aligns itself with the applied electric field. When the field oscillates, the dipole tries to align itself with the alternating electric field, which causes a phase discrepancy between the dipole's orientation and the field. Friction between the molecules is created by collisions, and the dipole loses energy that is subsequently transformed into heat.<sup>20</sup>

Because of the space between the molecules, this phenomenon only occurs in polar liquid substances and not in gaseous ones. However, if microwave heating is to be applied to apolar substances, a little quantity of miscible polar liquid must be added.

Since the frequency of electromagnetic waves affects rotational speed, the heating rate is influenced by that frequency. If the radiation frequency is too high, heating will not occur because the alignment is too slow, but if the frequency is too low, heating will not occur because the alignment is too fast.<sup>21</sup>

Ion conduction, which takes place in the presence of free charges, is the second process via which dielectric heating happens. Particularly, when charged with microwaves, positive ions go in the direction of the field and negative ions move in the opposite direction, creating an

apparent dipole moment. Ions move in response to oscillations in the electric field, which causes them to agitate, move and often they collide. This process dissipates energy and turns it into heat.

In comparison to dipolar polarization, ion conduction is more capable of producing heat.

### 3.3 Dielectric properties

When a material is exposed to microwave radiation, its dielectric characteristics influence how it heats up. The loss tangent  $\tan \delta$ , defined as follows (3.3), is used to characterize the capacity of matter to convert electromagnetic energy into heat at a particular temperature and frequency:

$$\tan \delta = \frac{\epsilon''}{\epsilon'} \quad (3.3)$$

The dielectric constant,  $\epsilon'$ , which represents the polarizability of molecules in the electric field, and the dielectric loss,  $\epsilon''$ , which is connected to the efficiency with which electromagnetic radiation is transformed into heat, make up the loss tangent<sup>21</sup>.

The loss tangents of some regularly used organic solvents are displayed in Table 3.3.

Table 3.3 Loss tangents ( $\tan \delta$ ) of organic solvents at 2.45 GHz and 20°C<sup>21</sup>

| Solvent             | $\tan \delta$ | Solvent            | $\tan \delta$ |
|---------------------|---------------|--------------------|---------------|
| Ethylene glycol     | 1.350         | DMF                | 0.161         |
| Ethanol             | 0.941         | 1,2-dichloroethane | 0.127         |
| DMSO                | 0.825         | Water              | 0.123         |
| 2-propanol          | 0.799         | Chlorobenzene      | 0.101         |
| Formic acid         | 0.722         | Chloroform         | 0.091         |
| Methanol            | 0.659         | Acetonitrile       | 0.062         |
| Nitrobenzene        | 0.589         | Ethyl acetate      | 0.059         |
| 1-butanol           | 0.571         | Acetone            | 0.054         |
| 2-butanol           | 0.447         | Tetrahydrofuran    | 0.047         |
| 1,2-dichlorobenzene | 0.280         | Dichloromethane    | 0.040         |
| Acetic acid         | 0.174         | Hexane             | 0.020         |

A high value of  $\tan \delta$  of the material allows for effective absorption of radiation and thus faster heating. This concept allows for the classification of reaction media into three groups: low ( $\tan \delta < 0.1$ ), medium ( $\tan \delta 0.1-0.5$ ), and high ( $\tan \delta > 0.5$ ) microwave absorption. For many processes, microwave heating works well because polar catalysts and reactants are typically present. The heating, which may be measured using  $\epsilon''$ , peaks at around 18 GHz.

Finally, the penetration depth  $x$  is defined as the point at which only 37% of the initially radiated microwaves are present. It can be shown that (3.4):

$$x \approx \frac{1}{\tan \delta} = \frac{\epsilon'}{\epsilon''} \quad (3.4)$$

This parameter is useful for quantifying the efficiency and uniformity of heating by microwave.

### 3.4 Comparison between traditional and microwave heating

In organic synthesis, conventional heating is accomplished with an external heat source, such as an oil bath. The three primary mechanisms involved are convection, conduction, and radiation. A number of variables, including the reaction mixture and the vessel's thermal conductivity as well as the convection currents produced inside the vessel, affect the heating efficiency. As a result, this heating technique may be sluggish and ineffective.

However, because of the way the mixture's molecules interact with the radiation, microwave irradiation is effective and quick.

The temperature gradients that result from microwave heating (left) and conventional heating (right) are shown to be inverted in Figure 3.5.

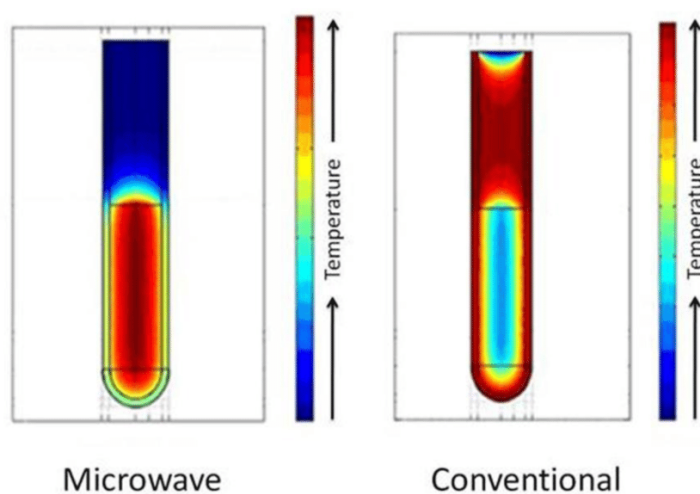


Figure 3.3 Temperature profiles generated after one minute of microwave heating (left) and traditional oil bath heating (right) (finite element modeling). Inverted temperature gradient: radiation increases the temperature throughout the volume simultaneously (bulk heating); in traditional heating oil bath the wall heats the mixture in contact with it first. Temperature scale in Kelvin<sup>21</sup>

Conventional heating involves the vessel being heated to a higher temperature while the interior volume is cooler. This can result in a temperature gradient inside the reaction mixture reaction and can cause local overheating, which can break down the reactants and substrate. Microwave heating involves the use of a material that lets microwaves go through the vessel, which are

directed to heat the core of mixture leaving the walls cool. Thus, it is possible to attain higher yield and purity using microwave irradiation.

### 3.5 Microwaves effects

Microwave heating has three effects on chemical reactions<sup>21</sup>: thermal effect (kinetic); specific microwave effect; non-thermal microwave effect.

#### 3.5.1 Thermal effect (kinetic)

The reaction rate increases due to a rapid and homogeneous rise in the reaction temperature throughout the volume; this effect is therefore purely thermal and kinetic.

Therefore, considering Arrhenius' law (3.5):

$$k = A \cdot e^{-\frac{E_a}{RT}} \quad (3.5)$$

where  $k$  is the kinetic constant and  $R$  the gas constant, only the temperature  $T$  is affected by the thermal effect while  $A$ , the pre-exponential factor, and  $E_a$ , the energy of activation remain unchanged.

This effect allows for shorter reaction times compared with conventional heating.

#### 3.5.2 Specific microwave effect

Thermal effects result from the unique characteristics of dielectric heating (refer to §3.2), which do not entail kinetics. These are known as particular microwave effects, because they cause chemical reactions and accelerations that would not happen with traditional heating. Reaction rate increases as a result of these impacts for a number of reasons.

There are no temperature gradients inside the reactor as a result of the mixture heating quickly and uniformly, a process known as mass heating. Furthermore, dielectric heating causes solvents to overheat at atmospheric pressure because the microwave power disperses across the reaction volume. Indeed, it has been shown that liquids heated by microwaves can reach temperatures 40°C higher than their boiling temperature at the same pressure<sup>22</sup>.

Because the energy is dispersed in the solvent where the reaction occurs and the way the reactor is build the walls of the reactor are not heated by the microwaves. As a result, the walls are cooler than the liquid, preventing catalysts and other substances that are sensitive to heat from deteriorating when they come into contact with the heated surfaces. As a result, there is a rise in the catalyst's efficiency and an increase in conversions.

One last crucial characteristic is the selective heating, which occurs when just certain of the mixture's components, the polar ones, absorb radiation and heat up; the other, apolar components only heat up by conduction. This behavior is highly beneficial when polar reactants



are present in a less polar mixture to form small hotspots, or when heterogeneous catalysts are activated, since they absorb microwaves more promptly.

The effects that were just discussed are purely thermal in nature and have nothing to do with the reaction's kinetics.

### 3.5.3 Non thermal microwave effect

Certain authors<sup>23</sup> postulate the presence of nonthermal microwave effects, according to which molecules' interactions with an electric field accelerate chemical processes rather than just thermal and kinetic effects alone.

According to some writers, the pre-exponential component  $A$  and the activation energy  $E_a$  of equation (3.5) change as a result of the dipolar molecules being oriented by the electric field. Specifically, when the reaction involves the transition state, the activation energy may be decreased by the contact with the magnetic field.

On the nonthermal effects of microwaves, which are still the focus of theories and investigation, some authors<sup>24</sup> differ.

## 3.6 Microwave reactors

Chemical synthesis is made possible by microwave reactors, which convert electromagnetic energy into heat in an effective and repeatable manner.<sup>25</sup>

A magnetron, which produces the microwaves, is the primary component of a reactor. The microwaves are then directed into waveguides, which are metal tubes, and into a metal cavity, which is where the sample is exposed to radiation. The reaction vessel is composed of materials that are transparent to microwaves, such Teflon®, quartz, or borosilicate.

Microwave reactors are currently equipped with temperature, pressure and radiation power, fiber-optic probes and IR sensors. There are basically two types of microwave reactors:

- Multimodal reactor, in which parallel synthesis is possible, that is, in the cavity are present in the rotor multiple irradiated reaction vessels;
- Single-mode reactor, or single-mode, in which only one vessel is irradiated at a time.

The multi-mode reactor's operation is seen in Figure 3.4. An agitator/antenna disperses the microwaves produced by one or two magnetrons inside the cavity after they enter through waveguides.

The microwaves interact chaotically with the material because they are reflected off the cavity's metal walls. Because they produce several pockets of energy with varying intensities within the cavity, hot and cold spots can therefore be created inside the reactor; to guarantee an equitable distribution of energy, the vessels are rotated.

Multi-mode reactors may produce large power outputs (between 1000 and 1400 W), but they

also have low power density and homogeneity of field.

Large-scale utilization of multimode reactors is also possible as they allow parallel synthesis

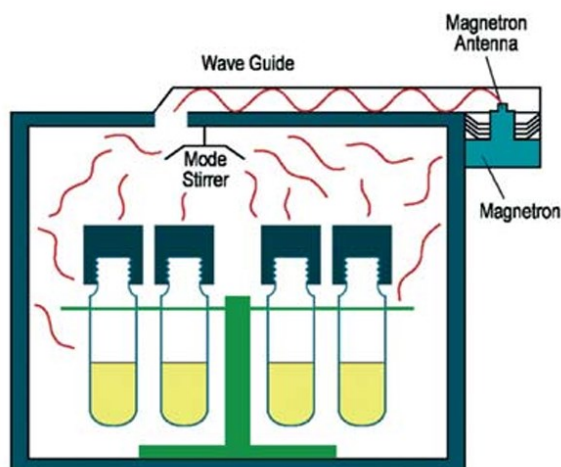


Figure 3.4 Multimodal microwave reactor<sup>26</sup>

In order to facilitate repeatable and scientifically valid results, microwave reactors have to be mechanically or magnetically stirred; possess precise temperature and pressure control; offer continuous power regulation; facilitate effective cooling; be computer-programmable; and have an explosion-proof cavity.

In this thesis work, a MicroSYNTH microwave reactor, supplied by Milestone, in Figure 3.5, whose wave frequency is 2.45GHz. The maximum power delivered by the two magnetrons is 1000 W, and the waves are distributed inside the reactor equally due to the patented pyramidal diffuser<sup>26</sup>. A fiber-optic probe placed within a single reference reactor, where a pneumatic sensor also controls pressure, is used to control temperature.

All additional reactors should be loaded identically to the reference reactor in order to ensure uniformity in the production process. Reactions may be seen and managed via an external terminal, and they can be carried out at a set temperature, pressure, or power.



Figure 3.5 MicroSYNTH® (Milestone) microwave reactor;

# Chapter 4

## Lignin liquefaction process

Lignin can be thermochemically converted into high-quality compounds by gasification, pyrolysis, combustion, or liquefaction<sup>27</sup>. Specifically, the latter is a solvent-assisted depolymerization process that yields to polyol as a liquefaction product, the properties of which are dependent on the reaction circumstances and which could be used to make polyurethane foams.

The majority of the information learned about the lignin liquefaction process is contained in Chapter 4. Specifically, the response mechanism, the components that impact the process the most and how they do so will be explained.

### 4.1 Lignin liquefaction

The process of liquefaction of lignocellulosic biomass is a solvolysis reaction by which there is the breaking of C-O and C-C chemical bonds to obtain oligomers with lower molecular weight and with higher functionality<sup>28,29</sup>.

The reaction is often carried out at high temperatures (150–170°C) using organic solvents and an acid catalyst (but basic catalysts are also sometimes used). Depending on the type of solvent utilized the end products can be utilized to create both rigid or flexible polyurethane. Polycondensation is a process that occurs in parallel with biomass depolymerization and reduces reaction efficiency by raising the proportion of insoluble residue. However, by maximizing the liquefaction parameters, such as temperature and duration, the amount of catalyst used, and the solvent/lignin ratio<sup>29</sup>, the polycondensation process may be restrained. The most important factor in the polycondensation process is reaction time. As the liquefaction time is increased, the yield of the reaction rises until the time set; if the other reaction parameters remain constant and the reaction is carried out for a longer period of time, the polycondensation reactions occur and the residue gradually increases<sup>30</sup>.

It has been proved that the using traditional heating in the liquefaction process is slower and more inefficient due to the low thermal conductivity of the reaction volume<sup>27</sup>, while microwaves allow to get a faster and homogenous heating. Indeed, they can accelerate the reaction due to the thermal and specific effect (Section §3.5).

### 4.1.1 Reaction mechanism

The entire process of lignin liquefaction cannot be adequately explained due to its complexity and lack of understanding<sup>31</sup>. Lignin is a high-molecular material with a three-dimensional structure, comprising carbon-carbon and carbon-oxygen linkages connecting phenyl-propane groups (see Section §2.1).

Research has demonstrated that the thermal stability of the bonds following lignin's heat treatment is:  $\beta\text{-5} > \beta\text{-}\beta' > \beta\text{-O-4'}$ . Lignin may be treated at high temperatures and with acid catalyst to break more easily the carbon-oxygen bond. Liquefaction produces aliphatic and alkyl low molecular weight phenols.

Phenol, ethylene glycol or polyoxy alcohols are solvents used to dissolve lignin, and will be explained in the following sections.

#### 4.1.1.1 Phenol process

The mechanisms of the acid-catalyzed and uncatalyzed liquefaction process were studied using guaiacylglycerol- $\beta$ -guaiacyl ether (GG) as the reference compound, which has a structure very similar to that of lignin<sup>32,33</sup>.

The reaction performed in the presence of an acid catalyst has a specific and different mechanism from that of the uncatalyzed reaction and, therefore, different products are obtained. Using acid catalysis, the product that is mainly obtained is guaiacylglycerol- $\alpha$ -phenyl- $\beta$ -guaiacyl ether but guaiacol, triphenylethane, diphenylmethane and benzocyclobutane are also produced<sup>32</sup>.

It has been shown that the kinetics of the reaction depend on the kind of acid used. Specifically, using 98% sulfuric acid accelerates catalysis compared to phosphoric and silicic acids. Studying the behavior of the reaction when the time and acidity of the catalyst vary and by analyzing the products of the reaction, it was possible to hypothesize a reaction mechanism, Figure 4.1.

The acid catalyst releases a hydrogen ion ( $\text{H}^+$ ), which attaches to the GG's hydroxyl alpha group; from this reaction it is obtained the benzene cation which reacts with the phenol, resulting in the formation of phenolate compounds. The weak  $\beta\text{-O-4'}$  bonds in newly formed compounds break, resulting in to the production of reactive intermediates, which can be involved in reactions of polycondensation reacting with each other or with phenol

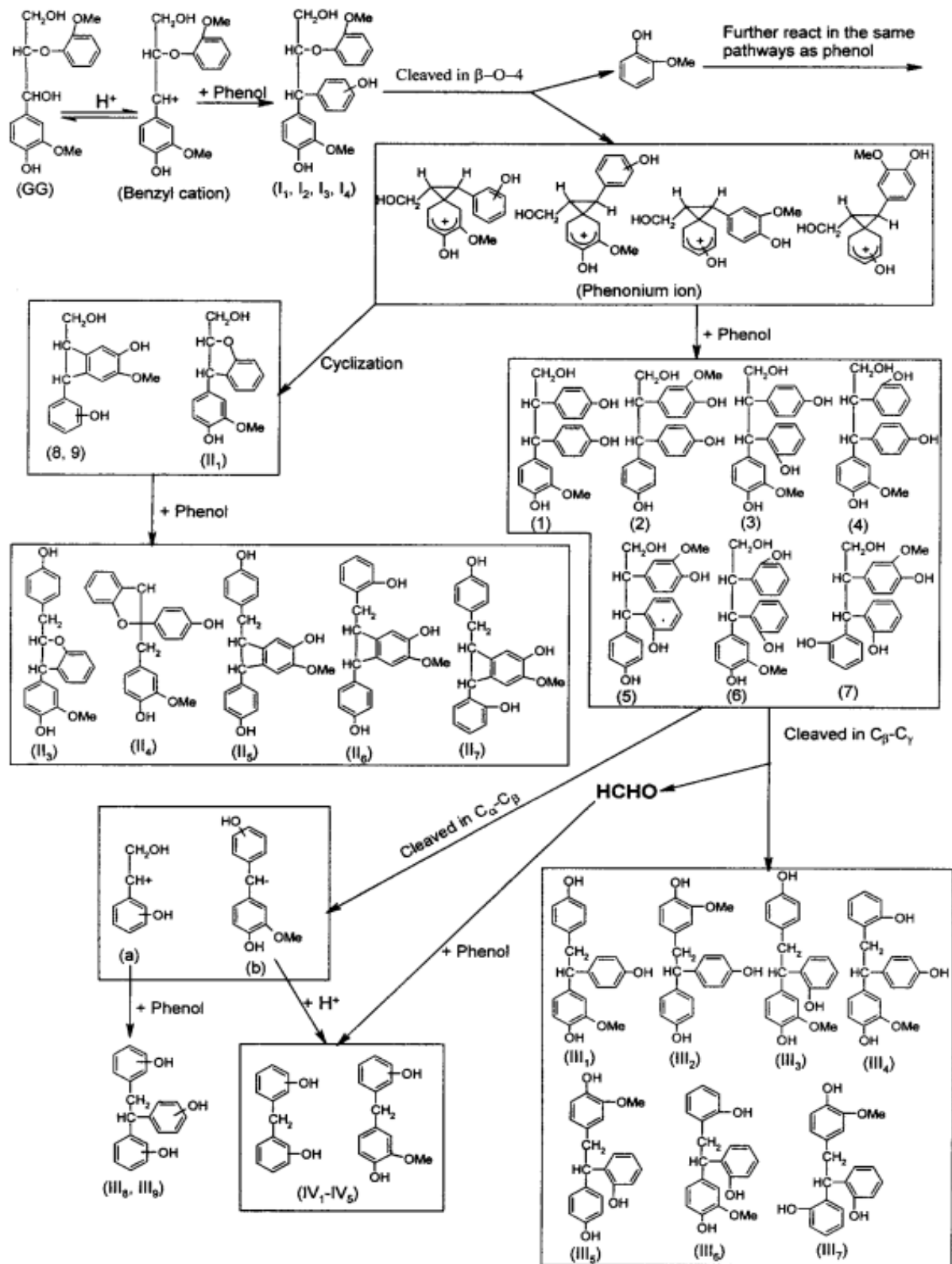


Figure 4.1 Depolymerization and polycondensation reactions involved in liquefaction of lignin in the presence of phenol and acid catalysis<sup>33</sup>

### 4.1.2 Ethyl glycol process

To determine the processes behind the lignin liquefaction process at 150°C with ethylene glycol, a study was conducted on the process<sup>34</sup>. A reduction in the proportion of secondary aliphatic hydroxyls to primary aliphatic hydroxyls may be the reason to assess that in the initial phase of the reaction (Figure 4.2), the EG attach itself to the  $\alpha$  group of the lignin's phenylpropane.

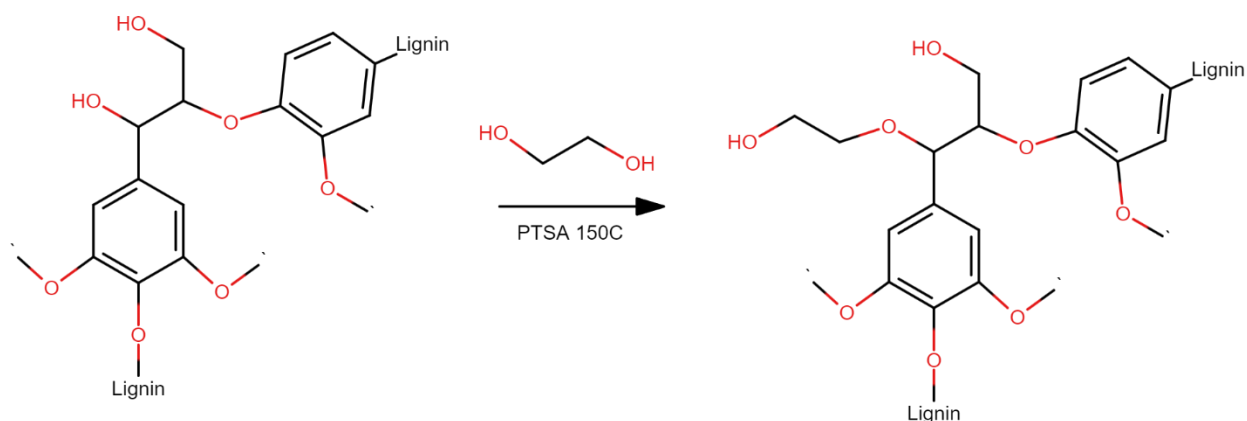


Figure 4.2 Reaction of EG with lignin and subsequent introduction into the  $\alpha$  position<sup>34</sup>

Depolymerization of lignin may follow from this reaction due to the breaking of the  $\beta$ -O-4' bond or the polycondensation reactions shown in Figure 4.3 may occur with subsequent formation of higher molecular weight compounds.

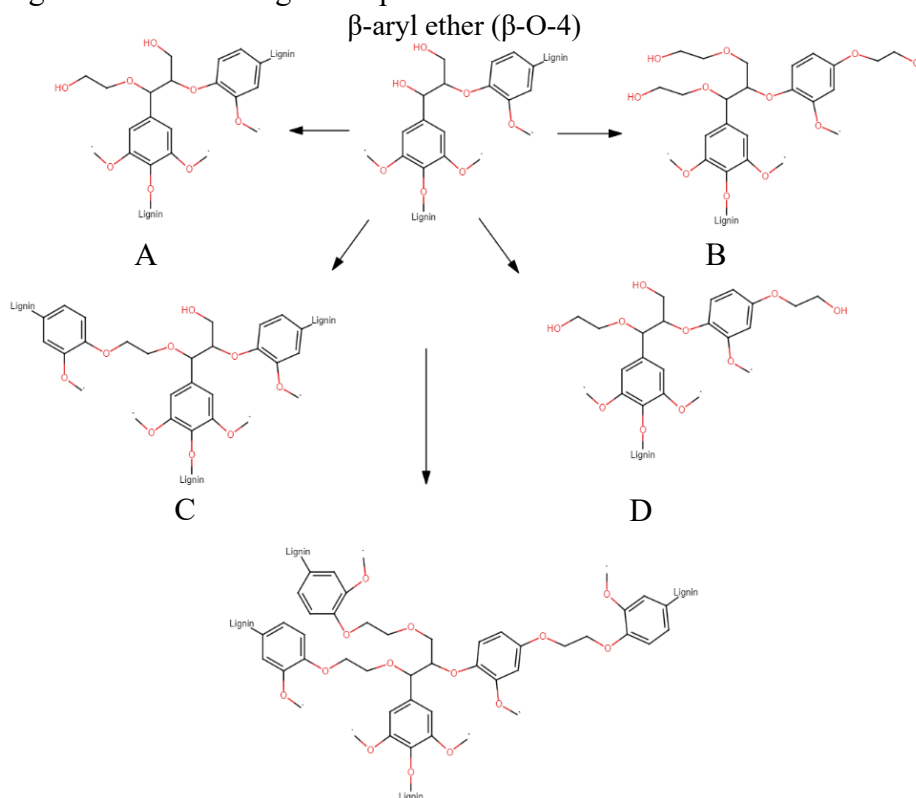


Figure 4.3 Polycondensation reactions involved in the lignin liquefaction process with di EG<sup>34</sup>

### 4.1.3 Reaction kinetics

Several writers<sup>35,36</sup> have focused their attention on examining the kinetics and mechanism of the lignocellulosic biomass liquefaction process in order to enhance its efficiency. The liquefaction process of polyoxydryl alcohols, PEG400, glycerin, or a combination of these has been reported to be multilevel<sup>34</sup>. Equation of Arrhenius (3.5), in which the activation energy  $E_a$  and the frequency factor  $A$  are found, was used to investigate the impact of temperature on the kinetic constant.

Yan et al.<sup>36</sup> found the values of the constants of (3.5) using a mixture of PEG400/glycerin (4/1 w/w), while Shi, Y. et al.<sup>35</sup> studied the kinetics using both PEG400 and glycerin as solvents, showing that glycerin is a more effective for liquefaction.

Table 4.1 shows the  $E_a$  and  $A$  values found in the different experiments that relate to the liquefaction of lignin.

Table 4.1 Activation energy,  $E_a$ , and rate factor,  $A$ , of the lignin liquefaction reaction performed using different solvents: PEG/glycerin, PEG400 and glycerin<sup>35,36</sup>

| Solvent                   | $E_a$ [kJ mol <sup>-1</sup> ] | $A$ [s <sup>-1</sup> ] |
|---------------------------|-------------------------------|------------------------|
| PEG400/glycerol (4/1 w/w) | 73.6                          | $8.8 \cdot 10^5$       |
| PEG400                    | 107.36                        | $7.41 \cdot 10^7$      |
| Glycerol                  | 89.10                         | $5.75 \cdot 10^8$      |

## 4.2 Liquefaction process parameters

Through many studies conducted on lignin liquefaction, it has been found that the yield and efficiency of the liquefaction reaction are related to several factors, such as temperature, time, type of solvent used and its ratio to lignin, type and amount of catalyst.

### 4.2.1 Effect of liquefaction solvent

Various solvents with distinct properties, including phenol, cyclic carbonates, ionic liquids, and polyhydroxy alcohols, can be used for the liquefaction process<sup>35</sup>.

It has been noted that many of these are effective in the liquefaction process, despite the fact that the liquefaction mechanism is not well known it occurs in the presence of polyhydroxy alcohols. Indeed, alcohols have a strong dipole moment, and the ionic and radical reactions that take place during the liquefaction process are favored by the solvent's polarity<sup>35</sup>.

Several studies have been conducted using as the main liquefaction solvent polyethynglycol<sup>37-39</sup> with which high yields can be obtained due to the limitation of the polycondensation reactions. The addition of 10-20% glycerol to the reaction mixture reduces the residue content and limits condensation reactions as well as speeding up the process. It has also been observed that by increasing the glycerin content in the starting mixture the hydroxyl number of the

product increases<sup>37,38</sup>. However, it has been studied<sup>37</sup> that higher amount of glycerin reduces the efficiency of liquefaction by dehydration.

The effect of the molecular weight of PEG in a PEG/glycerin mixture (80/20 by weight) was also investigated<sup>39</sup>. Experiments were conducted using PEG400, PEG600 and PEG1000, and it was been observed that the highest reaction yield, 97%, is achieved using the solvent with lower molecular weight; increasing the molecular weight decreases the yield to 89%. In parallel, the hydroxyl number decreases as the molecular weight increases: with the PEG400 a product having a hydroxyl number of 410 mgKOH/g can be achieved, with the PEG600 the hydroxyl value is 320 mgKOH/g and with PEG1000 of 190 mgKOH/g.

Gosz K. et al.<sup>27</sup> studied the liquefaction of lignin using a mixture of glycerin and 1,4-butanediol, without catalyst, with 15 percent biomass. At the optimal conditions of 150°C and for a time of 5 minutes, a yield of 93% and a hydroxyl number of 670 mgKOH/g was obtained.

### 4.2.2 Catalyst effect

The liquefaction's catalysis can be either acidic or basic, although most of the studies concern the former. Generally, basic catalysis requires higher temperatures (250°C) but is less corrosive to the equipment used<sup>29</sup>.

#### 4.2.2.1 Acid catalyst

Several acids can catalyze the liquefaction process by acting on the degradation and condensation mechanisms; their presence is very important because they allow the reaction to be conducted at lower temperatures and times and improve the yield. The most widely used catalyst is sulfuric acid, whose concentration relative to the reaction solvent must be optimized in order not to promote condensation reactions<sup>40</sup>. Increasing the concentration from 1% (w/w) to 3-4% (w/w) decreases the solid residue, so the yield increases, but further increasing the acid concentration does not affect the yield<sup>40</sup>. The hydroxyl number, on the other hand, decreases as the weight percentage increases of the acid<sup>39</sup>.

#### 4.2.2.2 Basic catalyst

Alma M.H & N. Shiraishi<sup>41</sup> used sodium hydroxide as catalyst, which is more economical, less corrosive and less polluting than sulfuric acid. The reaction was performed at 250°C for 2 hours, using PEG400 as solvent in a 4/6 ratio by weight with the biomass and using different concentrations of NaOH (0%, 2.5%, 5%). As the amount of catalyst increases, the solid residue decreases from 4.85% to 0.35%. The hydroxyl number of the product obtained using 5% soda ash is 169.9 mgKOH/g. The pH of the product increases as the soda content increases, but remains always close to neutral pH.



### **4.2.3 Temperature effect**

An increase in temperature, in general, accelerates the kinetics of reactions, and it is therefore necessary to find the optimum temperature value for which the reaction rate of condensation does not exceed that of decomposition. It has been investigated how the yield and hydroxyl number of the product vary with temperature in the range of 130°C to 170°C<sup>39</sup>. The maximum yield occurs at 150°C, then decreases as temperature increases due to the prevalence of polycondensation reactions. The hydroxyl number, on the other hand, decreases with increasing temperature.

### **4.2.4 Time effect**

Performing the liquefaction reaction for a very long time could result in the occurrence of condensation reactions, which is why reaction time is a fundamental parameter in liquefaction. Since liquefaction is a fast process the times considered are between 5-30 minutes<sup>42</sup>. Moving from 5 to 20 minutes the yield increases but after this value the polycondensation reactions occur and at 30 minutes a small decrease in yield is observed. The hydroxyl number, on the other hand, continues to decrease as the time increases<sup>39</sup>

### **4.2.5 Lignin-solvent ratio effect**

Changing the ratio of liquid to solid influences the liquefaction trend leading to a change in the hydroxyl number of the product and the yield of the process. If the lignin content is high, the number of reaction's intermediates increases favoring condensation and a decrease in yield happen. The hydroxyl number, on the other hand, decreases as the lignin content increases due to its reaction with the solvent<sup>39</sup>. An excess of solvent is therefore used. Considering a PEG400/glycerin mixture an optimal solvent/lignin ratio is 1/5-1/6



# Chapter 5

## Liquefaction materials and methods

In Chapter 5 will be described materials and methods utilized for the synthesized lignin-based polyols. The methodologies used for the characterization of the products of liquefaction will be also discussed

### 5.1 Materials

#### 5.1.1 Lignin type

In this thesis work, nine different types of lignin characterized by a different degree of purity: Borresperse® Ca, Borresperse® Na, Dealkaline lignin (TCI), Alkaline lignin (TCI), INDULIN® AT, Reax® 88A, Reax® 100M, Polyfon® O and Polyfon® T.

- *Borresperse® Ca*: is a spray-dried calcium lignosulphonate that is mostly made from the sulphite liquid of fermented spruce wood.
- *Borresperse® Na*: is a sodium lignosulphonate which comes from spruce wood sulphite liquid. It is a brown powder soluble in water.
- *Dealkaline lignin (TCI)*: is based on sodium lignosulfonate but different chemical modifications are applied like partial desulfonation, oxidation, hydrolysis and demethylations.
- *Alkaline lignin (TCI)*: is obtained by adjusting the pH value in the alkaline range, 8-10, of the Dealkaline lignin.
- *INDULIN® AT*: is a kraft lignin from pine, highly purified in which no hemicellulosic materials and sulfides are present, which is why it is usually used in the production of polymers. The lignin content is 97%. It is insoluble in benzene and hexane while it is completely soluble in dioxane and ethylene glycol.
- *Reax® 88A*: is a low molecular weight kraft lignin with a high content of sulfonated group and an acidic pH.
- *Reax® 100M*: is a highly sulfonated kraft lignin that is suggested for use in dry formulations and aqueous suspension like wettable powder and water dispersible granule.
- *Polyfon® O*: is a kraft lignin but with low sulphonation's degree and low molecular weight.

- *Polyfon® T*: is a kraft lignin but with low sulphonation's degree (higher than *Polyfon® O*) and low molecular weight.

Table 5.1 Main characteristic for the different types of lignin

| Lignin type              | pH   | Degree of sulfonation [mol/kg] | Site of sulfonic acid group  | MW averages [g/mol] |
|--------------------------|------|--------------------------------|------------------------------|---------------------|
| <b>Borresperse® Ca</b>   | 4.3  | 0.7                            | Aliphatic side and end chain | 30000 <sup>b</sup>  |
| <b>Borresperse® Na</b>   | 8.3  | 0.7                            | Aliphatic side and end chain | 30000 <sup>b</sup>  |
| <b>Dealkaline lignin</b> | 3    | max 1.9                        | Aliphatic side chain         | 60000 <sup>c</sup>  |
| <b>Alkaline lignin</b>   | 8    | max 1.9                        | Aliphatic side chain         | 60000 <sup>c</sup>  |
| <b>INDULIN® AT</b>       | 6.5  | 0                              | None                         | 4500                |
| <b>Reax® 88A</b>         | 4.3  | 2.9                            | hybrid                       | 3100                |
| <b>Reax® 100M</b>        | 8.8  | 3.4                            | hybrid                       | 2000                |
| <b>Polyfon® O</b>        | 10.3 | 1.2                            | Aliphatic side chain         | 2400                |
| <b>Polyfon® T</b>        | 10.5 | 2.0                            | Aliphatic side chain         | 2900                |

### 5.1.2 Liquefaction solvents

Liquefaction was conducted using EMEROX® polyols as solvents whose common characteristic is that they are derived from azelaic acid according to the process described in Chapter 2 (see Section §2.2).

In some tests, a polyol/glycerin mixture was used by varying the ratio from 50/50 to 100/0 (w/w). In contrast, the solvent/lignin ratio was held constant at 5/1 (w/w), the value most widely used in the literature<sup>43</sup>. Viscosity, functionality, hydroxyl number, average molecular weight and percentage of content from renewable sources of the polyols used are shown in Table 5.2.

<sup>b</sup> Tang Q, Sun Y *et al.* (2024)<sup>55</sup>

<sup>c</sup> Kane S, Hodge D *et al.* (2024)<sup>56</sup>

Table 5.2 Main characteristic of the Emerox® polyols

| Solvent            | Hydroxyl value<br>[mgKOH/g] | Functionality | Molecular weight<br>[g/mol] | Viscosity<br>[cps] | Biobased content<br>[%] |
|--------------------|-----------------------------|---------------|-----------------------------|--------------------|-------------------------|
| Emerox®<br>14511   | 106-114                     | 2             | 1043                        | 1680               | 78                      |
| Emerox®<br>14535xp | 355                         | 2             | 318                         | 250                | 69                      |

### 5.1.3 Catalysts

Both acid catalysts and basic catalysts can be used in the liquefaction process; in this thesis, the effect of both types of catalysis was studied and used different catalyst concentrations expressed as a percentage with respect to the weight of the liquefaction solvent.

The acid catalyst is 98% sulfuric acid, while anhydrous and caustic sodium hydroxide was used as basic catalyst.

### 5.1.4 Extraction solvent

Once the liquefaction reaction is complete, the polyol is dissolved in a solvent to facilitate the extraction of the same from the reaction mixture. The solvents used are acetone for the process with acid catalyst and a mixture dioxane/water 4/1 (w/w) for the process with basic catalyst.

## 5.2 Microwave lignin liquefaction

Microwave heating was employed in this work as the heating technique; Chapter 3 provided details on the mechanics. Therefore, the reaction was carried out in a Milestone-supplied MicroSYNTH® multi-mode microwave reactor (Figure 5.1a). One of the many reactors within the rotor is pressure- and temperature-controlled by a fiber-optic sensor (Figure 5.1b).

The reaction temperature may be controlled by automatically adjusting the microwave power. The temperature set can be reached in 5 minutes and maintained at that level for 20 to 30 minutes. The program is used to enter temperature and reaction time settings.

Magnetic stirrers are used to agitate the reaction mixture. A cooling system is also included in the reactor's setup.

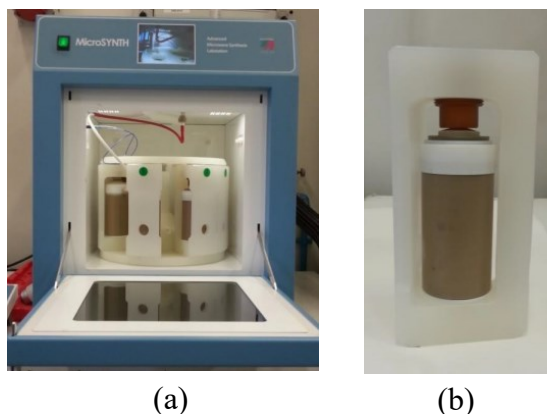


Figure 5.1 (a) MicroSYNTH® (Milestone) microwave reactor, (b) reactor pressure vessel

The process involves first adding the lignin, the solvent (or solvent combination) and the catalyst. The proportion of catalyst ranges from 1 percent to 3 percent, while the lignin to solvent ratio remains constant at 1/5 (w/w). Once the microwave liquefaction is complete, the mixture is cooled to room temperature and poured into an 800 mL beaker. Approximately 400-500 mL of extraction solvent, which could be acetone or a mixture of dioxane/water, is then added, and the mixture is stirred on a plate with a magnetic stirrer for one hour. A consistent decrease in viscosity can be observed, which facilitates the filtration process. The filtration setup consists of a vacuum pump, a Büchner funnel, and filter paper (Whatman 589/1 12-25 $\mu$ m). Before filtering, the polyol-acetone solution is centrifugate for 30 minutes at 3000 rpm to achieve preliminary separation. At the end of the filtration, the non-liquefied lignin will remain on the filter paper, which will be dried in an oven at 80 °C until the mass is constant and then weighted to calculate the liquefaction process yield. The filtrate will be transferred to the rotary evaporator for two main reasons: first, to recover the significant amount of extraction solvent (i.e. acetone or dioxane/water) and reuse it; the second reason is related to acetone because even small amounts of acetone could interfere with the foam formation process.

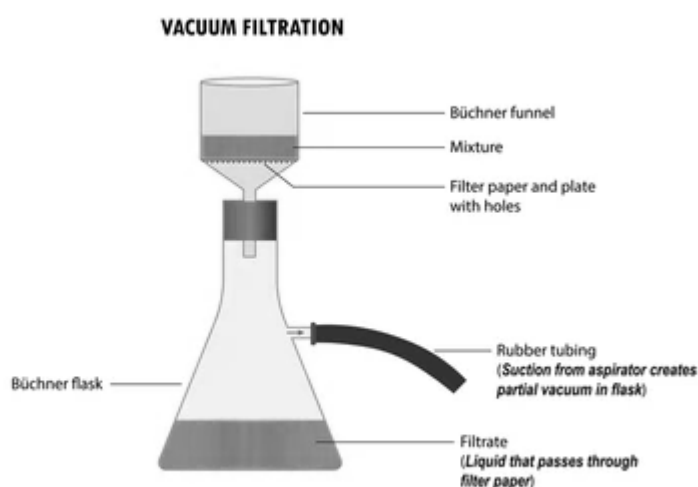


Figure 5.2 Vacuum filtration scheme

### 5.3 Yield calculation

The yield of the liquefaction process is calculated by considering the unreacted mass of the lignin, according to the following formula (5.1):

$$\eta = 1 - \frac{M}{M_0} \quad (5.1)$$

where  $M_0$  is the mass of lignin loaded into the reactor and  $M$  is the mass of lignin that is not depolymerized and insoluble in the dilution solvent that remains on the filter. The yield, therefore, allows to evaluate the efficiency of liquefaction by considering the percentage of lignin reacted.

### 5.4 Characterization method of polyols

The polyol obtained from the liquefaction process is characterized by titration, to determine the hydroxyl number, and by Gel Permeation Chromatography (GPC) for the molecular weight determination.

#### 5.4.1 Hydroxyl value

Along with liquefaction yield, hydroxyl number is used to assess the efficiency of liquefaction and is also needed to calculate the formulation of polyurethane foams according to equation (1.11). Determination of the hydroxyl number is done by potentiometric titration, according to DIN 53240-2:2007-11 standard.

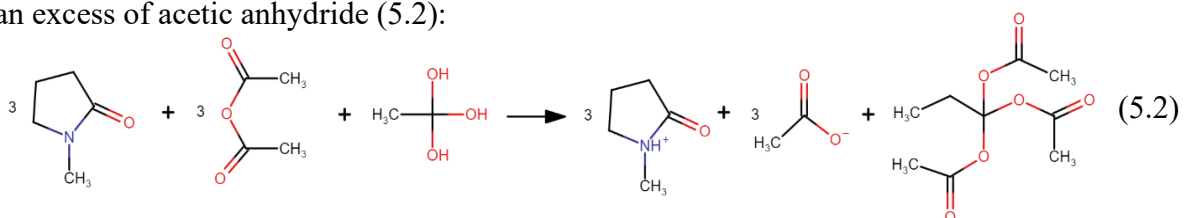
Titration is part of the volumetric analysis; it involves reacting a known volume of an unknown-titer solution containing the analyte until the reaction is finished with a solution of a known-titrant reagent.

The analyte concentration may then be computed using a straightforward method that takes the reaction's stoichiometry and titrant volume into account.

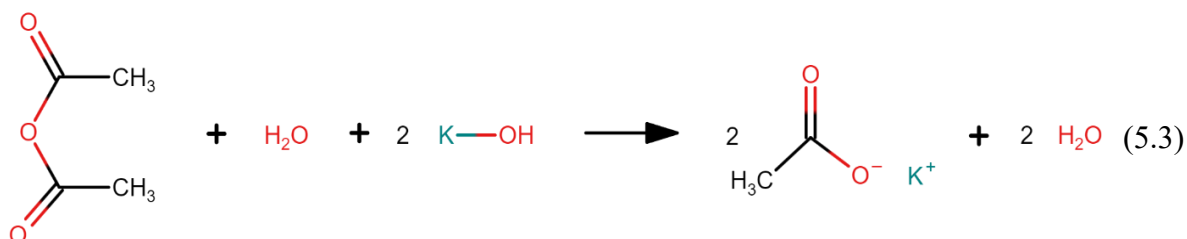
According to the previously mentioned standard, a polyol sample of known weight, between 0.2 and 0.5 g, is reacted for one hour at 55°C with an acetylating solution and a catalytic solution; the solution is continuously stirred during the reaction.

The acetylating solution consists of 100 mL of acetic anhydride in 1 liter of N-methylpyrrolidone (NMP) while the catalytic solution consists of 10g of 4-N-dimethylaminopyridine (DMAP) in 1000 mL of N-methylpyrrolidone.

In this first step, the acetylation reaction of the hydroxyl groups of the polyols takes place using an excess of acetic anhydride (5.2):



The solution is then allowed to cool while keeping it stirring, and then 3 ml of distilled water that is allowed to react, at least, for 15 minutes at room temperature so that the excess acetic anhydride that has not reacted with the polyol hydrolyzes to form acetic acid acetic acid; the latter is titrated by gradually adding a solution of known titer of KOH (0.5M in methanol) according to equation (5.3):



Titration is carried out until the reaction is finished, which may be determined in a few different ways: using an electrode that measures the pH of the solution and its fluctuation, which is the more accurate method, or using an indicator whose color varies based on the chemical environment in which it is found.

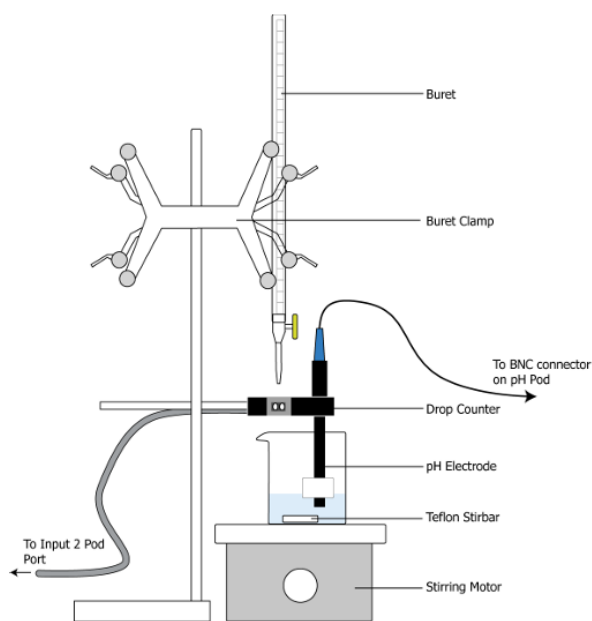


Figure 5.3 Potentiometric titration setup

Figure 5.3 shows the system that is used to titrate: a beaker containing the solution is agitated through a magnetic stirrer, an electrode is immersed inside the solution and a burette in which the titrant solution is added gradually.



To quantify the hydroxyl number, measured in mgKOH/g, the following equation:

$$nOH = \frac{(A - B) \cdot 5.6 \cdot M}{w} \quad (5.4)$$

where  $A$  is the volume of titrant used to titrate the blank, determined by the same procedure just described but without adding the sample to the catalytic solution and the acetylating solution,  $B$  is the volume of titrant used to titrate the sample, and  $M$  is the molarity of the titrant, in the present case KOH 0.5 molar, and  $w$  is the weight of the analyzed sample.

To determine the volume of the titrant needed to bring the reaction to completion, it is used the potentiometric curve, that is, the graph represented the potential value as a function of the volume of titrant (Figure 5.4).

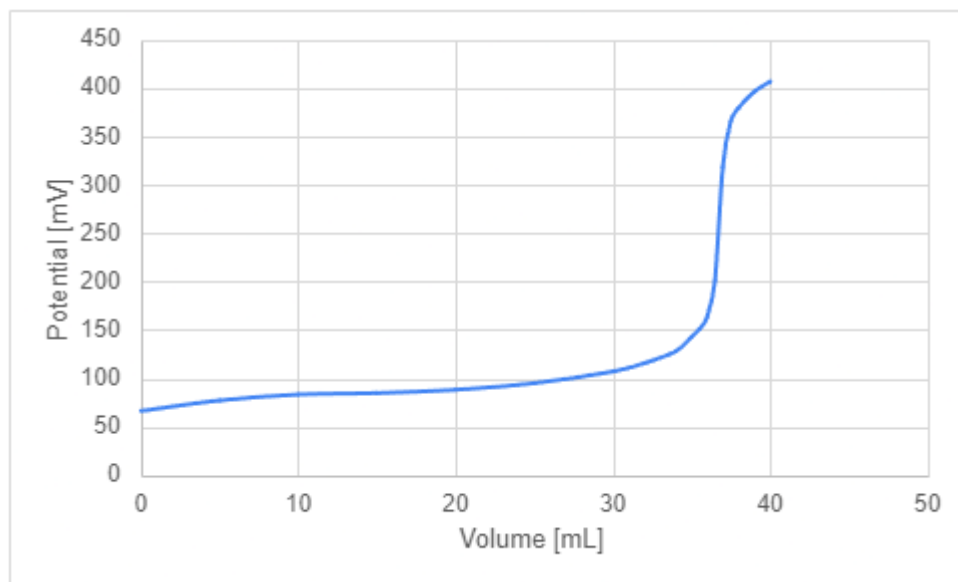


Figure 5.4 Potentiometric curve

Through the graphs of the first derivative (Figure 5.5) and second derivative (Figure 5.6) of the potentiometric curve, it is possible to precisely identify the point of equivalence, that is, the point at which the inflection of the potentiometric curve occurs. The first derivative ( $dE/dV$ ) has a maximum at the equivalence point, while the second derivative ( $d^2E/dV^2$ ) cross the zero when the reaction is completed.

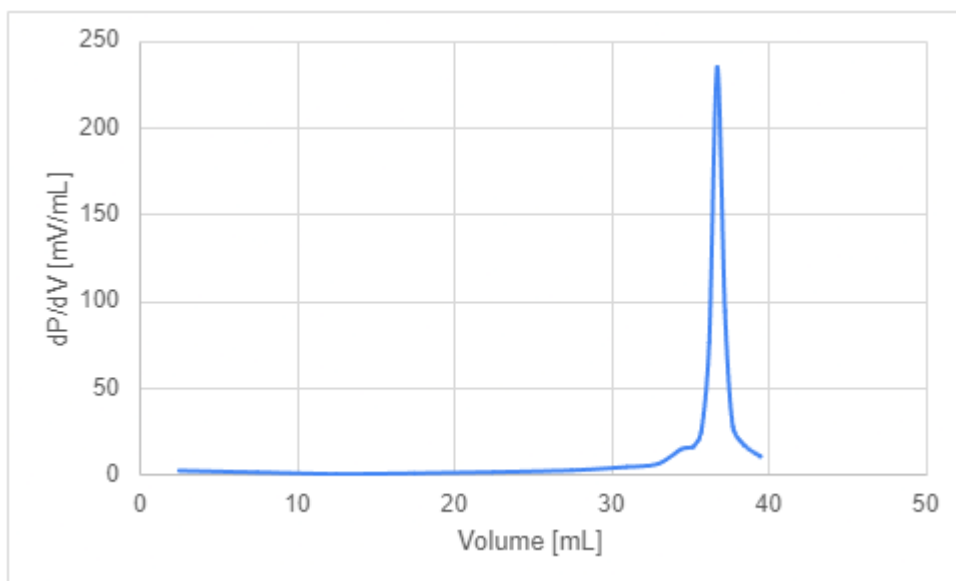


Figure 5.5 First derivative of the potentiometric curve

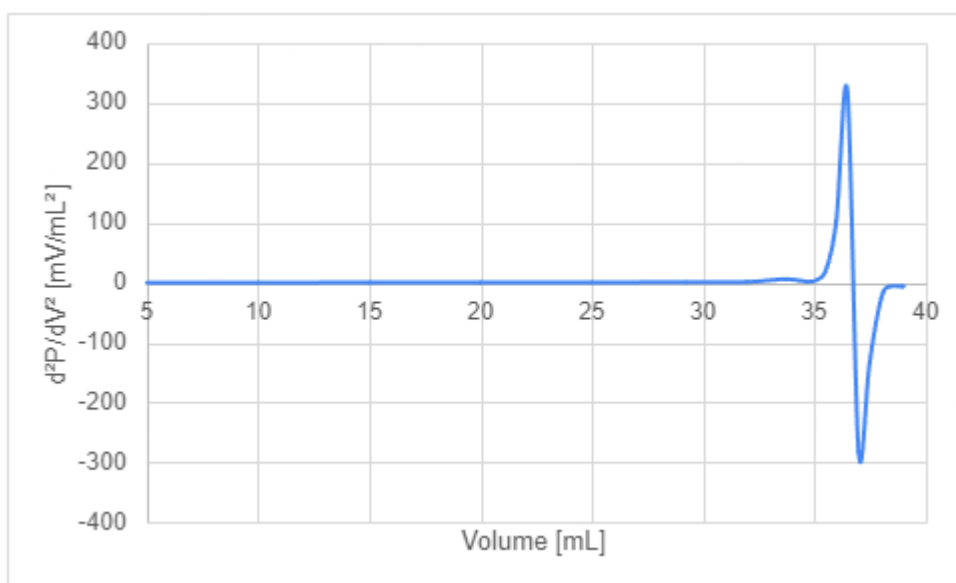


Figure 5.6 Second derivative of the potentiometric curve

### 5.4.2 Gel permeation chromatography

Gel permeation chromatography (GPC) is a technique used to assess the molecular weight of the polymers created during liquefaction. Understanding the polymer's molecular weight is crucial since it affects its technical characteristics.

Since the 1960s, the GPC technique has been utilized as a separation technique that permits the sample to be divided based on the size of the polymer chain.

The elution of a polymer solution in one or more columns with porous packing made of tiny, strongly cross-linked polymer particles is the basic idea behind GPC.

Depending on their size, the particles pass through the column at different times: particles with hydrodynamic volumes larger than the pore size pass into the interstices between the grains and escape faster; smaller particles penetrate into the pores and the smaller their size the more time they spend inside the pores slowing down their passage through the column. The total volume of the column is (5.5):

$$V_c = V_m + V_0 + V_p \quad (5.5)$$

where  $V_m$  is the volume of the solid matrix forming the porous packing;  $V_0$  is the interstitial volume between the particles, and  $V_p$  is the pore volume. The molecules are distributed between the interstitials and pores, and the retention volume  $V_e$  is given by (5.6)

$$V_e = V_0 + K_{SEC} \cdot V_p \quad (5.6)$$

$K_{SEC}$  is the distribution coefficient of the solute in the stationary phase and is one for molecules that have the largest volume of all pore sizes and zero for molecules with volume smaller than the size of all pores.  $V_e$  thus depends on the size of the chains and the pore size of the column, and from its distribution it is possible to derive that of the molecular weights. Usually, however, one elution time ( $t_r$ ) is measured.

The separation column, detectors, and solvent injection system/pump comprise the GPC (a schematic representation of which is provided in Figure 5.7.

The injection system maintains a steady solvent flow, while the pump generates high pressures to maintain a consistent solvent eluted flow.

According to the systems under consideration, different materials are used for the rigid or semi-rigid high-porosity packed spheres in the columns. For aqueous systems, rigid silica or glass particles or cross-linked gels of polyacrylamide are used; for organic systems, on the other hand, highly cross-linked polystyrene particles with *o*-divinylbenzene are used (as in this work).

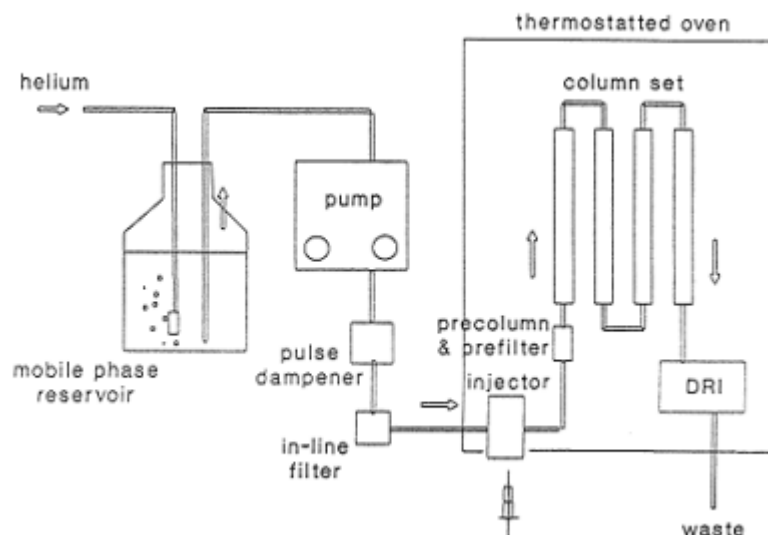


Figure 5.7 GPC scheme

A wide range of molecular weights is covered only if multiple columns (or one long) with a porosity distribution, because a single column can only measure a range of molecular weights that includes 1.5-2 orders of magnitude. It is very important the choice of solvent, in which the polymer to be analyzed must be soluble and in which do not occur secondary modes of separation. Typically, the following are used:

- *Tetrahydrofuran (THF)* with polymers solubilized at room temperature (as in this work);
- *o-dichlorobenzene* and *trichlorobenzene* at 130°C and 150°C with polyolefins;
- *2-chlorophenol* at 90°C with polyamides and polyesters.

Typically, the sample to be injected has a final concentration of 0.4% by weight; it must be verified that all the sample is dissolved into the eluent, after that the solution is filtered and finally injected into the machine. The analysis lasts approximately 35 minutes and the chromatogram will be shown at the end of it. A refractive index detector is utilized to create the chromatogram (Figure 5.8), which is a graph that displays the detector signal (proportional to concentration) as the volume or retention time varies. The detector measures the difference in index of refraction between the pure solvent and the solution that is flowing through the column continuously.

Calibration of the column is necessary to determine the correlation between the retention volume and molecular weight and thus transform the chromatogram into a distribution of molecular weights.

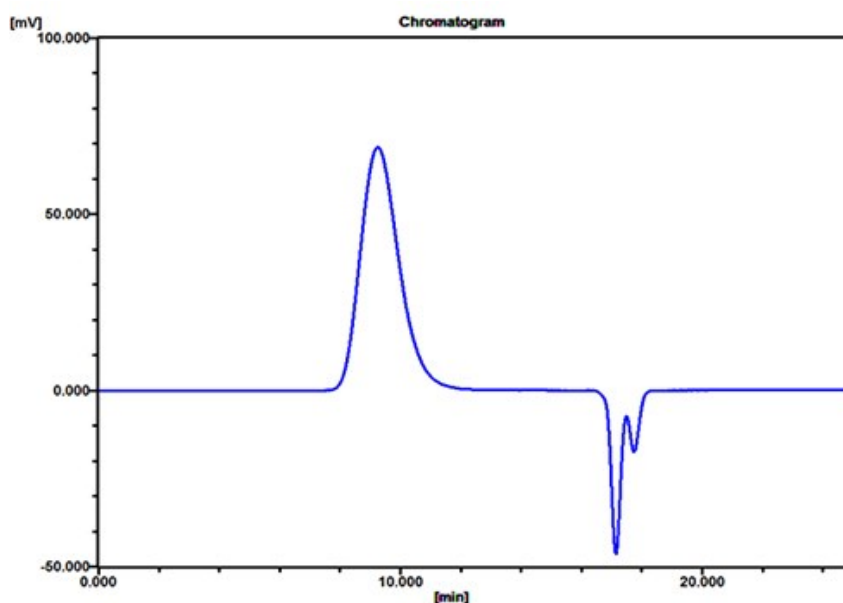


Figure 5.8 Typical chromatogram

To calibrate GPC, specified standard samples with known molecular weights (MW), limited distribution of molecular weights and known  $K_{SEC}$  are utilized. Based on polystyrene or polymethyl methacrylate, commercially available samples, typically have molecular weights between 2.9 million and 3000 u.m.a. In this work, polystyrene standards were employed.

The  $V_{idro}$  hydrodynamic volume is proportional to the molecular mass according to the calibration principle. The calibration procedure is the following: the refractive index change between the pure solvent and the entrained fraction is measured at the outlet after a 0.2% solution (2g/L) of sample in tetrahydrofuran is introduced into the chromatographic column. The calibration curve is made by representing in the abscissa the logarithm of the molecular weight and on the ordinate the retention volume for each injected solution.



# Chapter 6

## Methods for the characterization of polyurethane foams

Chapter 6 provides a description of the methods and equipment used in the characterization of the polyurethane foams produced in the present work. It is also outlined the basics concerning the combustion of polyurethanes.

### 6.1 Physical characterization

#### 6.1.1 Apparent density

Bulk density is the ratio of the mass to the volume of the foam, expressed in [kg/m<sup>3</sup>] and measured through the UNI 6349 standard. The mass ( $m$ ) and linear dimensions of the polymer are measured to determine the volume ( $V$ ) on a homogeneous sample. The density is then calculated as (6.1):

$$\rho = \frac{m}{V} \quad (6.1)$$

Density is very important in determining the mechanical properties of foam because as the density increases, the compressive strength increases according to the empirical relationship (6.2):

$$\sigma = K \cdot \rho^n \quad (6.2)$$

where  $\sigma$  is the compressive strength,  $\rho$  is the density and  $n$  is an empirical coefficient less than 2. It is also crucial that the density is not too high because one of the advantages of polymeric materials is their lightness.

#### 6.1.2 Thermal conductivity

Foams are usually also used in construction as thermal insulation, and therefore it is very important to evaluate their thermal conductivity. Thermal conductivity is measured by the heat flow meter method, following the standard UNI 7745, using a thermal conductivity meter (Figure 6.1).

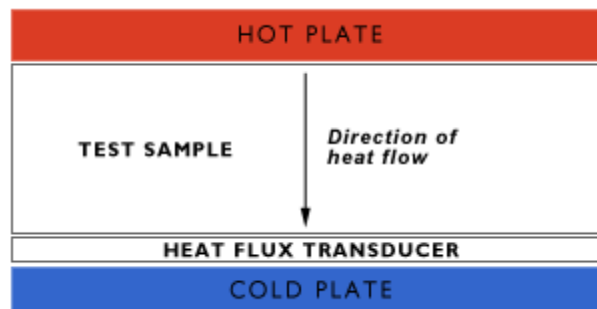


Figure 6.1 Thermoconductimetry scheme

The sample is placed between two plates that, being at different temperatures, generate a thermal gradient and thus a heat flux  $Q/A$  [ $\text{mW}/\text{m}^2$ ] that passes through the sample. The flux is measured by a transducer across an area of  $100 \text{ cm}^2$ , smaller than that of the sample to avoid the edge effect, i.e., lateral heat fluxes distorting the result.

Figure 6.2 shows the Holometrix Lambda 2300V thermal conductivity meter with which the the conductivity of the produced foams was measured.



Figure 6.2 Holometrix thermoconductimetry

Given the temperature gradient  $\Delta T$  [ $^{\circ}\text{C}$ ], the thickness  $s$  [ $\text{m}$ ] and the surface area of the sample in contact with the plates  $A$  [ $\text{m}^2$ ] and measuring the flux  $Q$ , it is possible to calculate the conductivity thermal  $k$  [ $\text{mW}/\text{m}\cdot\text{K}$ ] by inverting Fourier's law (6.3).

$$Q = \frac{k}{s} \cdot A \cdot \Delta T \quad (6.3)$$

From which derives equation (6.4)

$$k = \frac{Q \cdot s}{A \cdot \Delta T} \quad (6.4)$$



The heat flow through a 1 m<sup>2</sup> region of a 1 m thick panel when the temperature gradient is 1 K is therefore defined as thermal conductivity. Therefore, it can be inferred that as conductivity drops, heat transfer between two locations at differing temperatures also reduces, leading to a larger insulating power for the material.

Because polyurethane foams mostly consist of gas and only contain a little amount of solid material (about 3% by volume), they are commonly used as thermal insulators. As a result of their significantly lower heat conductivity than that of solids, gases make thermally insulating materials. In a material with a cellular structure, heat transfer occurs by conduction through the gas, by conduction through the solid, by radiation and convection. Given the size of the cells, the convective contribution is generally negligible, so the thermal conductivity of the foam is determined by the sum of the conductive contribution of the solid, the gas and the radiative contribution.

Since the expansion of gas outward and the inward diffusion of air, which has a greater conductivity, and so eventually reduce the insulating ability of the material, conductivity is tested on the first day of the foam's creation. As a result, thermal conductivity can be utilized as a gauge for foam aging, or the tendency for insulating power to diminish due to diffusive events. The number of closed cells has an impact on the initial temperature; the more closed cells, the lower the initial value.

### 6.1.3 Compression stress/strain

It is essential to know the mechanical properties of the material in order to assess whether it can be used for specific purposes, like cushioning, energy absorption and structural application. The tests are carried out following ISO 3386, using the Galdabini SUN 2500 dynamometer shown in Figure 6.3.



Figure 6.3 Galdabini SUN 2500 dynamometer

This standard requires that samples be either parallelepipeds or cylinders with a width/thickness or diameter/thickness ratio of 2:1, respectively. The thickness of the specimen

must be greater than 10 mm, preferably 50 mm, with an effective surface area of at least 2500 mm<sup>2</sup>. Once the specimen is prepared, it is placed between the plates so that the force acts along the centerline, and 4 compression cycles are performed up to a maximum of 70% ± 5%. The compression resistance values must be taken on the fourth cycle, both when the compression reaches 40% and at maximum deformation when compression reaches 70%. The compression stress is known to be influenced by the thickness and the tensile properties of the flexible cellular material. This parameter is important because measure the load-bearing properties of the material, which is not necessarily its capacity to sustain a load for long time.

#### 6.1.4 Compression set

For flexible foams, the compression set is an essential mechanical characteristic, especially in applications where the foam is compressed repeatedly or for an extended period of time, such as sealing, seating, and cushioning materials. It describes the foam's capacity to return to its initial thickness following compression and release. A high compression set implies that the foam experiences persistent deformation, which may impair its functioning, whereas a low compression set shows that the foam maintains its resilience and shape following compression. The density, cellular structure, and polymer makeup of the foam are the main factors that affect the compression set. How well the foam can withstand long-term compressive stress without permanently deforming is determined by these characteristics.

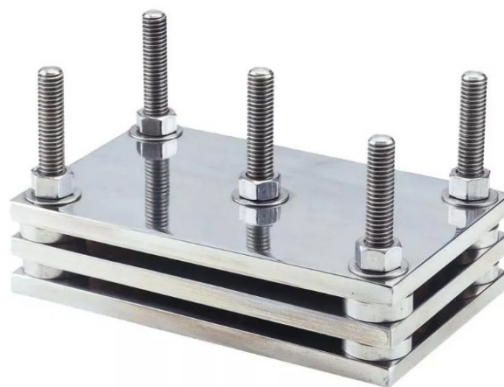


Figure 6.4 Compression set device for ISO 1856

For flexible foams, the compression set measurement is usually carried out in accordance with ISO 1856, the international standard that describes the methods for figuring out the compression set under particular conditions. The test involves the use of a device with two flat and parallel plates, which are larger in size than the specimen. The height of these plates must be maintained throughout the duration of the test. The specimen should be a parallelepiped measuring 50x50x25 mm. There are three different methods for performing the test; the one used here is briefly illustrated as Method A.

Using a caliber, the initial thickness of the sample is measured, and then a choice is made to

impose a deformation of either  $50\pm 4\%$  or  $75\pm 4\%$ . In this specific case, the first option was chosen. The samples are then placed between the plates, and within 15 minutes, they are placed in an oven at  $70^\circ\text{C}$  for  $22\pm 0.2$  hours. Once the time has elapsed, the specimens should be removed from the compression apparatus within one minute and left to rest on a surface with low thermal conductivity for 30 minutes. The thickness of the specimens is then remeasured, and the compression set factor is calculated as a percentage using the following formula:

$$C.S. = \frac{d_0 - d_r}{d_0} \cdot 100 \quad (6.5)$$

Where  $d_0$  represents the initial thickness, and  $d_r$  is the thickness after compression.

### 6.1.5 Dynamic mechanical analysis (DMA)

A useful method for assessing a material's mechanical characteristics in relation to temperature, frequency, time, and applied stress is dynamic mechanical analysis, or DMA. DMA is especially helpful for understanding the viscoelastic behavior of flexible foams, which is important for applications like seating, cushioning, and insulation when materials are subjected to dynamic loading conditions.

In compression mode DMA is used to assess the mechanical behavior of flexible foams under cyclic compressive stress. This is especially relevant for foams because of their ability to undergo significant deformation while maintaining functional properties such as cushioning and energy absorption. In DMA, compression testing provides information on the stiffness, damping, and fatigue resistance of the foam by gauging its response to cyclic or repetitive stress. This is done by providing information about their storage modulus, related to the elastic component, and loss modulus, which is related to the viscous component.



Figure 6.5 DMA Q800 TA Instruments

## 6.2 Morphological characterization. SEM (scanning electron microscope)

The cellular structure of the foams is analysed thanks to a scanning electron microscope. The main difference with optical microscopes is that, to achieve high resolutions, the radiation source is not light but an electron beam. Through a system of magnetic lenses, the electron beam is accelerated and focused on the sample in multiple scans that allow to get many signals from the interaction between sample and electrons. By processing the signals, the material can be characterized morphologically and structurally.

The outer surface is analysed by the signal from the secondary electrons, which are located at a depth of 10 nm, which create an image on the screen.

Figure 6.6 represents the schematic structure of the SEM. The main elements are:

- *Electron column* through which the electron beam is generated;
- *Vacuum chamber* in which the interaction between sample and the electron beam takes place;
- *Detectors* which acquire the signals of the interaction between the beam and the sample and transfer it to the processors;
- *Screen* on which the image of the sample is reconstructed through the received signal;

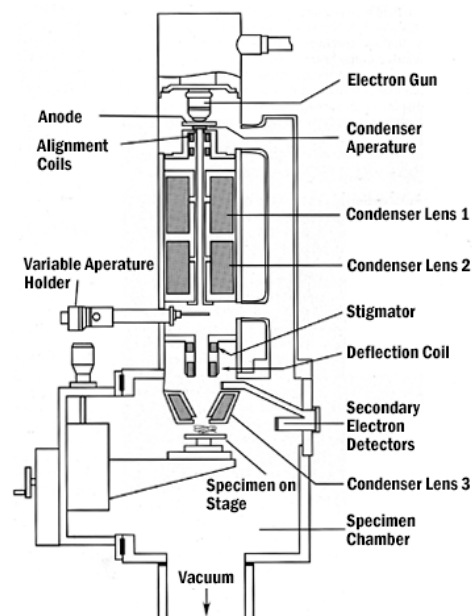


Figure 6.6 Schematic of a scanning electron microscope

The average cell size of foams may be calculated using sample images acquired by SEM. This is a crucial metric since it influences the material's heat conductivity. One may determine the average cell diameter by using ASTM D3576. It is crucial to adhere to a reference since the

cells differ in size from one another. This approach requires drawing five horizontal lines on the SEM images of the expanses, which should include around 400 cells, and counting the points where the reference line and the cell walls cross. Because the shear plane crosses the cell randomly rather than always passing through the center, the cell width is therefore calculated, necessitating an adjustment.

Dividing the length of the reference line by the number of intersections gives the z-chord that can be related to the average diameter of the randomly cut cells. Considering a generic circle  $x^2 + y^2 = r^2$  from (6.5) we obtain the mean value of the ordinates in the first quadrant:

$$\bar{y} = \frac{1}{r} \cdot \int_0^r \sqrt{r^2 - x^2} dx = \frac{\pi \cdot r}{4} \quad (6.5)$$

Where  $r$  is the radius of the cell in shear plane and  $\bar{y} = z/2$ .

Thus, it can be obtained the equation (6.6)

$$\frac{z}{2} = \frac{\pi \cdot r}{4} \quad (6.6)$$

And knowing that  $r = d'/2$  (6.7):

$$z = \frac{\pi \cdot d'}{4} \quad (6.7)$$

From (6.7) the (6.8) is obtained:

$$d = \frac{d'}{0.785} \quad (6.8)$$

Namely (6.9):

$$d = \frac{z}{0.785^2} = \frac{z}{0.616} \quad (6.9)$$

Alternatively, image analysis software can be used to calculate the average diameter of the cells. The variation of the gray tone in the image makes it possible to identify the cell wall. The measurement is preceded by calibration of the software by plotting a known dimension on the image.

### 6.3 Fire behaviour of polyurethane foams

The low thermal conductivity of polyurethane foams means that when their surface is subjected to radiation, negligible heat is dissipated resulting in a rapid rise in temperature and the reaching of the degradation temperature.

#### 6.3.1 Polymers combustion processes

The combustion of polymeric materials<sup>4,5,44-49</sup> occurs in a more complex manner than that of gases, since fuel is produced by the material as it degrades and that is why gases have varying rates and composition. Combustion is therefore related to different conditions such as the onset temperature of decomposition and kinetics of decomposition but also by the intensity of internal heating.

The combustion mechanism, schematized in Figure 6.7, thus includes several stages. Due to a heat source, pyrolysis of the solid substrate occurs, resulting in the development of heat and fuel. This, together with the oxygen in the air, can result in combustion, if the mixture is within flammable limits, with subsequent generation of heat that partly returns to the substrate and fuels combustion, and in part is dispersed to the environment ( $\Delta H_3$ ). Combustion occurs, in each case, when there is equilibrium between the processes involved.

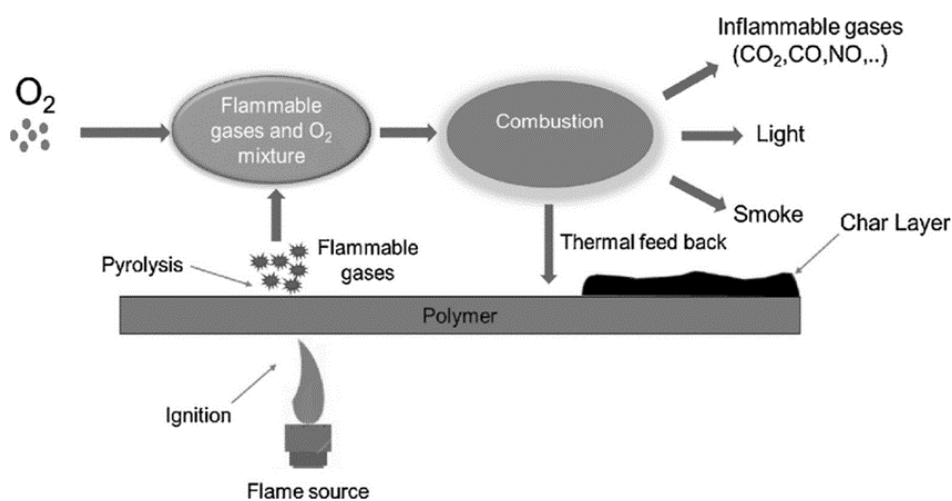


Figure 6.7 Polymer combustion mechanism

In the combustion of a polymer, in the specific case of polyurethane foams, there are four phases are distinguished:

1. *Preheating.*

Due to an external source, the polymer heats up according to the thermal intensity of the source, the thermal conductivity of the polymer and its specific heat. The moderate thermal conductivity of polyurethane foams results in a rapid increase in the temperature and critical conditions are quickly reached. In the range between 120-140°C, there is the release of moisture and other gases present.

2. *Decomposition.*

Under the critical conditions just described, weaker bonds are broken and the polymer begins to lose its characteristics: degradation begins. The initial depolymerization is followed by pyrolysis, due to which flammable gases such as hydrogen, methane, ethane and ethylene, and in parallel, a carbonaceous layer is formed on the polymer a carbonaceous layer called char. Parallel to pyrolysis, in the presence of oxygen, oxidation of the substrate can occur; in that case the material degrades at a rate that also depends on the diffusion of oxygen across the outer surface.

3. *Ignition.*

The amount of flammable gas produced increases as the degradation until the mixture falls within the flammable range. Ignition is also temperature-dependent, so depending on the presence or absence of an ignition source, the flash point and auto-ignition temperature are important.

4. *Combustion and propagation.*

The last stage is actual combustion in which new areas of the polymer are heated reaching the degradation temperature. The carbonaceous char is completely oxidized when about 510°C is reached. A combustion is called self-propagating if it continues even after removing the external ignition source; in this circumstance the heat that develops sustains both pyrolysis and combustion. If this does not occur, combustion dies out unless an external heat source is provided. The combustion process depends on several factors such as the rate of heat generation and heat transfer to the surface, the chemical structure and geometry of the surface, and the rate of decomposition. The extent of the flame is also related to the heat developed in the combustion of the polymer; the greater it is, the more heat the flame releases in sustaining the burning cycle.

### 6.3.2 Fire reaction characterization of polyurethane foams

There are different methods for characterizing the fire behavior of polymers and they allow to evaluate heat and matter transport to understand the contribution that the solid material provides to the fire when exposed to it. The different types of tests are related to the fact that there are three different regimes into which fire scenarios can be divided: ignition, for which it is necessary to understand the flammability of the material; propagation in which the main

parameters are flame spread and heat released; fire generalized in which factors such as load and flame penetration are important.

The small-scale tests that are usually used to characterize polyurethanes are the index of oxygen (LOI) and the cone calorimeter that relate to the ignition phase. The characterization of the fire behavior of polyurethane foams in the present work was done with both methods and they will be described below.

### 6.3.2.1 Limiting Oxygen index

According to ASTM D 2863, applied to perform the analysis, the oxygen index (Limiting Oxygen Index, LOI) is defined as the minimum amount of oxygen, in volumetric percent, in an oxygen-nitrogen mixture that can sustain combustion of a material under certain conditions. The oxygen index [%] is calculated according to (6.9):

$$LOI = \frac{100 \cdot O_2}{O_2 + N_2} \quad (6.9)$$

Where  $N_2$  and  $O_2$  are the volumetric fluxes [ $\text{cm}^3/\text{sec}$ ] of nitrogen and oxygen, respectively.

The specimens used to calculate the LOI of cellular polymers should be 125-150 mm and width and thickness of  $12 \pm 0.5$  mm.

The instrumentation needed to perform LOI are depicted in Figure 6.8.

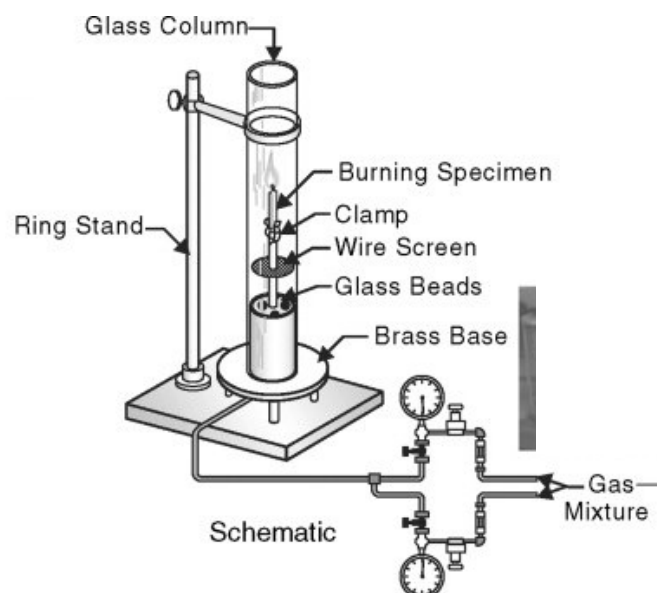


Figure 6.8 Limiting oxygen index apparatus

The specimen is placed in the clamp which is inside a glass column. By means of a torch fed with propane or other flammable gas, the specimen is ignited. The oxygen index is found by



changing the oxygen flow by trial and error until one found the one capable of sustaining combustion. If the index is less than 21%, it implies that combustion is self-sustaining in air; conversely if the index is above 21%. Polymers can be classified according to the oxygen index value: those whose value is between 21-26% are called low burning rate; those with a value above than 27% are called flame retardants; those with a value below 21 are called flammable.

### 6.3.2.2 Cone calorimetry

The cone calorimeter is one of the most extensively used and acknowledged methods for evaluating materials' fire performance. This instrument measures the key characteristics of combustion under controlled settings, providing useful information on a material's flammability, heat release rate (HRR), and overall fire behavior.

A cone calorimeter test involves exposing a tiny, flat sample of material (generally 100 mm × 100 mm) to a regulated external heat flux ranging from 10 to 100 kW/m<sup>2</sup>. The sample is positioned horizontally beneath a conical heating element, which evenly illuminates the surface. The name "cone calorimeter" refers to the conical shape of the heating source.

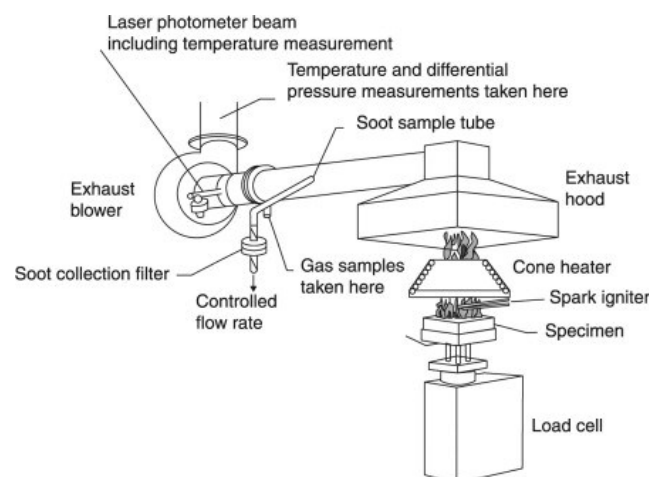


Figure 6.9 Typical cone calorimeter scheme

The following are the critical parameters that can be measured by the cone calorimetry analysis:

- *Heat Release Rate (HRR)*: the rate at which heat is emitted by the burning material is one of the most important fire testing criteria. Based on the idea that the rate of heat release is proportionate to the amount of oxygen used, it is commonly represented in kW/m<sup>2</sup> and is calculated by measuring the oxygen consumption during combustion.
- *Time to ignition (TTI)*: it is the duration of time between the start of the test and the onset of sustained ignition. It provides information on how long a material can be exposed to heat without igniting.

- *Total Heat Released (THR)*: by integrating the HRR during the course of the test, the total energy production during the combustion process is determined. MJ/m<sup>2</sup> is the usual unit of expression for this value.
- *Mass Loss Rate*: it is the mass of the material that reduces while it burns, and the mass loss rate (MLR) shows how quickly the fire is consuming the material. A load cell positioned underneath the sample is used to track this.
- *Smoke production*: it is the amount of smoke produced during combustion. This is a crucial metric for determining the safety of materials, particularly when it comes to fire scenarios where visibility and toxicity are concerns.
- *Effective Heat of Combustion (EHC)*: it measures how efficiently a material generates heat during combustion by estimating the total amount of heat produced per unit mass of material consumed.

To guarantee consistent and repeatable findings, the sample is conditioned in a controlled environment prior to the test (usually at 23°C and 50% relative humidity). After that, the sample is placed on a support underneath the conical heater. The external heat flux is applied, and the key parameters listed above are continually monitored. Usually, the test goes on until all of the material has been burned or until no further combustion takes place.

## 6.4 Thermal characterization.

### 6.4.1 Thermogravimetric analysis (TGA)

Thermal characterization of polyurethane foams was carried out by means of thermogravimetric analysis conducted in this thesis work with the TGA-SDT Q650, shown in Figure 6.10.



Figure 6.10 TA Instruments TGA SDT Q650

During this analysis, the sample is subjected to controlled heating and it is evaluated through a precision balance how the weight changes over time. The sample is located inside a furnace with a controlled atmosphere that can be either inert, for which nitrogen is sent, or oxidizing, for which air is sent. The sample can undergo either isothermal analysis, whereby the

temperature is kept constant, or to dynamic analysis, in which the temperature is made to rise at a rate programmed. Through TGA, the polymer can be characterized in several ways; thus, it can evaluate the content of volatiles, the temperature at which the polymer begins to decompose (onset), the content of inorganic substances, the effectiveness of flame retardants, etc.

It is important to be careful to set certain parameters in the realization of the thermogravimetric so that it is not distorted:

- the heating rate should not be too high because in this case the decomposition temperatures are higher;
- problems concerning heat transport can be created when the mass and sample size are too large, at the same time these must be sufficiently large to ensure the representativeness of the sample;
- the carrier gas flow must be large enough to allow the transport fast of the volatile products that develop so as to avoid secondary reactions but not too high to avoid disturbing degradation.



# Chapter 7

## Lignin Liquefaction

In the following chapter the procedure to produce the final polyol, starting from lignocellulosic biomass, will be presented. The objective of this study is the optimization of the final product investigating how the main parameters will affect its properties. This can be done by setting up a design of experiment (DoE). The optimized bio-polyol will be used for the synthesis of the flexible polyurethane's foams.

### 7.1 Lignin liquefaction methodology

As it been said in the previous chapters, the lignocellulosic polyols' production will be made by means of microwaves. The very first experimental phase was spent selecting and fine-tuning the liquefaction technique within the microwave reactor.

The microwave reactor is equipped with three cylindrical reactors, a total mass of 15 g of lignin and 75 g of solvent is divided equally among them. The solvent consists of a mixture of Emerox® polyols and glycerol. A catalyst (sulfuric acid or sodium hydroxide) is then added, and the reaction is ready to begin. After twenty minutes, the reaction product exhibited the formation of solid clumps and layers of solidified polyol on the upper and lower parts of the reaction mixture. This issue is closely related to inadequate mixing of the reagents. Although the reactors are equipped with a magnetic stirrer, it alone is not sufficient to homogenize the reactive mixture. Therefore, a pre-mixing step, which can also be performed manually, is necessary. The lignin and the solvent are placed in a beaker and initially mixed using a magnetic stirrer or a glass rod. Once the solution is homogeneous, the catalyst is added and mixed again. The resulting reactive mixture is then evenly distributed among the three reactors and exposed to microwave irradiation at 150°C for different reaction minutes. The final product obtained is a black-brownish coloured liquid. The yield, expressed as the solid lignin residue, played a crucial role in determining the optimal polyol. Issues related to this parameter involve the amount of solvent to use during washing, as a lack of solvent causes non-solvated polyol to deposit on the filter. Several studies have reported that the optimal quantities for the extraction solvent are 10 times the volume of the sample, but our experimental trails have shown that it is possible to reduce this ratio to 4:1.

## 7.2 Lignin screening

There are various types of lignin available on the market (Kraft, liginosulfonate, alkaline, and organosolv), each derived from different paper industries and differing in terms of extraction method and purity. For this study, nine types of lignin were used, see Table 7.1.

Table 7.1 Experimental set-up for different types of lignin

| LIGNIN TYPE           | TEMPERATURE [°C] | SOLVENT [1:5 ratio with respect to lignin] | CATALYST [%w on solvent basis]    | EXTRACTION SOLVENT | YIELD  |
|-----------------------|------------------|--|-----------------------------------|--------------------|--------|
| Lignin Alkaline TCI   | 150              | Emerox® 14535/glycerol (70/30)             | H <sub>2</sub> SO <sub>4</sub> 3% | Acetone            | 28%    |
| Lignin Dealkaline TCI | 150              | Emerox® 14535/glycerol (70/30)             | H <sub>2</sub> SO <sub>4</sub> 3% | Acetone            | 62%    |
| Borresperse CA        | 150              | Emerox® 14535/glycerol (70/30)             | H <sub>2</sub> SO <sub>4</sub> 3% | Acetone            | 70%    |
| Indulin AT            | 150              | Emerox® 14535/glycerol (70/30)             | H <sub>2</sub> SO <sub>4</sub> 3% | Acetone            | 99,85% |
| Reax 88A              | 150              | Emerox® 14535/glycerol (70/30)             | H <sub>2</sub> SO <sub>4</sub> 3% | Acetone            | -11%   |
| Reax 100M             | 150              | Emerox® 14535/glycerol (70/30)             | H <sub>2</sub> SO <sub>4</sub> 3% | Acetone            | 35%    |
| Polyfon O             | 150              | Emerox® 14535/glycerol (70/30)             | H <sub>2</sub> SO <sub>4</sub> 3% | Acetone            | 29%    |
| Polyfon T             | 150              | Emerox® 14535/glycerol (70/30)             | H <sub>2</sub> SO <sub>4</sub> 3% | Acetone            | 7%     |

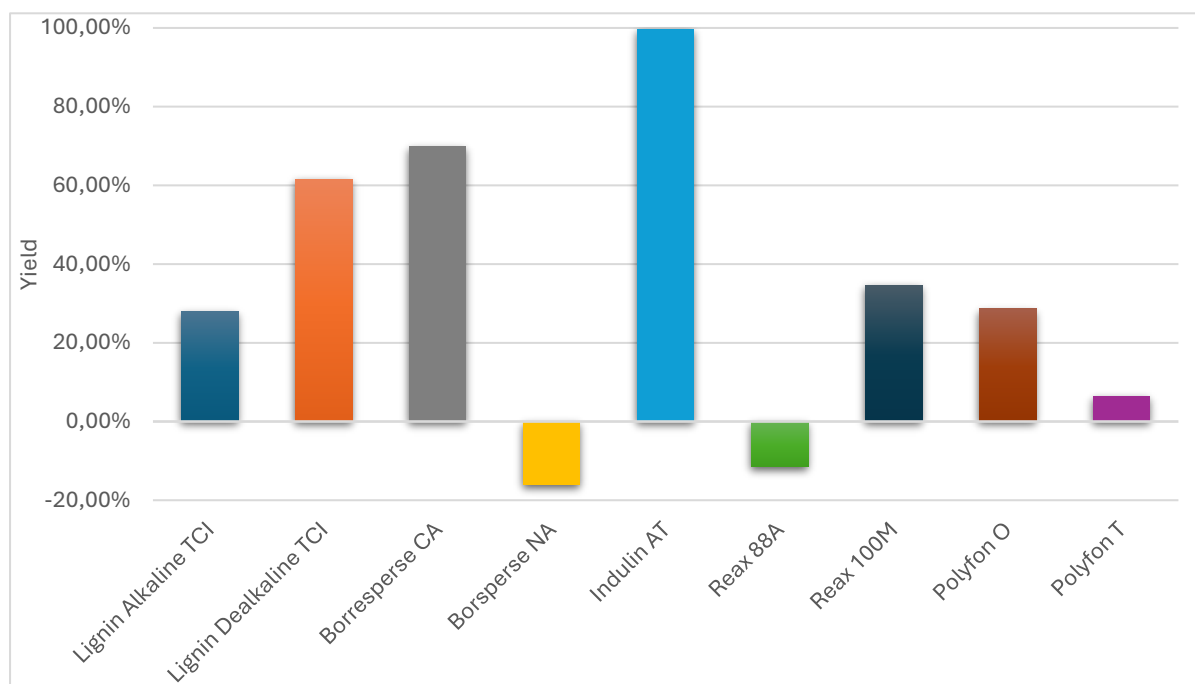


Figure 7.1 Yield for the different types of lignin calculated with the same experimental setup and condition

All experiments were performed with the same methodology and conditions to understand how different types of lignin responded to liquefaction in a solvent such as the Emerox®. Observing the tabulated yield values, only three types of lignin showed values above 50%, respectively Lignin Dealkaline TCI, Borresperse CA and Indulin AT. It is noteworthy that Reax 88A and Borresperse NA lignin resulted in negative yield values; from a mathematical point of view, this has no meaning but is justified by the fact that under certain conditions, rather than depolymerization reactions, the trend is reversed, and polycondensation phenomena occur, resulting in the accumulation of lignin and polyol on the filter paper.

In order to explain the differences in yield obtained by the latter experiments, various observations can be made regarding the inherent characteristic of the different types of lignin. No particular effect can be related to the position of the sulfonic group: for example, in Reax®100M they are on the aromatic ring and along the aliphatic side chain while in Polyfon® O they are bonded only on the aliphatic side chain. However, as it can be seen from Figure 7.1 their yields are similar. Nevertheless, some authors<sup>39</sup> also have hypothesized that the sulfonic groups, which increase the solubility in water, and so in the polyols, for alkaline pH values<sup>50</sup>, act like sulfuric acid, which is the catalyst of the liquefaction process, so the increase in their concentration makes the recondensation reactions more likely to occur.

A possible influence on the reaction yield could be related to the lignin's pH: indeed, yield values less than 40% there are obtained for the alkaline pH lignin, i.e., Polyfon®T, Polyfon®O, Reax®100M and alkaline lignin (TCI); yield ranging from 60% to 75% are achieved by the “acid” lignin, while the maximum yield is reached for neutral lignins, which can lead to

yield over 99%; despite this, Reax ®88A does not seem to follow this scheme.

Crucial role in the reaction yield is also played by the molecular weight distribution (MWD), that can be inferred considering the difference between the number average molecular weight (MW<sub>n</sub>), the weight average molecular weight (MW<sub>w</sub>) and the Z-average molecular weight (MW<sub>z</sub>): the larger the difference, the broader the MWD. Thus, given that the Indulin ® AT has the narrowest molecular weight distribution, namely it has lower amount of high MW fractions, it is reasonable to achieve higher yield in low molecular weight products.

### 7.3 Effects of the liquefaction solvent

The choice of liquefaction solvent is undoubtedly a crucial point, as several parameters must be considered, such as hydroxyl number, functionality, viscosity, and molecular weight. Two Emerox® polyols from the manufacturer Emery Oleochemicals, specifically 14535XP and 14511, were chosen because they were the only ones with hydroxyl values below 400mgKOH/g, specifically 355 and 106-114 mgKOH/g, respectively, and relatively low viscosity, allowing for easy mixing during liquefaction and adequate flowing during the final foaming stage. Both polyols have a functionality of 2. To evaluate the performance of the two solvents, all conditions for liquefaction were kept constant: the solvent-lignin ratio of 5:1, the amount of acidic catalyst equal to 3% in weight relative to the solvent, and the operating conditions set at temperature of 150°C and a reaction time of 20 minutes. The choice of these conditions is based on previous studies<sup>39</sup> in which it is confirmed that polycondensation reactions are less favoured, thus the depolymerization reactions are more likely to occur.

From a preliminary analysis, it is expected that the experimental hydroxyl number values will be lower for polyols produced starting from Emerox® 14511, because of the lower hydroxyl number (nOH) of the solvent mixture: indeed, comparing the two experiments conducted under the same conditions but with different bio-polyol, it was found to be almost halved.

*Table 7.2 Experimental condition and results of lignin liquefaction using different solvent*

| LIGNIN TYPE | TEMPERATURE [°C] | SOLVENT [1:5 ratio with respect to lignin] | CATALYST [%w on solvent basis]    | EXTRACTION SOLVENT | YIELD  | nOH   |
|-------------|------------------|--|-----------------------------------|--------------------|--------|-------|
| Indulin AT  | 150              | Emerox® 14535XP/glycerol (70/30)           | H <sub>2</sub> SO <sub>4</sub> 3% | Acetone            | 99,85% | 428,5 |
| Indulin AT  | 150              | Emerox® 14511/glycerol (70/30)             | H <sub>2</sub> SO <sub>4</sub> 3% | Acetone            | 99,98% | 251   |

From the above data the decrease of the hydroxyl value can be highlight; this is an important result for the synthesis of the flexible foams, since polyols with low nOH are needed.



## 7.4 Solvent/glycerol ratio

As mentioned in previous sections, a 5:1 ratio between solvent and lignin is maintained in the reaction. The solvent itself consists of Emerox® polyol and glycerol. Previous studies<sup>37,38</sup> have shown that increasing the percentage of glycerol increases the overall yield of the reaction; however, the hydroxyl number of the final polyol also increases, as the hydroxyl number of glycerol is 1800 mgKOH/g. To synthesize flexible polyurethane foams, it is necessary to have the lowest possible hydroxyl number, with an upper limit of approximately 300 mgKOH/g. It is therefore evident that the amount of glycerol in the solvent mixture must be limited without significantly reducing the yield of the liquefaction reaction.

For this reason, four experiments were performed varying the amount of glycerol from 0-30% by weight. The reaction conditions and the other reactants were kept constant. The experiments involved microwave irradiation for 20 minutes at 150°C of 15 g of Indulin AT lignin, 75 g of solvent, and 3% by weight of sulfuric acid as a catalyst.

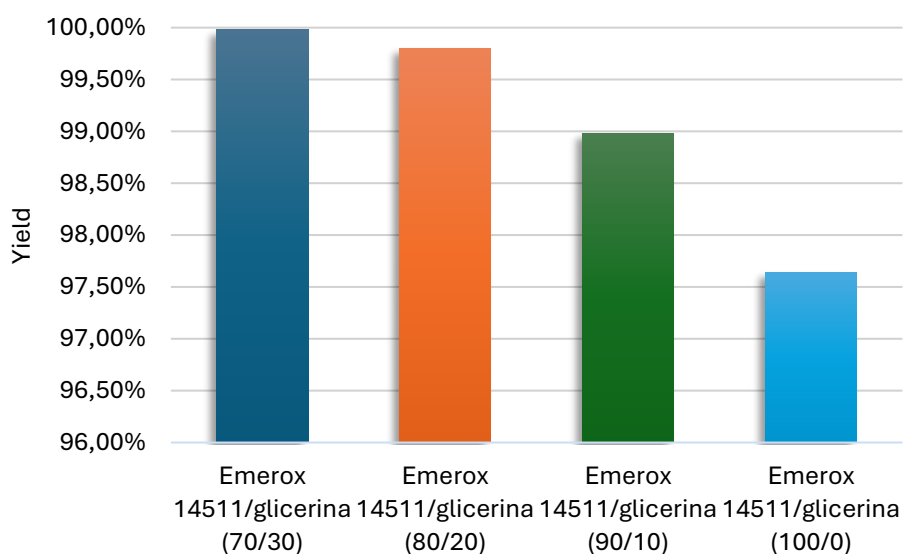


Figure 7.2 Yield histogram for the different percentage content of Emerox® 14511

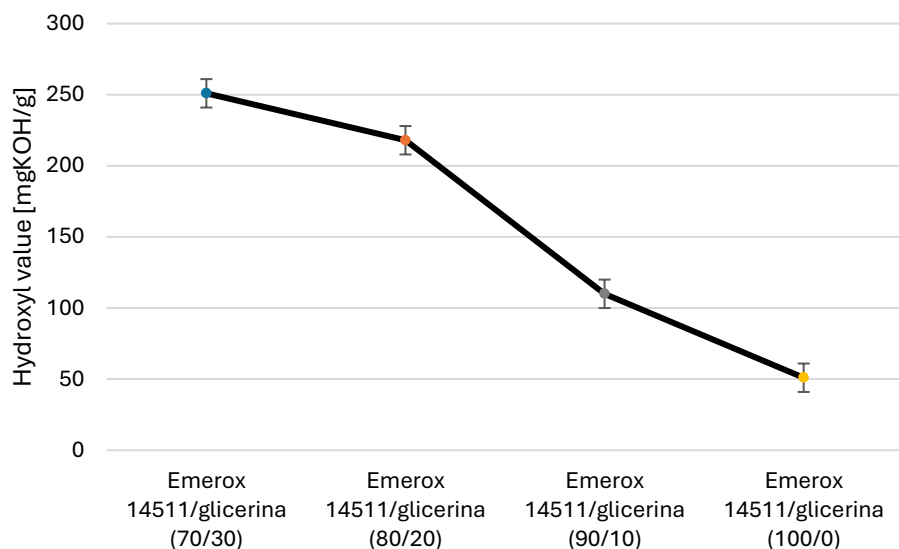


Figure 7.3 Hydroxyl values as the percentage of Emerox® 14511 varies

As expected, there is a decrease, even if not drastic, in yield, which however, still remains above 98%, and a reduction in the hydroxyl number with decreasing glycerol content; in particular, the lowest one results to be five times smaller than that obtained with 30% by weight of glycerin.

## 7.5 Type of catalyst

It is known from the literature<sup>43,51</sup> that lignin liquefaction can be catalysed in either acidic or basic environment. The two most commonly used substances are sulfuric acid and sodium hydroxide. The use of these catalysts has both advantages and disadvantages. Regarding acid catalysis, depolymerization reactions predominate with respect to condensation ones, and yield evaluation is facilitated because filtration is performed using acetone as a washing solvent. However, during the foam formation phase, the acidity of the mixture can lead to higher consumption of (basic) catalysts, reducing cost-effectiveness and compromising the stability of the foam itself. For this reason, a basic catalyst was also considered and tested in the liquefaction phase since it would not interfere with the foaming catalysis. The main problem is the washing solvent used during filtration. According to the literature<sup>52</sup>, a 1:4 mixture of dioxane and water is used, but the evident toxicity problems associated with this substance have prompted the search for substitutes, as it will be explained in the following.

### 7.5.1 Acid Catalysis

As mentioned earlier, the main issue related to the use of an acid catalyst, specifically sulfuric acid, is the interference that it can cause during the synthesis of polyurethane foams. Despite

it is known from the literature that 3% by weight relative to the solvent is the optimal concentration for obtaining a polyol with the desired characteristics and high yields<sup>53</sup>, it was attempted to reduce its concentration to 1% by weight. To optimize yield values and hydroxyl numbers, eight total tests were compared, differing only in the concentration of the acid used; thus, reaction times, temperatures, and reagents were kept the same, specifically at 20 minutes and 150°C. Again, a range of liquefaction solvent compositions was covered from 70% to 100% of Emerox® 14511.

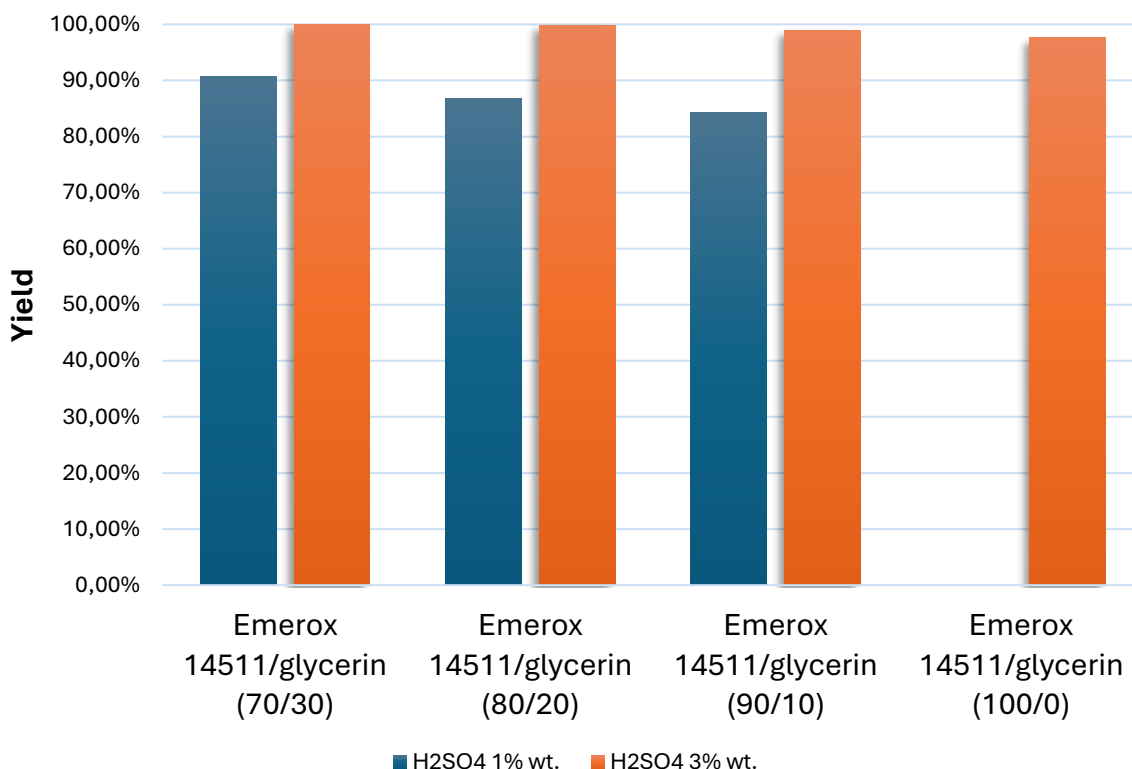


Figure 7.4 Liquefaction yield at 1% and 3% concentration of sulfuric acid

The first observation from the graph above is about the reduction in yield associated with the decrease in catalyst concentration. Nevertheless, yields are still above 90%, except in the test with 20% glycerol, where the yield is slightly lower, but higher than 85%. Another important consideration is the impossibility of liquefying lignin using only Emerox® and an acid concentration of 1% by weight. This is because of the decrease in glycerin and catalyst content, which are both very effective in promoting liquefaction. Further considerations can be made by looking at the hydroxyl number reported in the figure below.

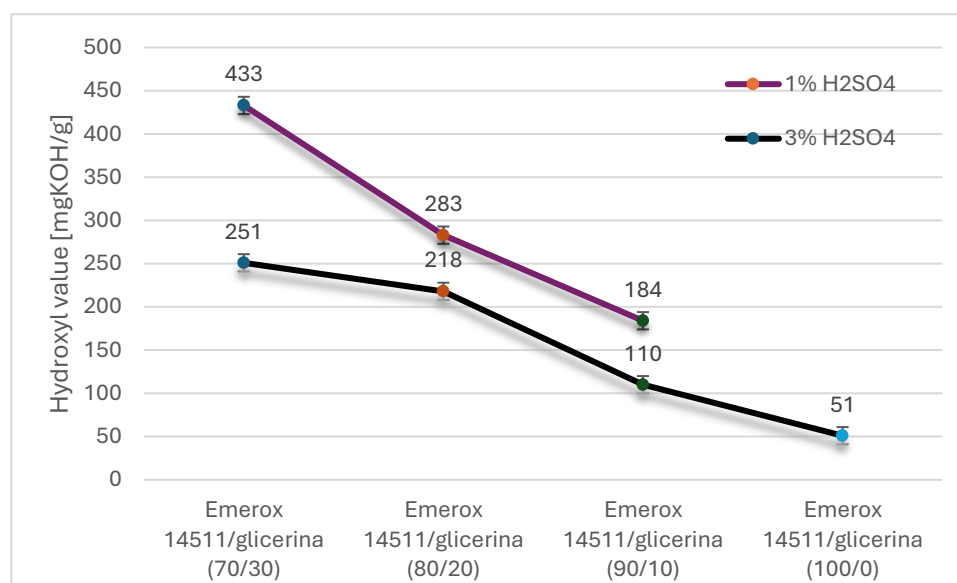


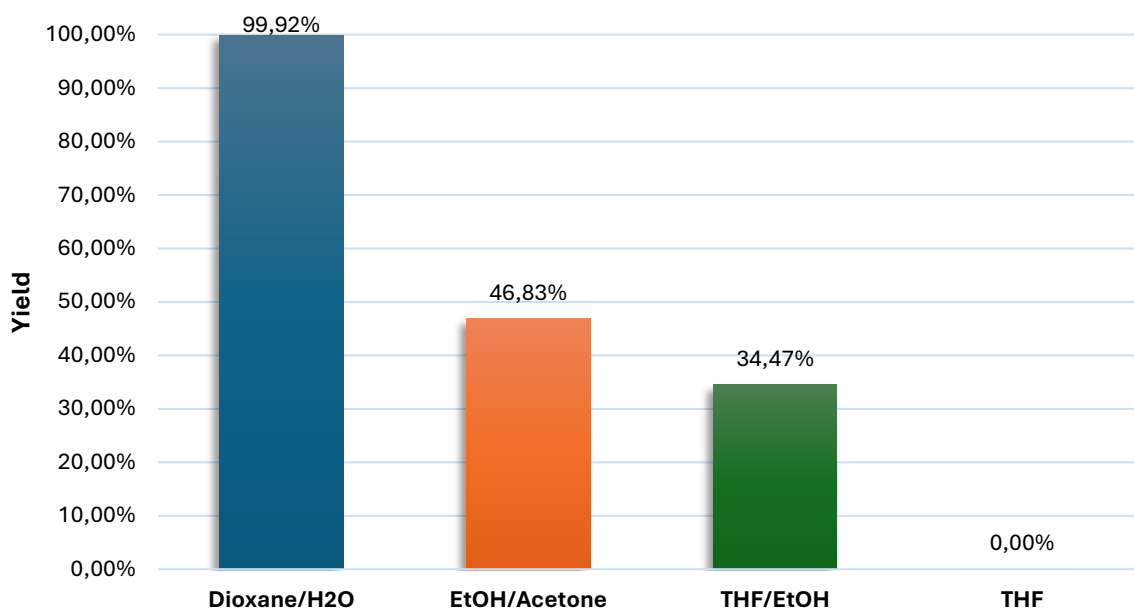
Figure 7.5 Hydroxyl value as the concentration of Emerox® and sulfuric acid

Looking at the graph above, it is evident that in all cases where 1% sulfuric acid was used, the hydroxyl number is higher, indicating that liquefaction is less efficient. Despite this, the experiment employing 20% glycerol proves to be a possible candidate to produce flexible polyurethane foams.

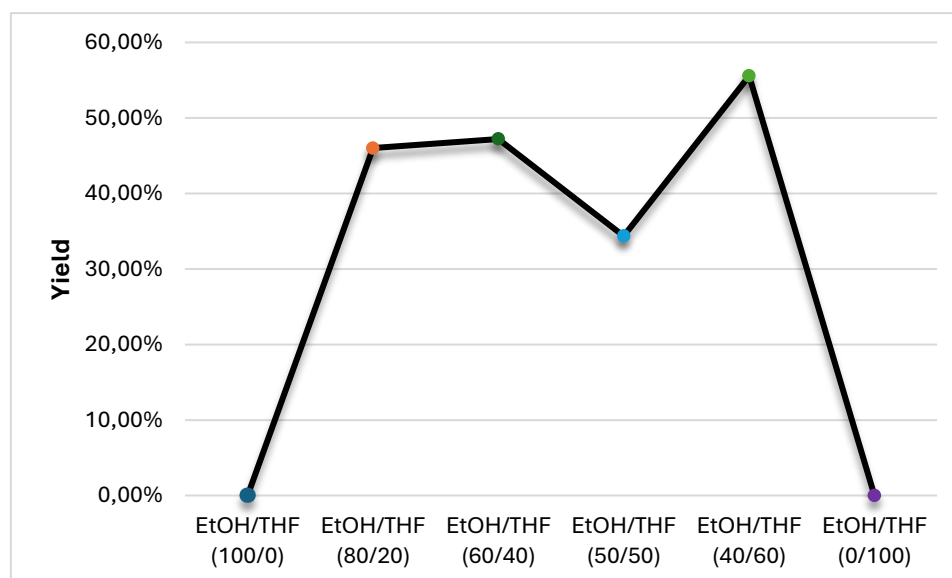
### 7.5.2 Basic catalyst

In order to solve the low pH of the polyol when it is produced by using an acid catalyst, several tests were carried out using a basic catalyst, specifically the sodium hydroxide. There are relatively few studies on the liquefaction of lignin in a basic environment<sup>52</sup>, even though this offers various benefits during foaming process, in terms of cost-effectiveness and also the production of less corrosive substances. For this purpose, the standard set of conditions used in the initial experimental trials was maintained, keeping the Emerox®/glycerol ratio at 70/30% by weight and 3% by weight, relative to the solvent, of catalyst. This first experiment was not successful because it showed the formation of solid agglomerates in the reactor. Thus, the polyol/glycerol ratio was then changed to 50/50% by weight, and a liquid product was obtained. According to studies<sup>52</sup> in the literature, to calculate the yield, a diluted dioxane solution with water is used as a washing solvent. It is known that dioxane has been identified as a potentially carcinogenic substance, so an attempt was made to find a possible substitute. Various washing tests were conducted with different solvents, including acetone, EtOH/acetone mixtures, and THF/EtOH at different ratios; these mixtures have been chosen because of their solubility parameter (defined by Hildebrand<sup>54</sup>), also known as  $\delta$ -value,  $\delta = (-E/v^1)^{\frac{1}{2}}$ , the term  $-E$  represents the energy of vaporization at zero pressure, while  $v^1$  is the liquid molal volume. Only with the latter it was possible to achieve measured yields between 50-60%, but they are lower

than those obtained with the dioxane mixture; this is due to the low solubility of the lignin in these mixtures, not to the effectiveness of the process. Moreover, because of the high content of glycerin required with basic catalyst, the hydroxyl number of the final polyol shows a value incompatible with the synthesis of flexible polyurethane foams, which should be less than 300 mgKOH/g.



a)



b)

Figure 7.6 a) Effect of different extraction solvent on yield, b) effect of different ethanol-THF ratio on the yield

## 7.6 Design of experiment

All studies done up to this point, aimed at understanding how the type and amount of solvent, catalytic environment, and lignin type affects lignin liquefaction for the polyol production, have served as a screening phase to optimize the synthesis of the new bio-polyol. A design of experiment (DOE) was therefore applied to the current study. The optimization objectives for the new polyol were primarily twofold: to maximize liquefaction yield and minimize the hydroxyl number. As seen in the previous sections, however, the yield of reactions involving Indulin AT lignin is above 98%, so further attempts to maximize an already high parameter would bring minimal benefits. Therefore, the focus was placed on minimizing the hydroxyl number. With the aid of Minitab software, a multilevel factorial design with four factors was generated. Based on the previous results, a constant weight (3%) of acid catalyst has been used, while the variable representing the percentages of Emerox® 14511 in the Emerox®/Glycerol solvent mixture was not considered as a continuous variable but rather a categorical variable, preventing subsequent alterations in the ratios of this variable.

*Table 7.3 Factors and level of the DOE multilevel factorial design*

|   | LEVEL 1 | LEVEL 2 | LEVEL 3 |
|---|---------|---------|---------|
| <b>EMEROX®<br/>14511/GLYCEROL<br/>[%W/%W]</b> | 80/20   | 90/10   | 100/0   |
| <b>TEMPERATURE [C]</b>                        | /       | 150     | 170     |
| <b>TIME [MIN]</b>                             | 5       | 10      | 20      |

Using the combination of the parameters listed above, the software provided a set of 18 reactions. For each reaction, yield and hydroxyl number were calculated according to the procedures outlined in the previous sections.

Table 7.4 Design of experiment generated by Minitab

| Run Order | Emerox®/Glycerol<br>[%w/%w] | Catalyst<br>[%w] | Temperature<br>[°C] | Time<br>[min] |
|-----------|-----------------------------|------------------|---------------------|---------------|
| 1         | 80/20                       | 3                | 170                 | 10            |
| 2         | 90/10                       | 3                | 150                 | 10            |
| 3         | 100/0                       | 3                | 170                 | 5             |
| 4         | 100/0                       | 3                | 170                 | 10            |
| 5         | 80/20                       | 3                | 150                 | 10            |
| 6         | 90/10                       | 3                | 170                 | 10            |
| 7         | 100/0                       | 3                | 170                 | 20            |
| 8         | 100/0                       | 3                | 150                 | 10            |
| 9         | 80/20                       | 3                | 170                 | 20            |
| 10        | 80/20                       | 3                | 150                 | 5             |
| 11        | 90/10                       | 3                | 170                 | 5             |
| 12        | 90/10                       | 3                | 150                 | 5             |
| 13        | 90/10                       | 3                | 170                 | 20            |
| 14        | 80/20                       | 3                | 170                 | 5             |
| 15        | 90/10                       | 3                | 150                 | 20            |
| 16        | 100/0                       | 3                | 150                 | 5             |
| 17        | 100/0                       | 3                | 150                 | 20            |
| 18        | 80/20                       | 3                | 150                 | 20            |

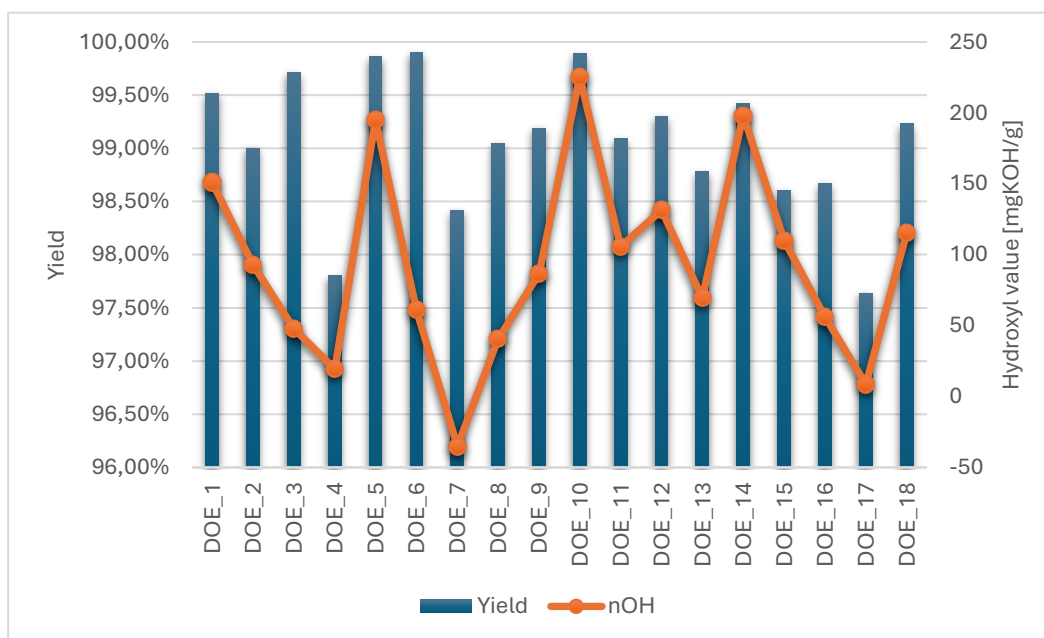


Figure 7.7 Yield and Hydroxyl value of the design of experiment

As shown in the graph above (Figure 7.7), yields are greater than 97.5%, confirming that optimizing this parameter would not bring significant benefits. In contrast, the hydroxyl

number, when compared to that of virgin industrial polyol (28 mgKOH/g), shows considerable variability. It is worth pointing out that there is a negative hydroxyl number value, which, although it has no physical meaning, could be due to the non-depolymerization of lignin. For subsequent DOE analyses, this test (number 7) was excluded.

After obtaining yield and hydroxyl values for all tests, the DOE response surface was analysed, and the backward elimination method was chosen with an alpha factor of 5% (i.e.,  $p < 0.05$ ) and, consequently, a confidence level of 95%. Recall that the alpha factor represents the significance level of a variable or interaction. The model summary is reported below:

Table 7.5 Linear regression equations resulting from the model

| Emerox® 14511/Glycerol | Regression equation  |
|------------------------|--|
| 80/20                  | $nOH = 431.6 - 1.148 \cdot Temperature - 7.369 \cdot Time$ |
| 90/10                  | $nOH = 303.2 - 1.148 \cdot Temperature - 2.50 \cdot Time$  |
| 100/0                  | $nOH = 248.7 - 1.148 \cdot Temperature - 3.104 \cdot Time$ |

$$\begin{aligned}
 nOH = & 327.8 - 1.148 \cdot Temperature - 4.326 \cdot Time + 103.77 \cdot EM / GLY_{80} - 24.64 \cdot EM / GLY_{90} \\
 & - 79.13 \cdot EM / GLY_{100} - 3.043 \cdot Time \cdot EM / GLY_{80} + 1.821 \cdot Time \cdot EM / GLY_{90} \\
 & + 1.221 \cdot Time \cdot EM / GLY_{100}
 \end{aligned} \tag{7.1}$$

The Table 7.5 Table 7.5 Linear regression equations resulting from the model shows the regression equations for each categorical variable, while equation (7.1) collects all the categorical variable in just one *regression equation*. The absence of second and higher-degree terms in all three equations indicates a linear trend.

For the purposes of the study, the variable representing the percentages of Emerox® 14511 in the Emerox®/Glycerol solvent mixture was not considered as a continuous variable but rather a categorical variable, preventing subsequent alterations in the ratios of this variable.

Table 7.6 Main characteristic of the DOE model response surface

| S       | R-sq   | R-sq(adj) | R-sq(pred) |
|---------|--------|-----------|------------|
| 12,5142 | 97,87% | 96,59%    | 84,89%     |

This model shows an R-sq (adj) factor above 95%, indicating high reliability of the model in providing a significant explanation of the observed variations, with value close to 85% for the model's predictive factor.

From the Pareto chart, analysing the hydroxyl number as the response, it is evident that among



all possible interactions, the only one significant within the model is between *Time* and the variable indicating the ratio of Emerox® 14511 to glycerol, see equation (7.1).

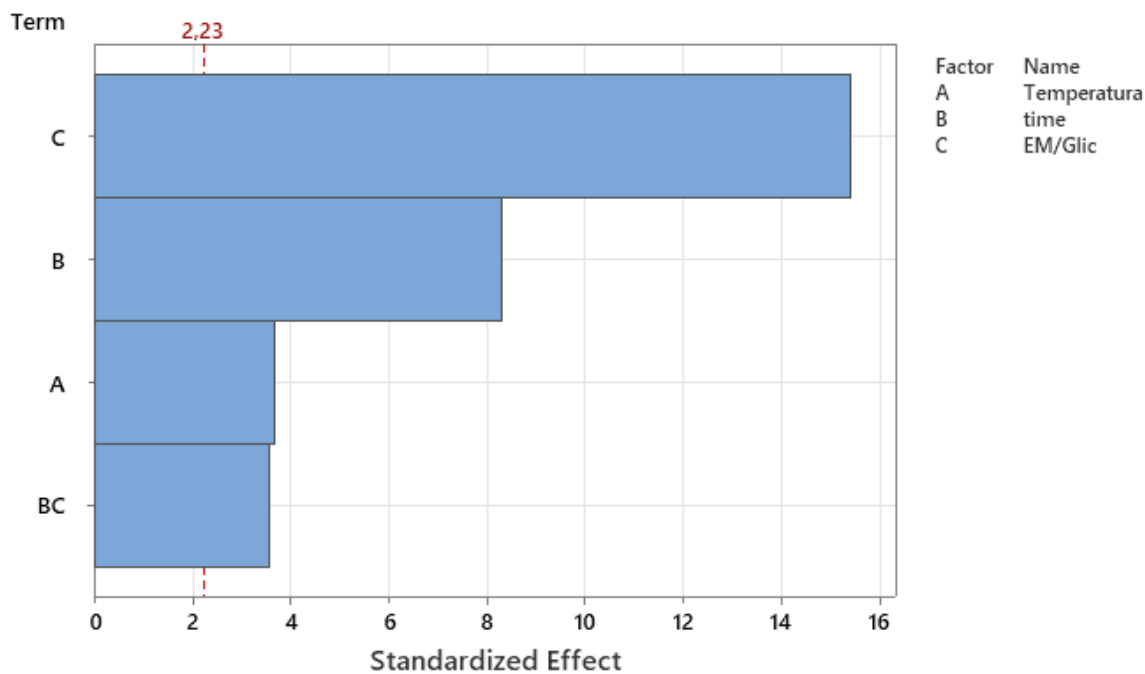


Figure 7.8 Pareto chart of the response surface model

Below there are the graphs related to the residual analysis.

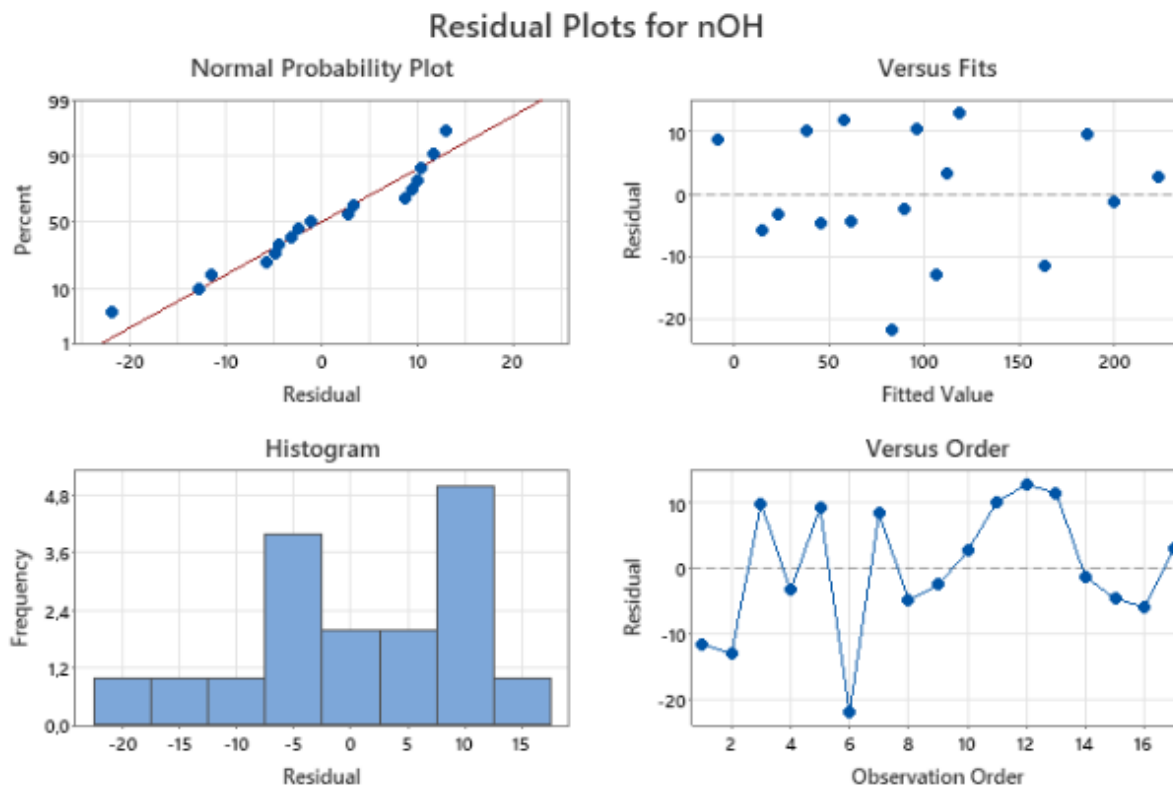


Figure 7.9 Residual plots for the response surface model

Starting from the normal probability plot, it can be seen that the points follow the line, suggesting that the residuals are normalized; however, some outliers are present, appearing to deviate from the normality conditions. Observing the Versus Fits plot, no particular patterns are noticeable, and the residuals appear to be well distributed around zero, indicating that the model is appropriate. Regarding the histogram, the distribution is neither normal nor symmetrical, likely due to the presence of outliers, as observed in the first graph. In the last graph, the Versus Order plot, a trend is observed towards the end, indicating the presence of correlation with the sequential order of observations, suggesting the presence of non-random effects over time. Overall, the model appears to be appropriate, but there might be slight violations of normality or independence of variables that should be considered.

### 7.6.1 Hydroxyl number optimization

After analyzing the response surface of the model, the next step is to optimize the response. Specifically, this involves minimizing the hydroxyl value since the ultimate goal of this work is to synthesize flexible polyurethane foams, which require the lowest possible number.

It was decided to set the target value to that of the petroleum-based polyol, specifically the PM6000 polyol, which has a hydroxyl number of 28 mgKOH/g. Minitab provided the following five solutions for the optimization problem:

Table 7.7 Optimal conditions set for achieving the requested hydroxyl value

| Solution | Temperature [C] | Time [min] | Emerox®/Glycerol [%w/%w] | nOH Fit [mgKOH/g] | Composite Desirability |
|----------|-----------------|------------|--------------------------|-------------------|------------------------|
| 1        | 160,000         | 11,9276    | 100                      | 28,0000           | 1,00000                |
| 2        | 150,000         | 15,6254    | 100                      | 28,0000           | 1,00000                |
| 3        | 168,068         | 8,9441     | 100                      | 28,0000           | 1,00000                |
| 4        | 170,000         | 5,9324     | 100                      | 35,1318           | 0,96385                |
| 5        | 153,493         | 5,0370     | 100                      | 56,8603           | 0,85372                |

The parameters that minimize the response are as follows, as can be noted, the first of the five proposed solutions was chosen:

Table 7.8 Chosen variable in order to achieve the optimal hydroxyl value

| Variable        | Value   |
|-----------------|---------|
| Temperature [C] | 160     |
| Time [min]      | 11,9276 |
| EM/Glic [%w/%w] | 100     |

Table 7.9 Confidence and probability intervals relative to the first solution proposed

| Response | Fit   | SE Fit | 95% CI         | 95% PI         |
|----------|-------|--------|----------------|----------------|
| nOH      | 28,00 | 5,11   | (16,61; 39,39) | (-2,12; 58,12) |

In the Table 7.9, two intervals can be seen: the first is the confidence interval, within which the response has a 95% probability of falling. A similar argument can be made for the second interval, which represents the prediction interval of the response.

Table 7.10 Experimental setup and calculated hydroxyl numbers of the optimal polyol and for the two experiments used to check the validity of the model

| ID             | Emerox®/glycerin | Temperature | Time | nOH  |
|----------------|------------------|-------------|------|------|
| <b>Optimal</b> | 100/0            | 160         | 12   | 38.1 |
| <b>Check 1</b> | 100/0            | 168         | 9    | 30.2 |
| <b>Check 2</b> | 100/0            | 160         | 7.5  | 36.3 |

As shown in the Table 7.10, which reports the experimental conditions of the tests performed, the hydroxyl values obtained fall within the 95% confidence interval. To check the reliability of the model, other two tests were carried out; different nOH have been tested. As can be seen in Table 7.10, these tests show the experimental values fall within the confidence interval because the values obtained are 30.2 and 36.3 mgKOH/g.

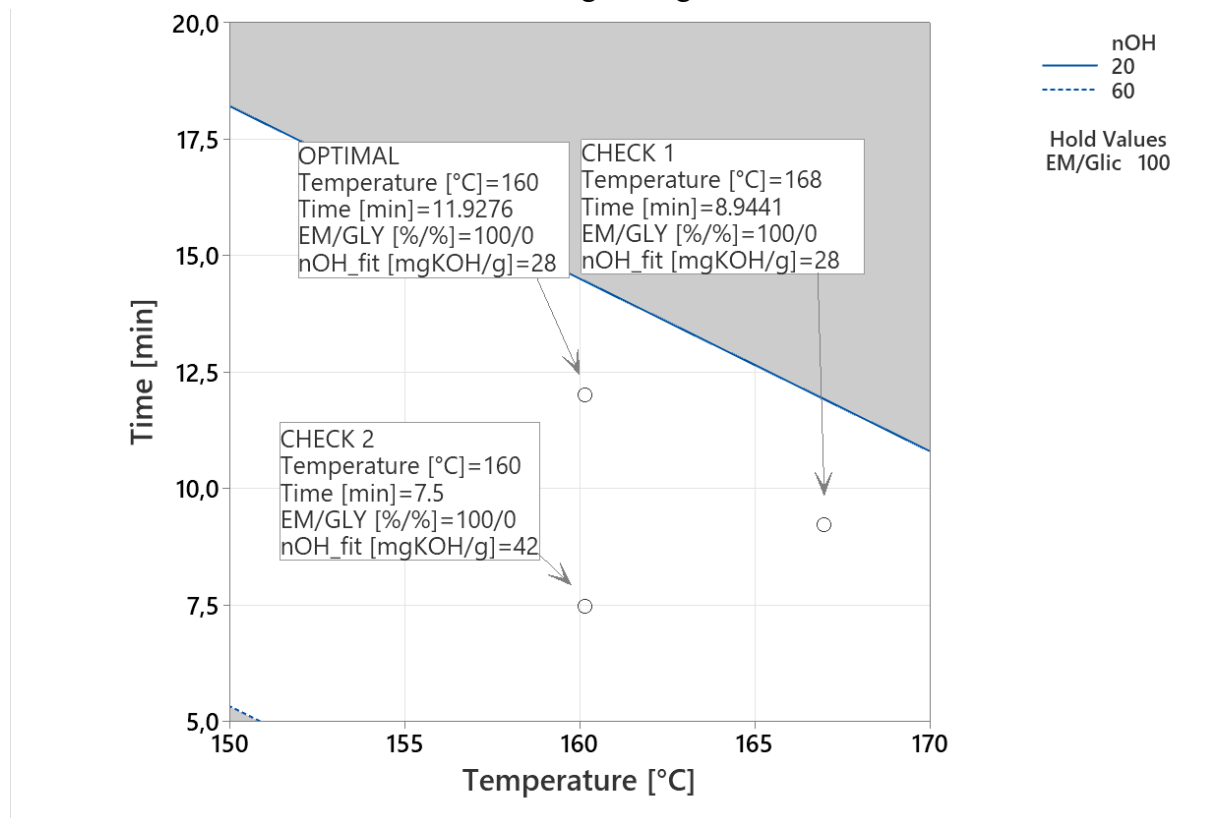


Figure 7.10 Contour plot for the hydroxyl value response

## 7.7 Gel permeation chromatography analysis

It is known from the data give by the manufacture that the lignin Indulin AT has an average molecular weight of 4500 g/mol. Thus, it has been decided to perform a gel permeation chromatography in order to verify the efficiency of the lignin liquefaction process through microwave. First of all, the sample must be prepared, so in a 10 mL flask must be weighted 0.02 g of lignin-based polyol, which will be dissolved in 5 g of THF, which is the eluent.

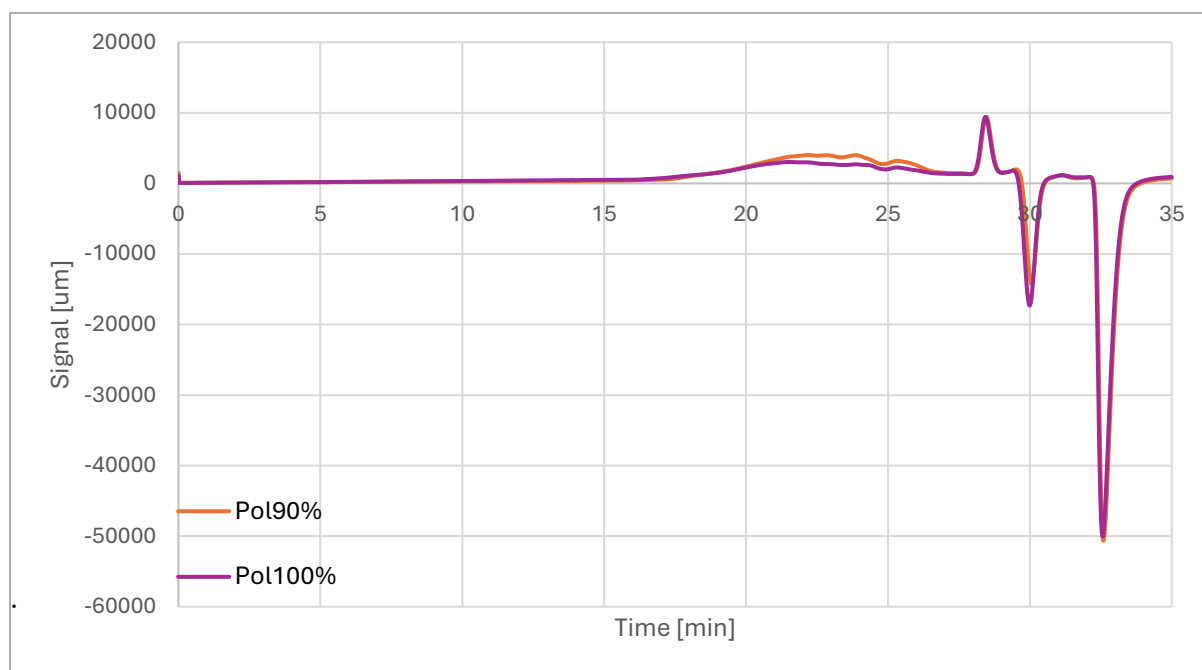


Figure 7.11 Chromatogram of the two lignin based polyols used as starting point for the design of experiment

The graph showed above represents the chromatograms of the bio-polyol with 100% of Emerox® 14511 and the bio-polyol containing the 90% of Emerox® 14511 and 10% by weight of glycerol. The Pol100% has a slightly higher molecular weight compared to the Pol90%, see Figure 7.11, this is due to the presence of glycerol which makes more efficient the liquefaction of lignin.

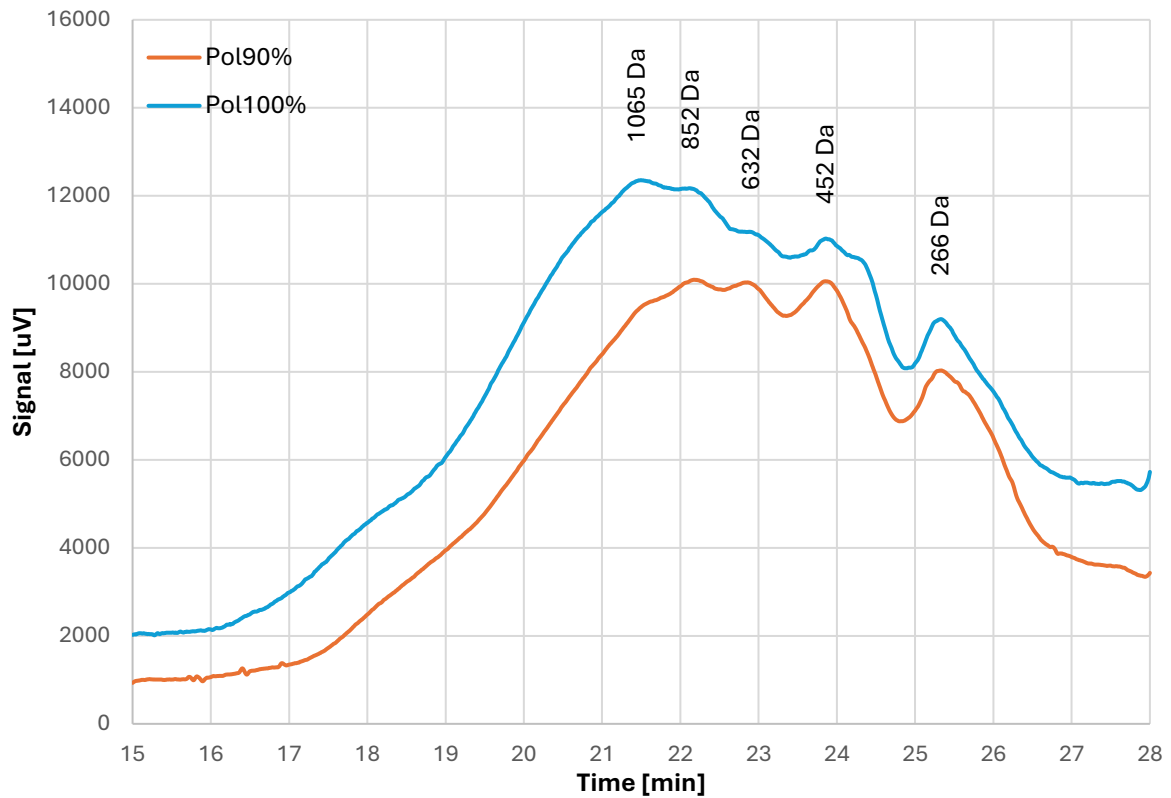


Figure 7.12 Magnification of the two lignin base polyols, namely the one with 100% Emerox 14511 and the other with 90% of Emerox 14511 and 10% of glycerol

From the graph reported in Figure 7.13 is interesting noticed how the time affects the molecular weight distribution. The general trend seems to be maintained along the time but the concentration of lighter molecules increases.

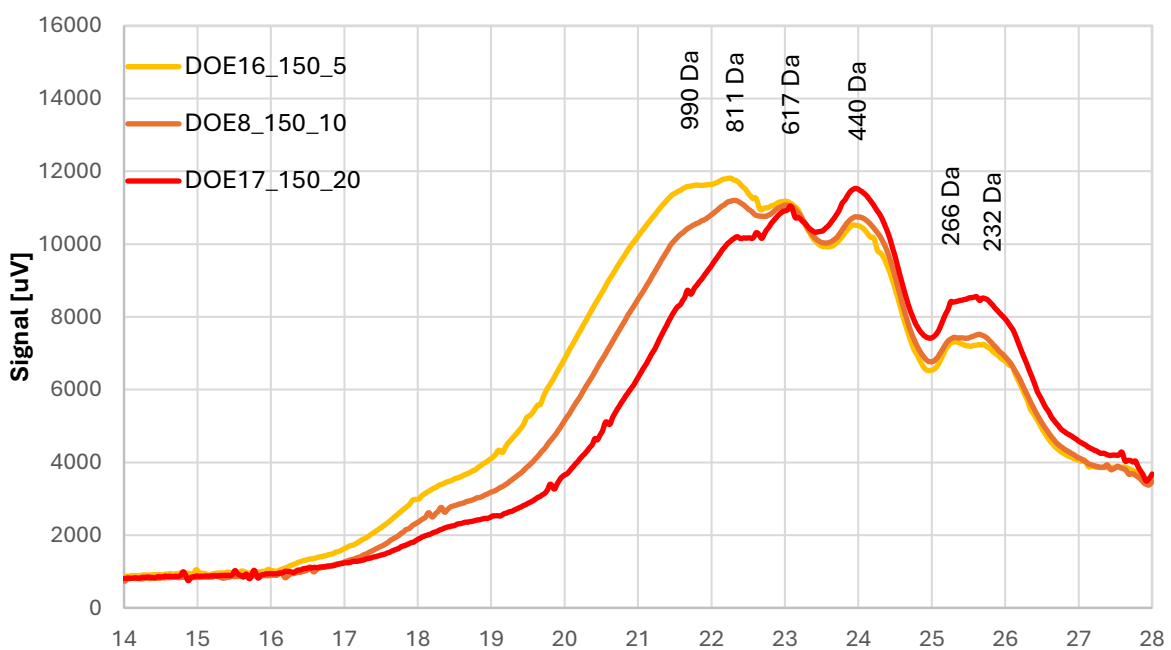


Figure 7.13 Effects of time on molecular weight distribution at fixed temperature of 150 C

Same consideration can be done if the Figure 7.14 is take into account, at 170 C if the time is increased from 5 minutes to 20 minutes the molecular weight distribution goes towards lower values.

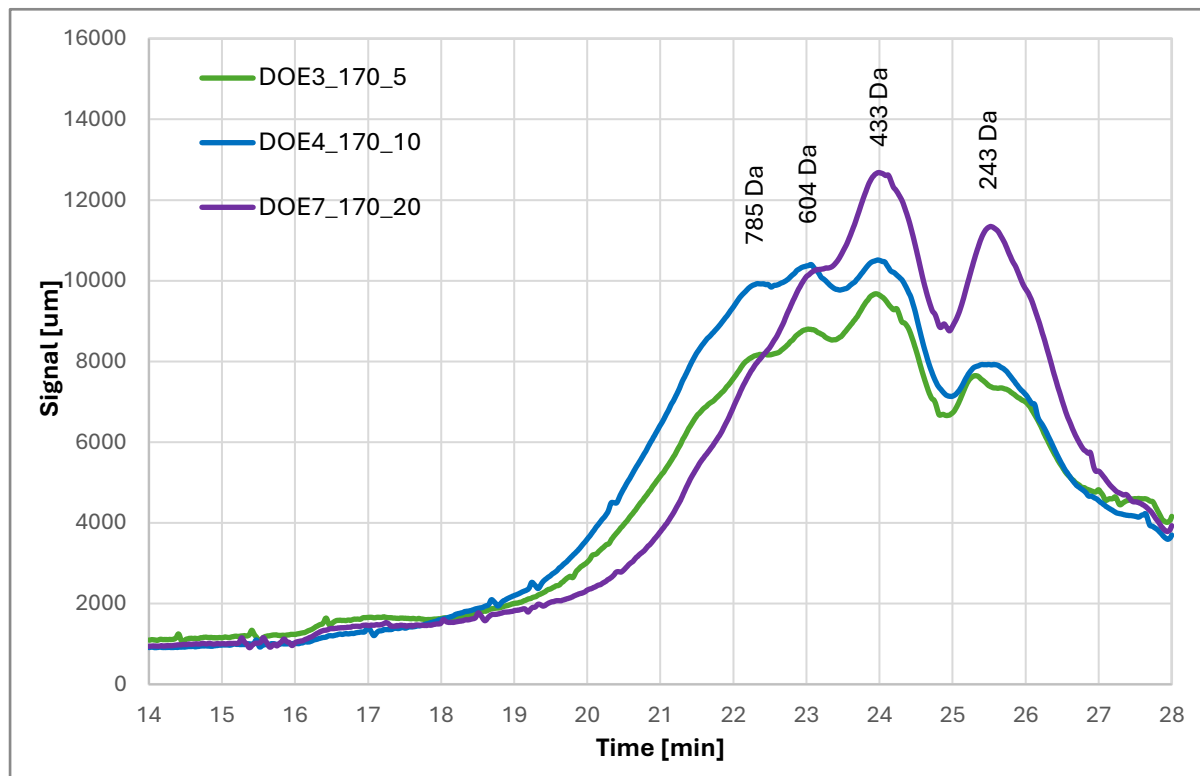


Figure 7.14 Effects of time on molecular weight distribution at fixed temperature of 170 C

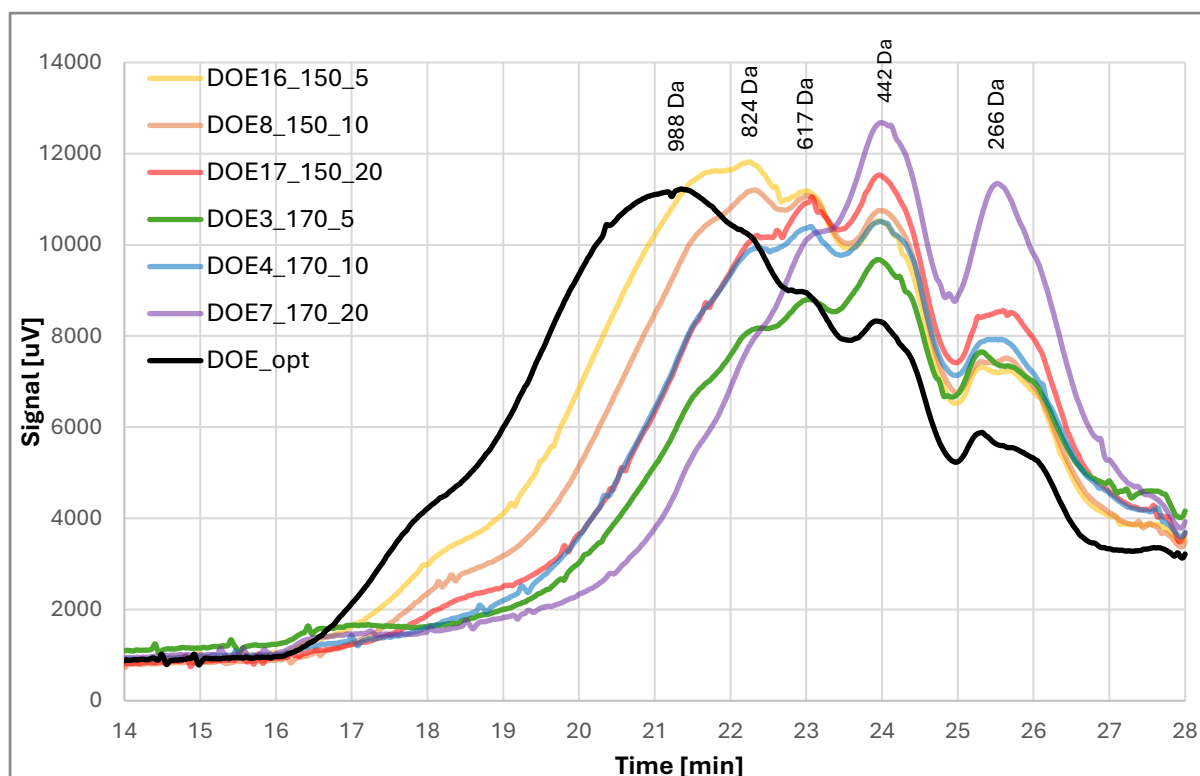


Figure 7.15 Chromatogram of the optimal polyol according to the DOE analysis. It was synthesized at 160 C for 12 minutes

In Figure 7.15 is shown where the optimized polyol is collocated together with the other experiments. As can be seen the molecular distribution is shifted towards higher values.





# Chapter 8

## Foam synthesis and characterization

In the following chapter, the synthesis of flexible polyurethane foams, the final product of the recycling process, will be illustrated. The methodologies and characterization of the foams are described to define their physical, morphological, and thermal properties.

### 8.1 Raw material for the synthesis of the polyurethane foams

In this paragraph will be presented all the main substances used to synthesize the flexible polyurethane foams

#### 8.1.1 Polyols from liquefaction

For the synthesis of flexible polyurethane foams, the two polyols that exhibit the best characteristics for this study were chosen (Section §7.6), along with what will be referred to as the optimized polyol. This optimized polyol is the one with the minimized hydroxyl number according to the model developed using DOE (Design of Experiments). Their main properties are reported in Table 8.1. The molecular weight has been evaluated by the GPC analysis while the functionality has been calculated by using equation (1.9).

Table 8.1 Experimental conditions and main characteristics of the three polyols used for the foams' synthesis

| Polyol                | Emerox®<br>14511<br>[%w] | Glycerol<br>[%w] | H2SO4<br>[%w to the<br>solvent] | Hydroxyl<br>value<br>[mgKOH/g] <sub>exp</sub> | Functionality | Molecular<br>weight <sub>exp</sub><br>[g/mol] |
|-----------------------|--------------------------|------------------|---------------------------------|---|---------------|---|
| Pol_90% <sup>4</sup>  | 90                       | 10               | 3                               | 110   | 3.2           | 1620  |
| Pol_100% <sup>5</sup> | 100                      | 0                | 3                               | 55  | 2             | 2067  |
| Pol_opt               | 100                      | 0                | 3                               | 38  | 1.6           | 2312  |

It should be specified that the first two polyols were synthesized using microwave irradiation at 150°C for 20 minutes, while the optimized polyol was synthesized at 160°C for 12 minutes.

<sup>4</sup> Known as DOE\_15 (Section §7.6, Table 7.4)

<sup>5</sup> Known as DOE\_17 (Section §7.6, Table 7.4)

## 8.2 Formulation of the polyurethane foams

This section presents the formulations and characteristic times of the foams produced. Specifically, it includes the reference foam made with petroleum-based polyol (PM6000) and those obtained with recycled polyols containing liquefied lignin. Since it is not known how lignin might act within the system and considering that achieving a good flexible polyurethane foam requires the right balance between reagents, we started with a standard formulation that was then adapted and optimized for the needs of this study, which required several trials. The Table 8.2 summarizes the quantities of reagents for the reference foam, where no recycled polyols were used

Table 8.2 Reference foam formulation

|                                       | <i>Reference</i> |
|---------------------------------------|------------------|
| <b>Formulation</b>                    |                  |
| <i>PM6000 [g]</i>                     | 90               |
| <i>Polyol_100% [g]</i>                | /                |
| <i>Polyol_90% [g]</i>                 | /                |
| <i>Cell opener Rokopoll M1170 [g]</i> | 5                |
| <i>Tegostab B8629 [g]</i>             | 1.5              |
| <i>Water [g]</i>                      | 3.038            |
| <i>Jeffcat Z110 [g]</i>               | 0.8              |
| <i>NiAx A1 [g]</i>                    | /                |
| <i>DTBL [g]</i>                       | /                |
| <i>Isotech TCC 105 [g]</i>            | 78.1             |
| <b>Times</b>                          |                  |
| <i>Cream [s]</i>                      | 29               |
| <i>Gel [s]</i>                        | 87               |
| <i>Tack.free [s]</i>                  | 160              |

Considering three recycled polyols containing liquefied lignin (Pol90, Pol100, Pol\_opt), it was possible to synthesize seven foams that differ in the amount of bio-polyol used:

- Foam Pol90%\_20: Contains 20% by weight of bio-polyol, which is composed of 90% Emerox® 14511 and 10% glycerol, relative to the total amount of the polyol.
- Foam Pol90%\_30: Contains 30% by weight of bio-polyol, which is composed of 90% Emerox® 14511 and 10% glycerol, relative to the total amount of the polyol.

- Foam Pol100%\_20: Contains 20% by weight of bio-polyol, which is composed of 100% Emerox® 14511, relative to the total amount of the polyol.
- Foam Pol100%\_30: Contains 30% by weight of bio-polyol, which is composed of 100% Emerox® 14511, relative to the total amount of the polyol.
- Foam Pol100%\_40 Contains 40% by weight of bio-polyol, which is composed of 100% Emerox® 14511, relative to the total amount of the polyol.
- Foam Pol\_opt\_20: Contains 20% by weight of bio-polyol, which is composed of 100% Emerox® 14511, relative to the total amount of the polyol.
- Foam Pol\_opt\_30 Contains 30% by weight of bio-polyol, which is composed of 100% Emerox® 14511, relative to the total amount of the polyol.

Table 8.3 Recycled lignin polyol foam formulations

|                            | <i>Foam</i>      | <i>Foam</i>      | <i>Foam</i>       | <i>Foam</i>       | <i>Foam</i>       | <i>Foam</i>       | <i>Foam</i>       |
|----------------------------|------------------|------------------|-------------------|-------------------|-------------------|-------------------|-------------------|
|                            | <i>Pol90%_20</i> | <i>Pol90%_30</i> | <i>Pol100%_20</i> | <i>Pol100%_30</i> | <i>Pol100%_40</i> | <i>Pol_opt_20</i> | <i>Pol_opt_30</i> |
| <b>Formulation</b>         |                  |                  |                   |                   |                   |                   |                   |
| <i>PM6000 [g]</i>          | 70               | 60               | 70                | 60                | 50                | 70                | 60                |
| <i>Polyol_100% [g]</i>     | /                | /                | 20                | 30                | 40                | 20                | 30                |
| <i>Polyol_90% [g]</i>      | 20               | 30               | /                 | /                 | /                 | /                 | /                 |
| <i>Cell opener</i>         | 5                | 5                | 5                 | 5                 | 5                 | 5                 | 5                 |
| <i>Rokopoll M1170 [g]</i>  |                  |                  |                   |                   |                   |                   |                   |
| <i>Tegostab B8629 [g]</i>  | 1.5              | 1.5              | 1.5               | 1.5               | 1.5               | 1.5               | 1.5               |
| <i>Water [g]</i>           | 1.62             | 1.654            | 3.038             | 2.762             | 2.792             | 3.349             | 2.743             |
| <i>Jeffcat Z110 [g]</i>    | /                | /                | /                 | /                 | /                 | /                 | /                 |
| <i>Niax A1 [g]</i>         | 1.2              | 1.2              | 1.6               | 1.6               | 1.8               | 1.6               | 1.6               |
| <i>DTBL [g]</i>            | 3.8              | 3.8              | 3.8               | 3.8               | 4                 | 3.8               | 3.8               |
| <i>Isotech TCC 105 [g]</i> | 42.1             | 45.1             | 63.1              | 60.4              | 61.8              | 69.9              | 59.3              |
| <b>Times</b>               |                  |                  |                   |                   |                   |                   |                   |
| <i>Cream [s]</i>           | 23               | 29               | 20                | 27                | 31                | 16                | 20                |
| <i>Gel [s]</i>             | 58               | 65               | 70                | 95                | 110               | 53                | 77                |
| <i>Tack free [s]</i>       | 78               | 97               | 114               | 164               | 170               | 109               | 160               |

The polyols containing lignin were obtained by using sulfuric acid, and thus, given their low pH value, it has been studied how this affected the catalysis of the foams. In general, it is known that the catalysts used belong to two main categories: amines or tin octoates; both exhibit basic behaviour. When they encounter the acidic sites of the lignin, they are consumed and partially

lose their catalytic function. This can be observed through two key factors, both summarized in the Table 8.3. The first factor concerns the change of catalyst, from Jeffcat Z110 to Niax A1, which are blow catalysts, and the second concerns the addition of DBTDL (a tin octoate) that improve the gel phase. Attempts were made to reduce the reaction times of some foams, particularly referring to the last two foams reported in the table above (Table 8.3), but the addition of higher amount of catalysts led to the collapse of the foam's cellular structure. It also should be considered that the addition of lignin primarily increases the tack-free time.

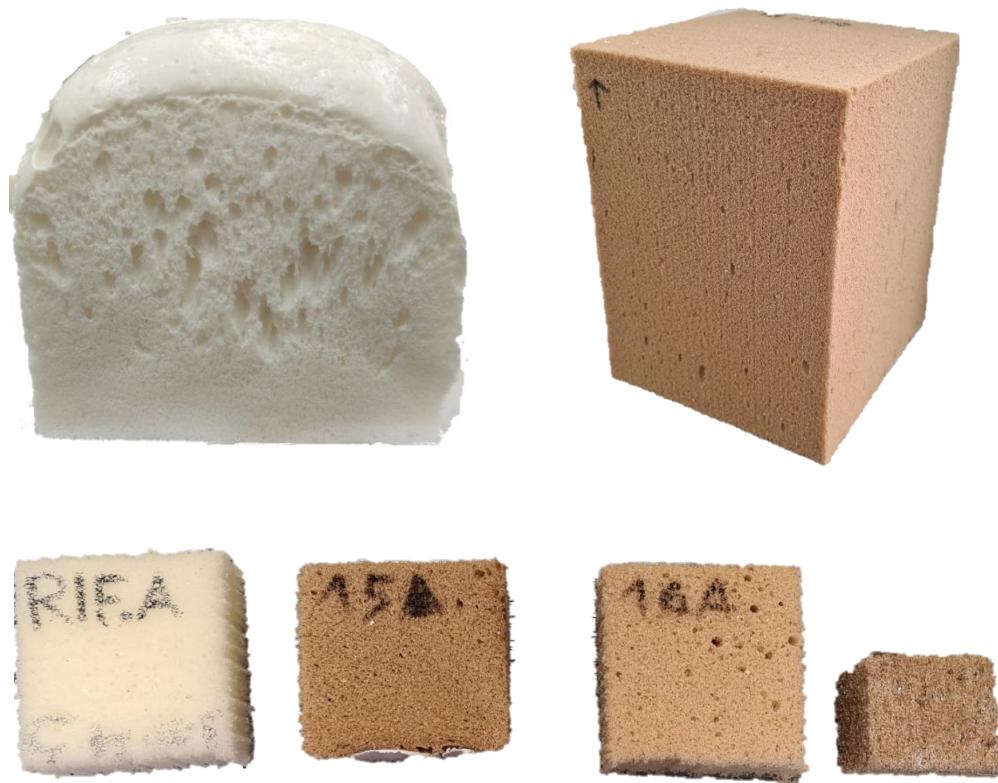


Figure 8.1 Reference and bio-based lignin polyols foams

### 8.3 Physical properties

One of the most important physical characteristics for polyurethane flexible foams is their low density, which should be below 40 kg/m, but it should also be noted that an increase in density generally leads to an improvement in the mechanical properties of the polymer. In addition to density, the thermal conductivity of the flexible polyurethane foam was also measured, although it is not important since the final purpose is not thermal insulation due to its open-cell structure.

In fact, it is known that thermal conductivity is lower when the diameter of the individual cells that make up the foam is smaller.

Table 8.4 Density and Thermal conductivity of recycled lignin foams

|  | Reference | Pol90%_20 | Pol90%_30 | Pol100%_20 | Pol100%_30 | Pol100%_40 | Pol_opt_20 | Pol_opt_30 |
|--|-----------|-----------|-----------|------------|------------|------------|------------|------------|
| Density<br>[kg/m <sup>3</sup> ]              | 43        | 70        | 68        | 37         | 51         | 61         | 38         | 44         |
| Thermal<br>conductivity<br>@10°C<br>[mW/m K] | 37.7      | 39.0      | 38.0      | 37.8       | 38.6       | 38.6       | 37.0       | 39.5       |

From the values reported in the Table 8.4, it is possible to observe how the density varies within a range from 37 kg/m<sup>3</sup> to a maximum of 70 kg/m<sup>3</sup>. A further reduction in density leads to the collapse of the foam, while the thermal conductivity evaluated at average temperature of 10°C, with a temperature difference between the plates of 20°C, ranges from a minimum of 37.7 mW/m K for the reference foam to a maximum of 39 mW/m K for the Pol90%\_20 foam. Both tests were performed after a maturation period of 24 hours in an oven at 70°C.

## 8.4 Foams filled with biochars

To improve the thermal properties and mechanical resistance of the foams, it was decided to introduce fillers, in particular biochars, into the formulation. Since higher content of lignin polyols lead to a more probable foam collapse, and since this effect can be caused also by fillers introduced into the foam formulation, biochars filled foams have been produced starting from the foam synthesized using 20% by weight of polyol with 100% Emerox® 14511, Thus, once again, a reference foam was prepared, which in this case coincides with the Pol100%\_20 foam, along with three foams in which 5% by weight of three different fillers (rice husk, Arundo Donax, and Tetrapack waste) were added. It was found that further addition of filler, namely greater than 5% in weight, within the foam leads to structural failure, causing the foam to collapse. The formulations are reported in the Table 8.5.

Table 8.5 Formulation of reference and biochar additive foams

| <b>Formulation</b>          | <i>Foam</i>       | <i>Foam</i>           | <i>Foam</i>           | <i>Foam</i>           |
|-----------------------------|-------------------|-----------------------|-----------------------|-----------------------|
|                             | <i>Pol100%_20</i> | <i>Pol100%_20_D_5</i> | <i>Pol100%_20_L_5</i> | <i>Pol100%_20_T_5</i> |
| <i>PM6000 [g]</i>           | 70                | 70                    | 70                    | 70                    |
| <i>Polyol_100% [g]</i>      | 20                | 20                    | 20                    | 20                    |
| <i>Polyol_90% [g]</i>       | /                 | /                     | /                     | /                     |
| <i>Biochar [g]</i>          |                   | 8.79                  | 8.79                  | 8.79                  |
| <i>Cell opener Rokopoll</i> |                   |                       |                       |                       |
| <i>M1170 [g]</i>            | 5                 | 5                     | 5                     | 5                     |
| <i>Tegostab B8629 [g]</i>   | 1.5               | 1.5                   | 1.5                   | 1.5                   |
| <i>Water [g]</i>            | 3.038             | 3.038                 | 3.038                 | 3.038                 |
| <i>Jeffcat Z110 [g]</i>     | /                 | /                     | /                     | /                     |
| <i>Niax A1 [g]</i>          | 1.6               | 1.6                   | 1.6                   | 1.6                   |
| <i>DTBL [g]</i>             | 3.8               | 3.8                   | 3.8                   | 3.8                   |
| <i>Isotech TCC 105 [g]</i>  | 63.1              | 63.1                  | 63.1                  | 63.1                  |
| <b>Times</b>                |                   |                       |                       |                       |
| <i>Cream [s]</i>            | 20                | 17                    | 17                    | 19                    |
| <i>Gel [s]</i>              | 70                | 50                    | 50                    | 53                    |
| <i>Tack.free [s]</i>        | 114               | 70                    | 75                    | 86                    |

As can be seen from the table, the different foams have the same formulation, the only difference is the type of additive:

- Foam Pol100%\_20\_D\_5 This foam consists of 20% by weight of polyol containing 100% Emerox® 14511 and 5% by weight of filler derived from Arundo donax.
- Foam Pol100%\_20\_L\_5 This foam consists of 20% by weight of polyol containing 100% Emerox® 14511 and 5% by weight of filler derived from rice husk.
- Foam Pol100%\_20\_T\_5 This foam consists of 20% by weight of polyol containing 100% Emerox® 14511 and 5% by weight of filler derived from waste tetrapack.

Looking at the reaction times in the Table 8.5, it can be immediately seen the difference between the reference and biochar-additive foams of 20 sec in the gel time, and about 45 sec, on average, in the tack free time. This indicates that the fillers accelerate the development and formation of the cell structure.

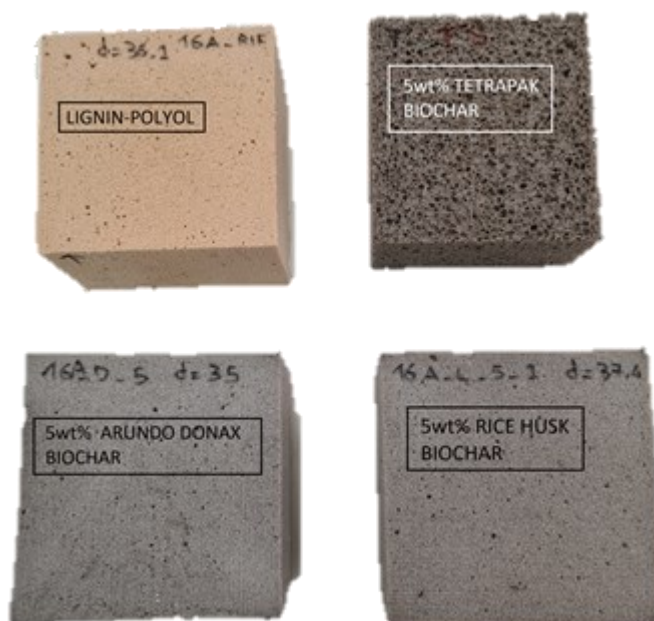


Figure 8.2 Reference and biochar filled foams

The physical properties, specifically density and thermal conductivity of biochar-filled foams are summarized below (Table 8.6):

Table 8.6 Density and Thermal conductivity of biochar additive foams

|                                     | Pol100%_20 | Pol100%_20_D_5 | Pol100%_20_L_5 | Pol100%_20_T_5 |
|-------------------------------------|------------|----------------|----------------|----------------|
| Density [kg/m <sup>3</sup> ]        | 37         | 35             | 37.6           | 44.4           |
| Thermal conductivity @10°C [mW/m K] | 37.8       | 40.6           | 45.0           | /              |

From the Table 8.6, it can be observed that the apparent density values do not significantly deviate from the reference, except for the flexible foam in which Tetrapack waste was used. However, the thermal conductivity shows a different trend. Again, it is worth noting that thermal conductivity is not a crucial property in the specific context of this study. An increase of a few mW/m K units indicates that the cell structure has "enlarged", meaning that the cell diameter is larger compared to the reference foam. It is also evident from the Table 8.6 that the thermal conductivity of the foam containing Tetrapack is missing because, even though the foam has not collapsed, it shows evident cellular defects visible to the naked eye. For this reason, it was decided that characterization tests of Tetrapack foam would not be carried out.

## 8.5 Foam characterization

Once the formulation was prepared, the foams were synthesized and placed in an oven to cure for at least 24 hours at 70°C. The foams were then ready for characterization. The following paragraphs present the different analyses performed and the corresponding results.

### 8.5.1 Compression stress

The Table 8.7 reports the compression stress carried out on the flexible polyurethane foams.

Table 8.7 Compression resistance's value for reference and recycled foams

|                                  |               | Referenc<br>e | Pol90%_2<br>0 | Pol90%_3<br>0 | Pol100%_<br>20 | Pol100%_<br>30 | Pol100%_<br>40 | Pol_opt_2<br>0 | Pol_opt_<br>30 |
|----------------------------------|---------------|---------------|---------------|---------------|----------------|----------------|----------------|----------------|----------------|
| $\sigma_c$<br>@Compression = 40% | Average [kPa] | 3.0           | 3.7           | 5.5           | 3.0            | 4.7            | 6.0            | 5.0            | 4.8            |
|                                  | Std.dev       | 0.1           | 0.25          | 0.35          | 0.2            | 0.5            | 0.35           | 0.2            | 0.3            |
| $\sigma_c$<br>@Compression = 70% | Average [kPa] | 9.3           | 16.8          | 24.7          | 16.8           | 23.4           | 29.5           | 21             | 23             |
|                                  | Std.dev       | 0.3           | 1.2           | 1.6           | 1.2            | 2.2            | 0.6            | 0.3            | 3.0            |

From the Table 8.7, it can be seen that the foams with 20% of lignin polyols have roughly the same stress at the imposed deformation of 40%, but there is also an increase of more than 50% when the specimen is compressed to 70%. The foams containing glycerol exhibit more markedly this behavior. This is especially evident at maximum deformation, where the compression stress is, in some cases, three times higher than that of the reference. This is probably due to both the aromatic ring content of the lignin, which makes the polymeric chain more rigid, and to the glycerin content that increases the crosslinking density of the foams.

Table 8.8 Compression resistance's value for biochar additive foams

|                                  |              | Pol100%_20 | Pol100%_20_D_5 | Pol100%_20_L_5 |
|----------------------------------|--------------|------------|----------------|----------------|
| $\sigma_c$<br>@Compression = 40% | Average[kPa] | 3.0        | 3.4            | 3.6            |
|                                  | Std.dev      | 0.2        | 0.5            | 0.3            |
| $\sigma_c$<br>@Compression = 70% | Average[kPa] | 16.8       | 22             | 17             |
|                                  | Std.dev      | 1.2        | 3.0            | 0.5            |

The Table 8.8 shows the results of the compression test for flexible foams with biochar additives. Here, too, there is an increase in the stress at both 40% and maximum deformation. This is particularly noticeable in the specific case of the foam with *Arundo donax* additives.



### 8.5.2 Compression set

The compression set values for the different samples are shown in the following Table 8.9:

Table 8.9 Compression set results for reference and recycled foams

|     |                  | <i>Referenc</i><br><i>e</i> | <i>Pol90%_2</i><br><i>0</i> | <i>Pol90%_3</i><br><i>0</i> | <i>Pol100%_2</i><br><i>0</i> | <i>Pol100%_3</i><br><i>0</i> | <i>Pol100%_4</i><br><i>0</i> | <i>Pol_opt_2</i><br><i>0</i> | <i>Pol_opt_3</i><br><i>0</i> |
|-----|------------------|-----------------------------|-----------------------------|-----------------------------|------------------------------|------------------------------|------------------------------|------------------------------|------------------------------|
| C.S | Average<br>e [%] | 6.50                        | 41.40                       | 39.30                       | 43.00                        | 46.20                        | 48.20                        | 42.70                        | 42.60                        |
|     | Std.dev          | 0.3                         | 1.9                         | 1.7                         | 0.1                          | 0.35                         | 0.8                          | 0.30                         | 0.2                          |

It is evident from the tabulated values that the presence of liquefied lignin in the polyol results in a deterioration of the compared compression set behavior compared to the reference foam, which is good to remember that is 100% petroleum-based. However, the values are slightly above 40%, which is considered the limit for an acceptable flexible foam. This lack in performance could be due to the high aromatic content in the lignin-based recycled polyol, which stiffens the polymer chain.



Figure 8.3 Compression set samples after running the test. Lignin based polyols foam on the left, reference on the right

The following table shows the compression set factor for the additivated foams:

Table 8.10 Compression set results for biochar additive foams

|      |                | <i>Pol100%_20</i> | <i>Pol100%_20_D_5</i> | <i>Pol100%_20_L_5</i> |
|------|----------------|-------------------|-----------------------|-----------------------|
| C.S. | Average<br>[%] | 43.00             | 48.20                 | 44.4                  |
|      | Std.dev        | 0.1               | 0.5                   | 1.2                   |

In general, the addition of biochar seems to slightly worsen the performances, inhibiting the flexibility of the foam.



*Figure 8.4 Biochar filled ample foams for the compression set. Samples in the first row have 5% wt. rice husks, while the second row's samples are filled with 5% wt. of Arundo donax*

### 8.5.3 Dynamic mechanical analysis (DMA)

This section presents the DMA analyses of the various foams. This technique involves applying an oscillatory stress to the sample, in this specific case, a compressive stress, during which the temperature, frequency, and amplitude of deformation are varied in a controlled manner. The settings for the analysis are provided below.

- DMA multi-frequency strain
- Temperature ramp/frequency sweep
- Amplitude 30  $\mu\text{m}$
- Soak time 5 min
- Heating rate 3  $^{\circ}\text{C}/\text{min}$

From the analysis run with the above mentioned settings, the following graphs are obtained (Figure 8.5).

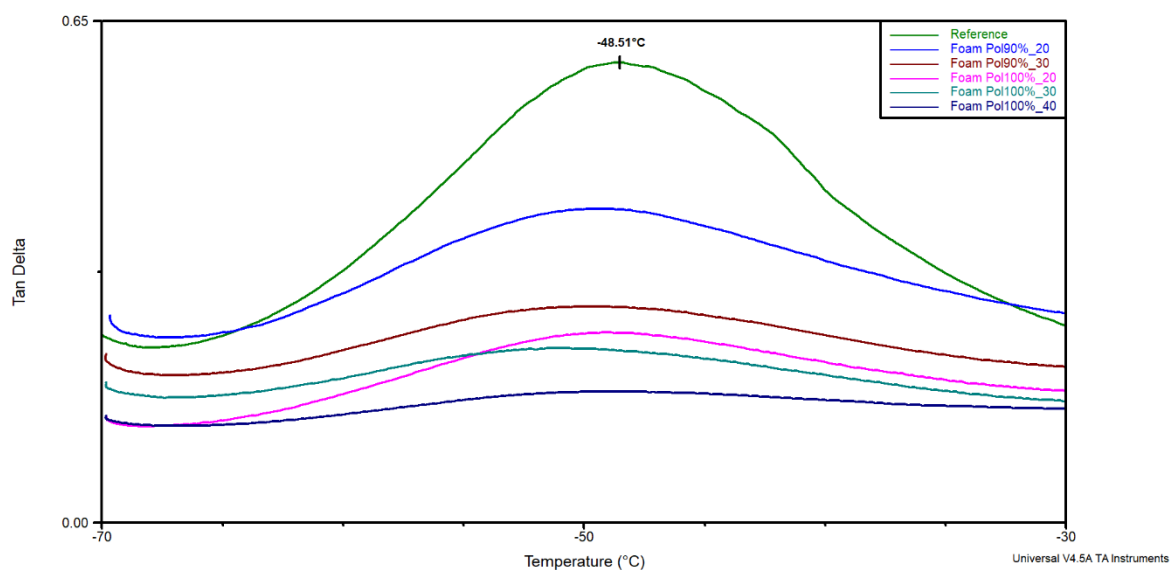


Figure 8.5 Graph representing the transition glass temperature for the reference and different recycled lignin foams

In Figure 8.5 the glass transition temperature for the reference foam is reported, i.e.  $-48^{\circ}\text{C}$ , this foam does not contain neither lignin nor Emerox<sup>®</sup> bio-based polyol. In Table 8.11 are listed all the glass transition temperatures, they differ from each other just for 1-2  $^{\circ}\text{C}$  which can be associated to the experimental error, thus the lignin content, like the percentage of glycerin, does not affect the glass transition temperature. What can be exploited from the graph is related to the area below the curves. The area below the Tan Delta curve represents the damping capability of the foam, so we can conclude that the increase in the lignin content within the foam reduces the energy dissipation ability if compared to the reference. In particular this last result is in agreement with the compression set results.

Table 8.11 Glass transition temperature for the reference and lignin recycled foams

| ID Specimen     | Glass transition temperature [ $^{\circ}\text{C}$ ] |
|-----------------|---|
| Reference       | -48   |
| Foam Pol90%_20  | -49   |
| Foam Pol90%_30  | -50   |
| Foam Pol100%_20 | -49   |
| Foam Pol100%_30 | -51   |
| Foam Pol100%_40 | -50   |

The Figure 8.6 represents the DMA analysis for the foams that were made up with the optimized polyols obtained from the DOE analysis. The curves refer to the reference, the two foams realized with the optimized polyol (substitution of 20% and 30% by weight), and the corresponding two foams synthesized with the pol100%.

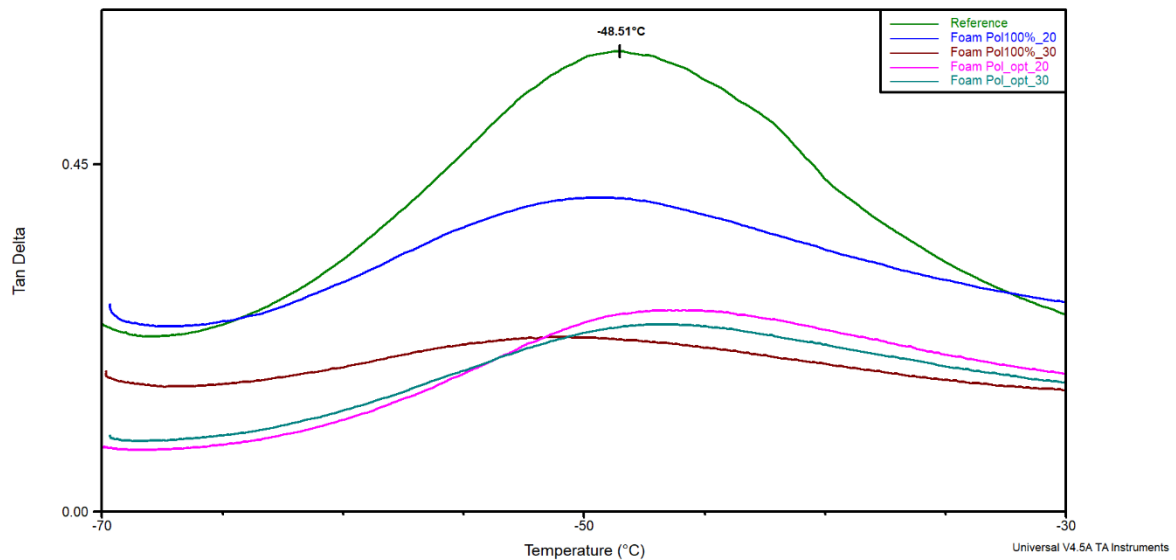


Figure 8.6 Graph representing the transition glass temperature for the optimal polyol foams

Table 8.12 Glass transition temperature for the reference and optimized polyol foams

| ID Spicemen     | Glass transition temperature [C] |
|-----------------|----------------------------------|
| Reference       | -48                              |
| Foam Pol100%_20 | -49                              |
| Foam Pol100%_30 | -51                              |
| Foam Pol_opt_20 | -46                              |
| Foam Pol_opt_30 | -47                              |

From Figure 8.6 the following characteristic can be noted: the height of maximum peak and the area below the curve of the reference are greater than the others, meaning that the damping ability of the lignin foam is reduced. Dealing with Tg temperature, the optimal polyol seems to make stiff the foam more flexible, because of the lower glass transition temperature detected. Indeed, if compared to the Tg temperature of the other foams, this shows a temperature difference of  $-4^{\circ}\text{C}$  on the Tg value, thus meaning that the polymeric chains have higher mobility. About the area below the tan-delta curves, it can be observed that all the lignin based foams have reduced capability of energy dissipation if compared to the reference foam.

Figure 8.7 reports the DMA analysis for the foams filled with the biochar as additive, and their reference, namely the lignin foam chosen as base model. Also in this case, it can be noted that the introduction of biochar in the foam does not significantly affect the Tg; again, a reduction of the damping capability was also registered.

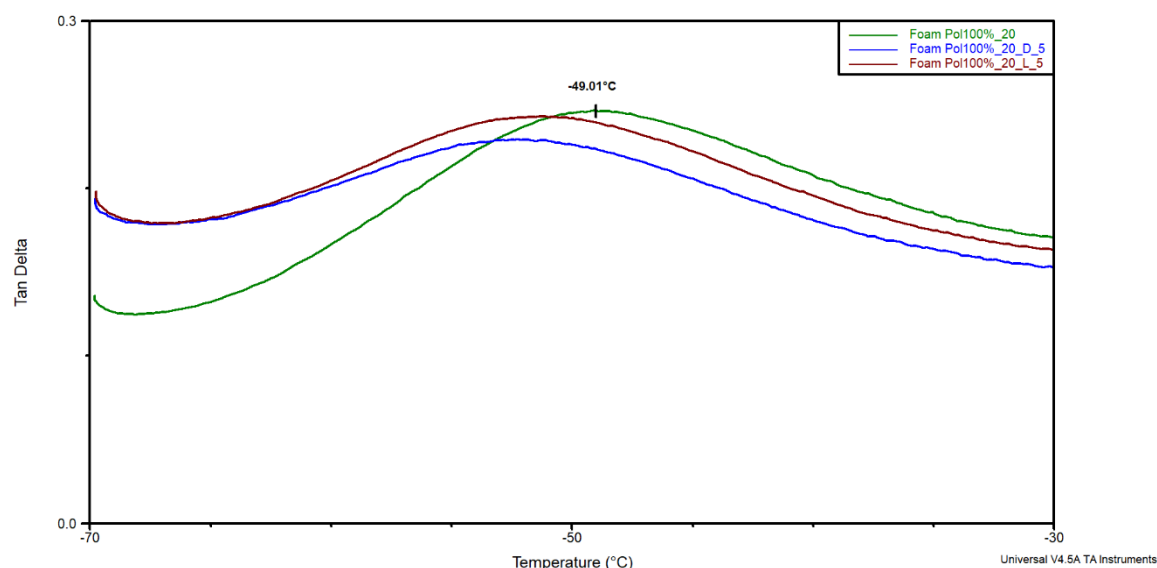


Figure 8.7 Graph representing the transition glass temperature for the biochar additive foams

Table 8.13 Glass transition temperature for biochar additive foams

| ID Specimen         | Glass temperature transition [C] |
|---------------------|----------------------------------|
| Foam Pol100%_20     | -49                              |
| Foam Pol100%_20_D_5 | -51                              |
| Foam Pol100%_20_L_5 | -52                              |

#### 8.5.4 Thermogravimetric analysis (TGA)

Moving on to analyses aimed at characterizing polyurethane foams from a thermal perspective, one of the most common characterizations is thermogravimetric analysis (TGA). Aluminum pans containing approximately 5-20 mg of sample are placed in the furnace. These are heated up to 800°C at a rate of 20°C/min with chromatographic air.

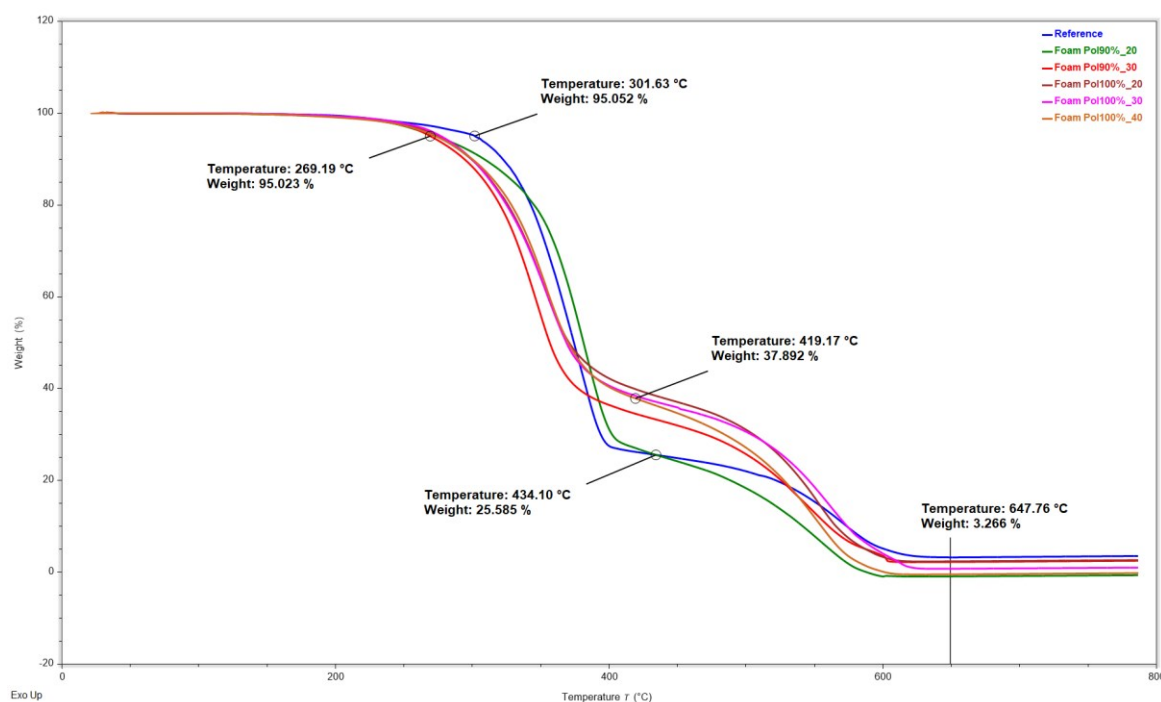


Figure 8.8 Thermogravimetric curves of the reference and different recycled lignin foams

This type of analysis allows the evaluation of the percentage weight loss of the sample as a function of temperature. From the Figure 8.8, two key aspects should be noted: the first concerns the presence of two degradation steps occurring in two different temperature ranges, specifically between 300-400°C and from 450 to 600°C. In the first phase, depolymerization of the chain occurs, with the breaking of urethane bonds and polyol chains, while in the second stage, there is typically a breakdown of unsaturated C=C bonds, which are also present in aromatic rings, which are typically very stable.

The second aspect concerns the influence of the different polyols on the thermal stability; excluding Pol90%\_20 foam, which is very similar to the reference one, the remaining foams show better thermal stability, compared to the reference, in the temperature range between 450-600°C.

Table 8.14 Weight loss and temperature at maximum degradation rate for reference and lignin based foams

| ID Specimen    | Weight loss                 | Temperature @ max degradation rate | Weight loss                 | Temperature @ max degradation rate |
|----------------|-----------------------------|------------------------------------|-----------------------------|------------------------------------|
|                | 1 <sup>st</sup> stage [%wt] | 1 <sup>st</sup> stage [C]          | 2 <sup>nd</sup> stage [%wt] | 2 <sup>nd</sup> stage [C]          |
| Reference Foam | 70.539                      | 383.74                             | 21.423                      | 573.4                              |
| Pol90%_20      | 70.753                      | 381.16                             | 25.147                      | 556.89                             |
| Pol90%_30      | 61.745                      | 346.63                             | 30.967                      | 547.9                              |
| Pol100%_20     | 57.298                      | 351.50                             | 35.556                      | 554.03                             |
| Pol100%_30     | 58.788                      | 354.55                             | 35.438                      | 560.12                             |
| Pol100%_40     | 59.325                      | 354.28                             | 36.325                      | 554.92                             |

A comparison between foams obtained by using two polyols selected from the initial screening (Pol100% and the optimal one suggested by the design of the experiment) is shown in the Figure 8.9.

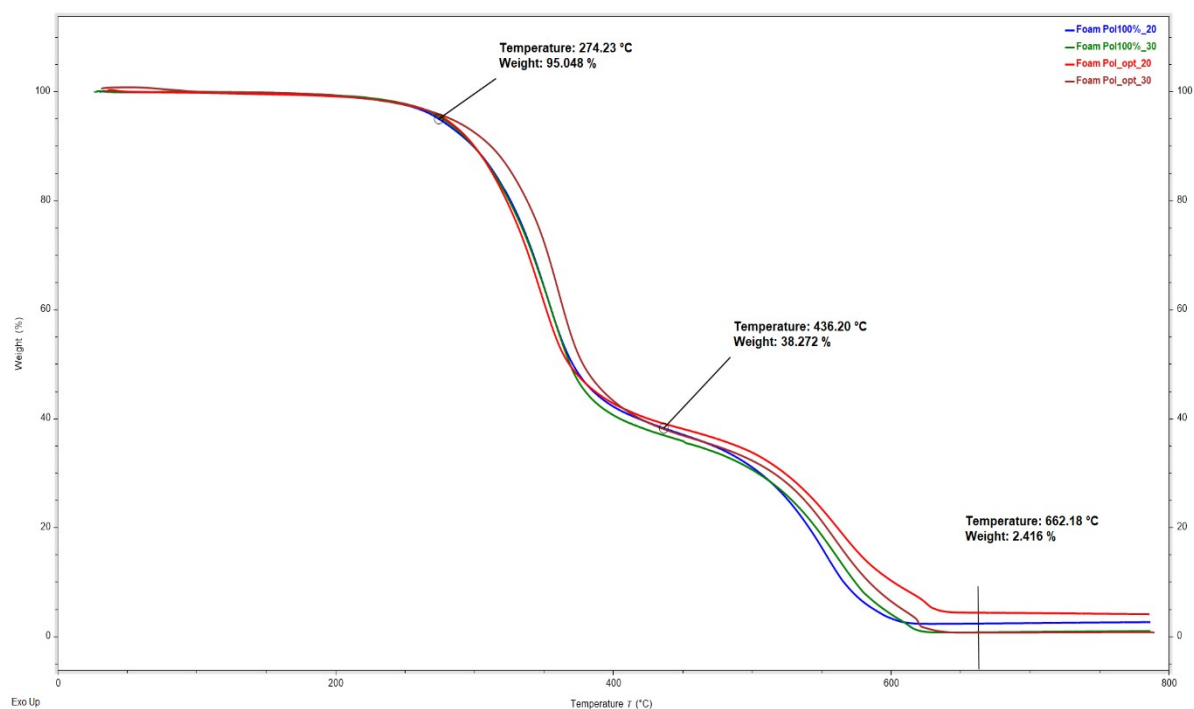


Figure 8.9 Thermogravimetric curves of the optimized polyol foams

It is observed that in the first phase of material degradation, the foams exhibit the same behaviour except for the one synthesized with the optimal polyol at 30% by weight relative to the formulation, which shows a slight shift in the curve of about ten degrees. In the second phase, in the range between 450°C and 620°C, the foam derived from the optimized polyol again exhibits slightly greater stability, but this time it is the one containing 20% by weight.

Table 8.15 Weight loss and temperature at maximum degradation rate for optimized polyol foams

| ID Specimen     | Weight loss                 | Temperature @ max degradation rate | Weight loss                 | Temperature @ max degradation rate |
|-----------------|-----------------------------|------------------------------------|-----------------------------|------------------------------------|
|                 | 1 <sup>st</sup> stage [%wt] | 1 <sup>st</sup> stage [C]          | 2 <sup>nd</sup> stage [%wt] | 2 <sup>nd</sup> stage [C]          |
| Foam Pol100%_20 | 57.298                      | 351.50                             | 35.556                      | 554.03                             |
| Foam Pol100%_30 | 58.788                      | 354.55                             | 35.438                      | 560.12                             |
| Foam Pol_opt_20 | 57.053                      | 348.21                             | 34.045                      | 561.99                             |
| Foam Pol_opt_30 | 59.621                      | 361.37                             | 35.325                      | 557.88                             |

The following graph shows the TGA analysis performed on the foams with added biochar.

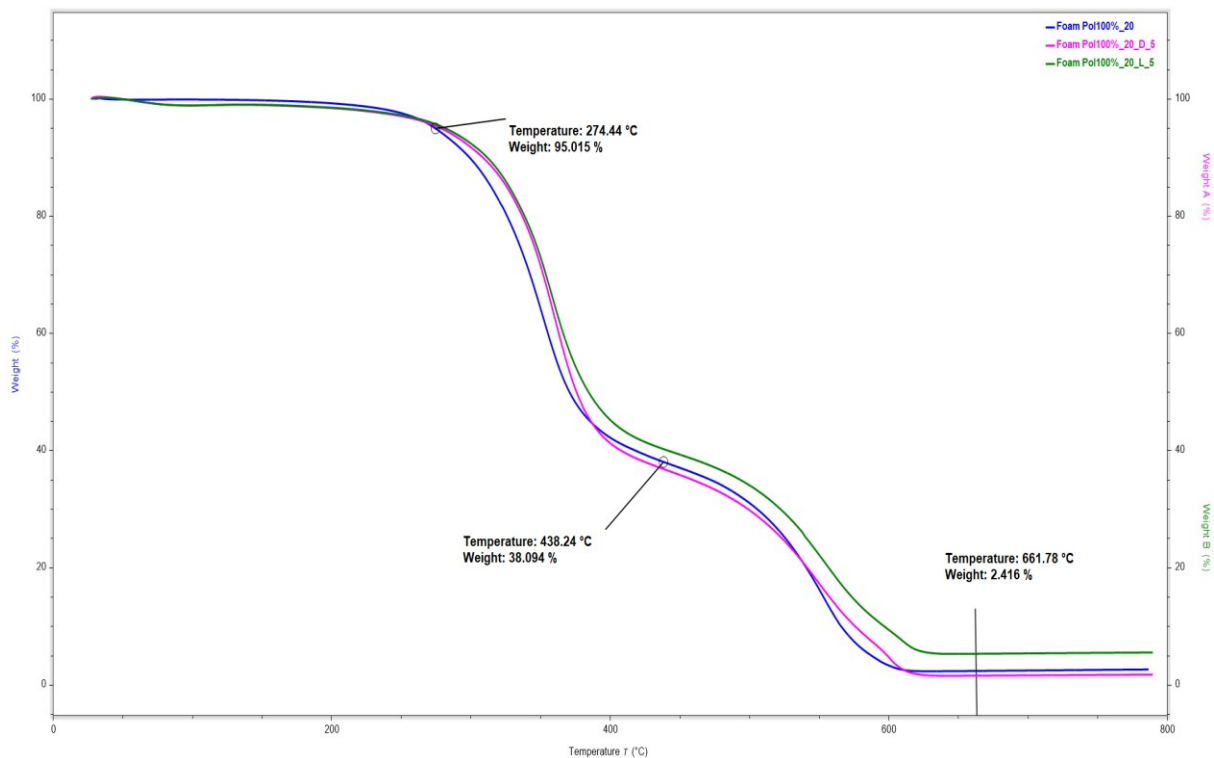


Figure 8.10 Thermogravimetric curves of the biochar additive foams



In this case as well, the trend of the two curves remains similar to that of the reference foam, i.e., Pol100%\_20. A slight improvement in the thermal stability can be observed over the entire temperature range in the foam containing biochar derived from rice husk. Despite having a high (about 20%) silica content, the small amount of biochar utilized in the foam is insufficient to significantly alter the thermal stability.

Table 8.16 Weight loss and temperature at maximum degradation rate for additive biochar foams

| ID Specimen         | Weight loss                 | Temperature @ max degradation rate | Weight loss                 | Temperature @ max degradation rate |
|---------------------|-----------------------------|------------------------------------|-----------------------------|------------------------------------|
|                     | 1 <sup>st</sup> stage [%wt] | 1 <sup>st</sup> stage [C]          | 2 <sup>nd</sup> stage [%wt] | 2 <sup>nd</sup> stage [C]          |
| Foam Pol100%_20     | 57.298                      | 351.50                             | 35.556                      | 554.03                             |
| Foam Pol100%_20_D_5 | 58.708                      | 360.22                             | 35.148                      | 548.36                             |
| Foam Pol100%_20_L_5 | 55.614                      | 357.85                             | 34.155                      | 553.73                             |

### 8.5.5 Limiting Oxygen Index (LOI) analysis

The oxygen index was measured according to the standard normative ISO 4589. This factor represents the minimum volume percentage of oxygen in an oxygen-nitrogen mixture at which the combustion of the polymer self-sustains. The LOI thus provides information on ignition, with a higher value of this index implying a lower probability that the foam will act as the ignition source of a fire. Below a table with the LOI values of the various foams is reported (Table 8.17).

Table 8.17 Limiting oxygen index for the reference and the lignin recycled foams

| Specimen ID | LOI [%] |
|-------------|---------|
| Reference   | 19.5    |
| Pol90%_20   | 20.3    |
| Pol90%_30   | 20      |
| Pol100%_20  | 20      |
| Pol100%_30  | 20.3    |
| Pol100%_40  | 21      |
| Pol_opt_20  | 20.1    |
| Pol_opt_30  | 20.5    |

The tabulated values show that in all cases, there is an increase in LOI with respect to the reference foam, which is a positive outcome. Two observations can be made from these data: first, the presence of glycerin (Pol90%) increases the oxygen index, probably due to a greater

degree of cross-linking; the same trend is observable when the percentage of recycled polyol with the lignin is increased, for the higher aromatic content.

Table 8.18 Limiting oxygen index for the biochar additive foams

| Specimen ID    | LOI [%] |
|----------------|---------|
| Pol100%_20     | 19.7    |
| Pol100%_20_D_5 | 20.3    |
| Pol100%_20_L_5 | 20.4    |

The presence of fillers within the foam results in slight improvements of the LOI; since the amount of biochar is equal to 5% by weight relative to the total mass of polyurethane and blowing agent, the improvement is limited.

### 8.5.6 Calorimetry analysis

Fire behaviour has also been studied by cone calorimetry using a heat flux of 35kW/m<sup>2</sup>. The heat release rate (HRR) and total smoke product (TSP) are shown in Figure 8.11.

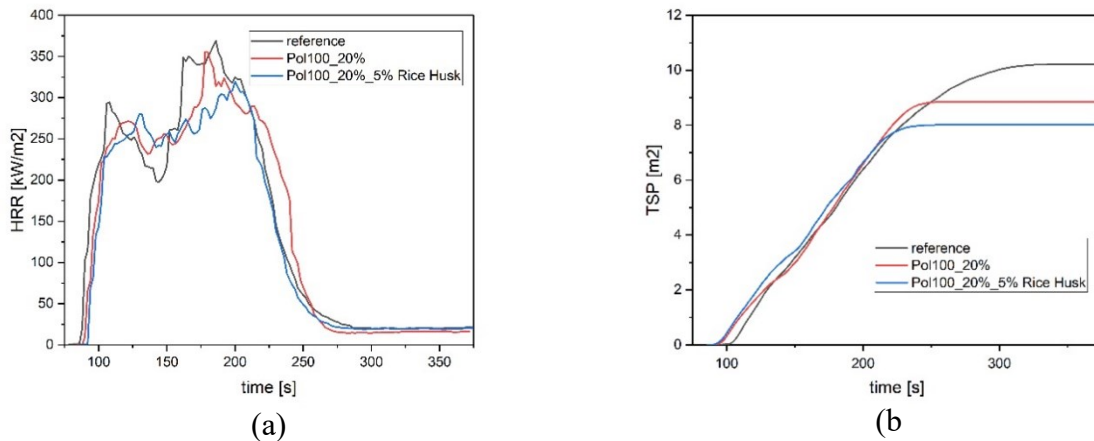


Figure 8.11 Calorimetry analysis, (a) represent the Heat release rate while (b) the total smoke product

From the first plot reported above, it can be observed that the heat release rate (HRR) peak is the same for all foams, but the time to peak HRR is longer for the lignin based polyol foams; this behavior can be explained by the increase of the aromatic content of the polymeric chain. By looking at the area below the HRR curves, it can be assessed that lignin based polyols improve the total heat released and decrease the total smoke production (TSP). The addition of rice husk biochar leads to some further improvements

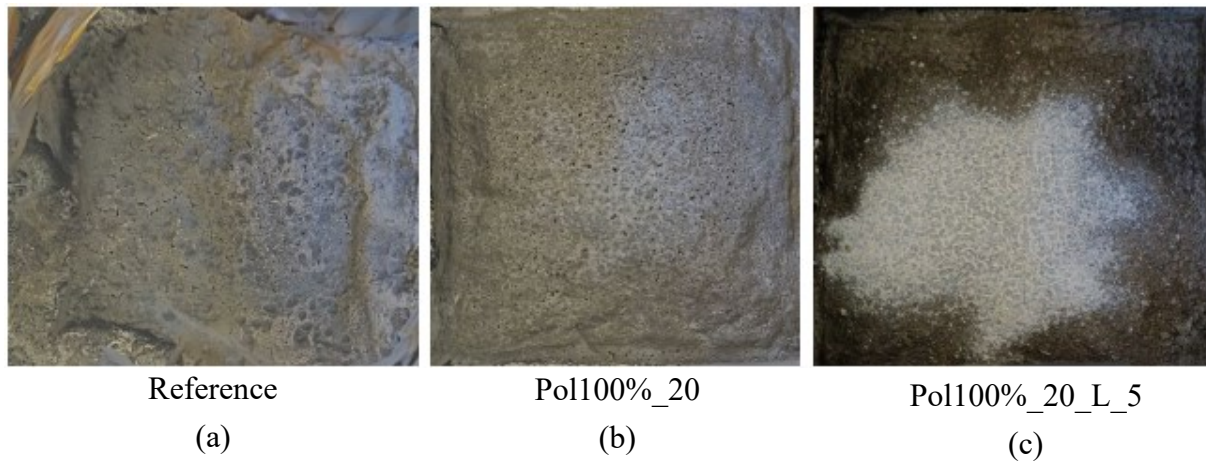


Figure 8.12 Residues after cone calorimetry tests (35 kW/m<sup>2</sup> irradiative heat flux).

These results are related to the composition of the char layer that forms during combustion in the cone (Figure 8.12). It is evident that the char is denser for lignin-based foams (Figure 8.12b) than for reference foam (Figure 8.12a); additionally, a protective silica layer is formed in the presence of biochar (Figure 8.12c) due to the silica content of such biochar.

### 8.5.7 Morphological characterization, SEM analysis

The morphology of a polyurethane foam can be analyzed using SEM (Scanning Electron Microscopy) analysis. This technique provides information on the cellular structure which greatly affects the mechanical performance of the material. It should be noted that the analysis was performed parallel to the growth direction of the foam.

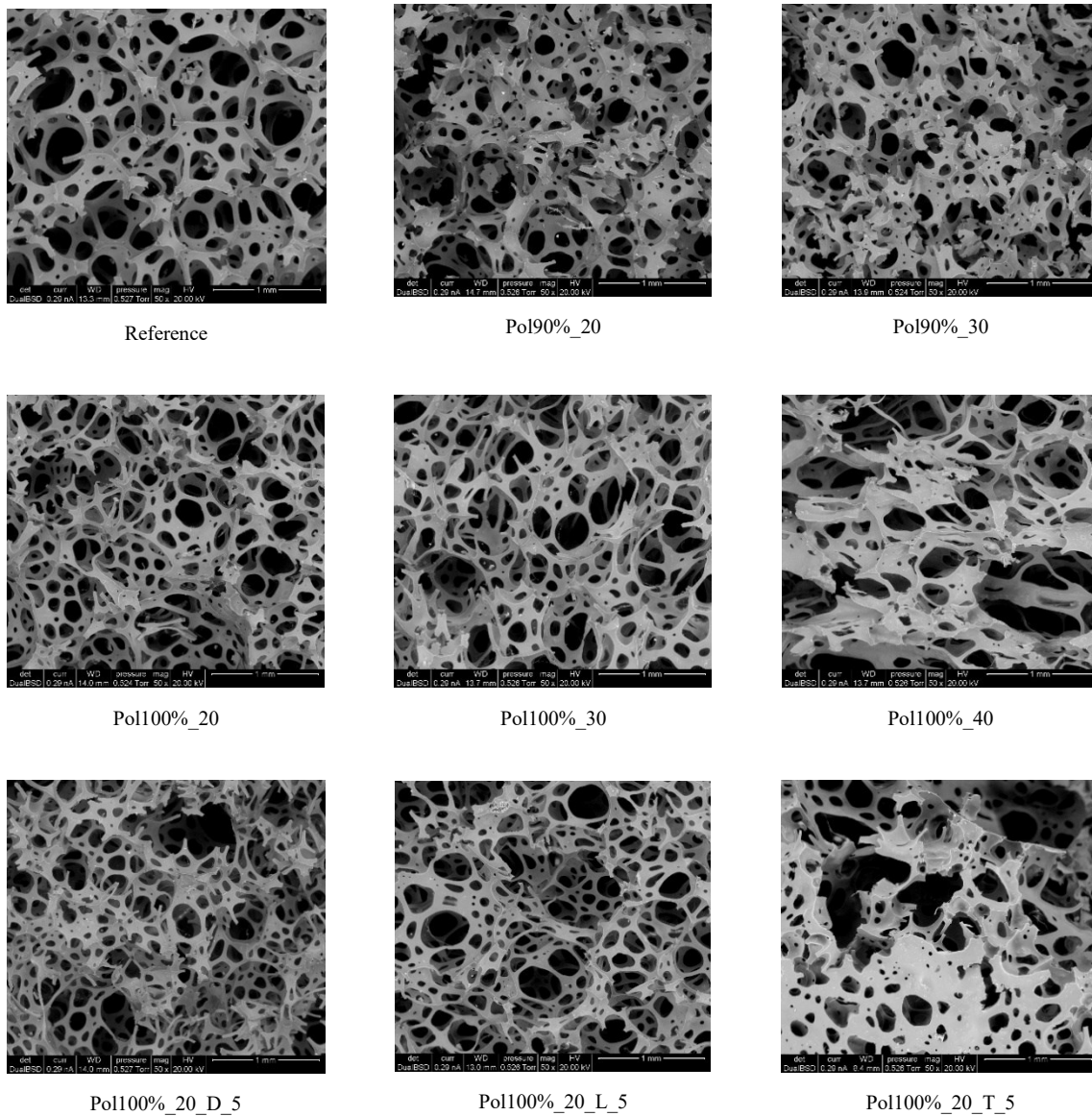


Figure 8.13 SEM foams images of the reference, of the lignin based polyol and the biochar additive

The images reported above represent the foam cellular structure. Analysing the 50x magnification, some considerations about the cell's wall and the porous structure of the foam can be drawn. The reference foam has a regular structure with a uniform distribution of the porous, which have variable dimension. The two foams made with the 90% of Emerox® 14511 (Pol90%) present a different structure compared to the reference: the cells seem to be smaller and walls are thicker. Going on with the SEM images, there are three foams made with 20, 30 and 40% of recycled lignin polyol, which contain 100% Emerox® 14511 (Pol100%). At 20 and 30% the cell structure is similar to the reference: in the first one the cells dimension is comparable but the walls seem to be thinner, while in the second one it can be observed an increase in cells dimension and also in this case the wall are thinner with respect to the

reference. For the foam synthesized with the 40% of lignin's polyol, it can be noted that the cells are wider and stretched, maybe because of a coalescence phenomenon. Thus, it can be hypothesized that the increase of lignin percentage will produce a more fragile and unstable cellular structure. Similar conclusion can be reached also with reference to the glycerol content in the foam, as it can be seen comparing the wall thickness of the first two rows. The last three images refer to the biochar additive foams. They have the same formulation as the Pol100%\_20 with the addition of 5% in weight of biochar. The one with *Arundo donax* and rice husks have similar cell structure, but greater cells dimension if compared to the foam without the biochar. The last foam is the worst one: the presence of waste tetrapack makes the cell extremely wider and more irregular. It can be observed the presence of large holes that alternate between thin and thick cells' walls.

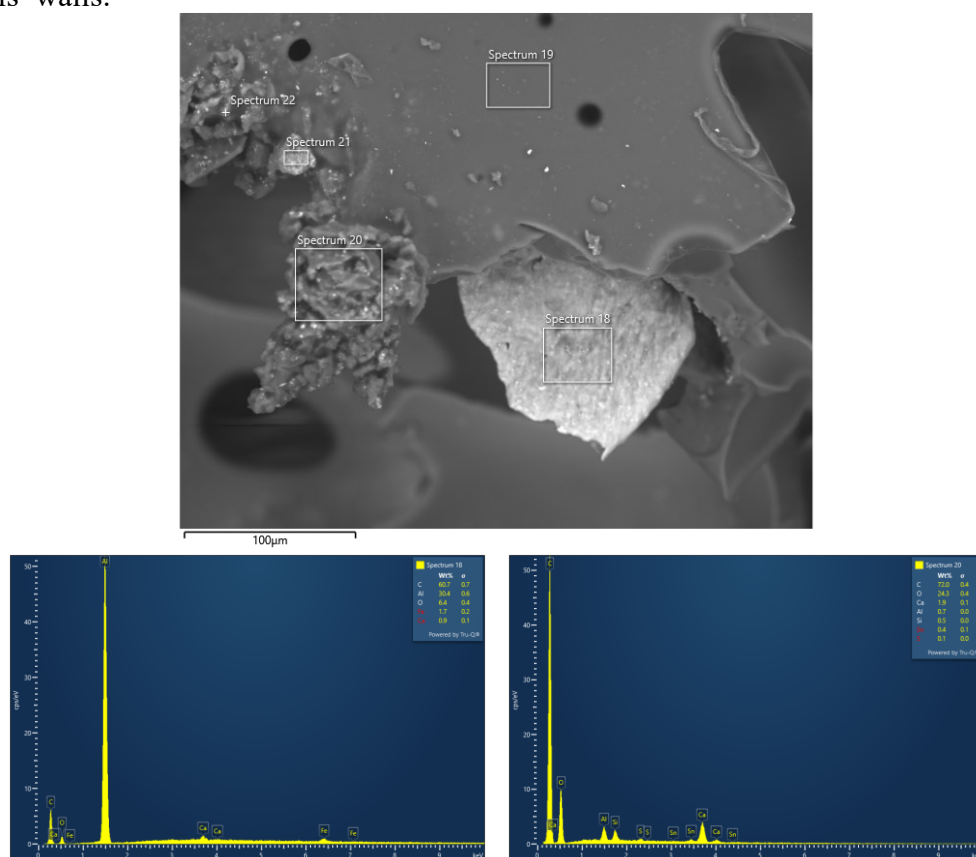


Figure 8.14 Magnification of tetrapack additive foam cell structure and relative spectrum analysis

The images reported above is a magnification of the waste tetrapack additive in the foam (Figure 8.14). By looking at the EDX spectra, it can be asserted that spectrum 18 refers to tetrapack biochar, while spectrum 20 identifies a micro piece of lignin residue.

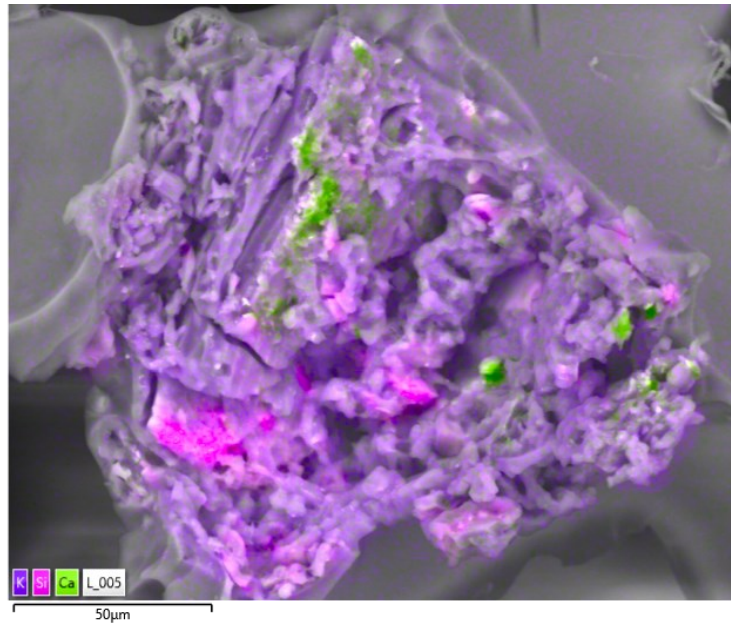


Figure 8.15 Analysis of a residue of rice husks additive within the cellular structure of the foam

The image above (Figure 8.15) shows the magnification of a piece of rice husks biochar, as it can be see the main component are the potassium and silicon.

### 8.5.8 FT-IR analysis

Fourier Transform Infrared Spectroscopy (FT-IR) can be used to analyse the content in terms of free isocyanate and the main functional groups within the foam. This can help in better understanding the behaviour of the various samples. In the image reported below (Figure 8.16), two spectra are showed. The main difference is around the 1700  $\text{cm}^{-1}$  where the presence of carbonyl group seems to be more pronounced in the foam with the 30% of the optimised lignin-based polyol.

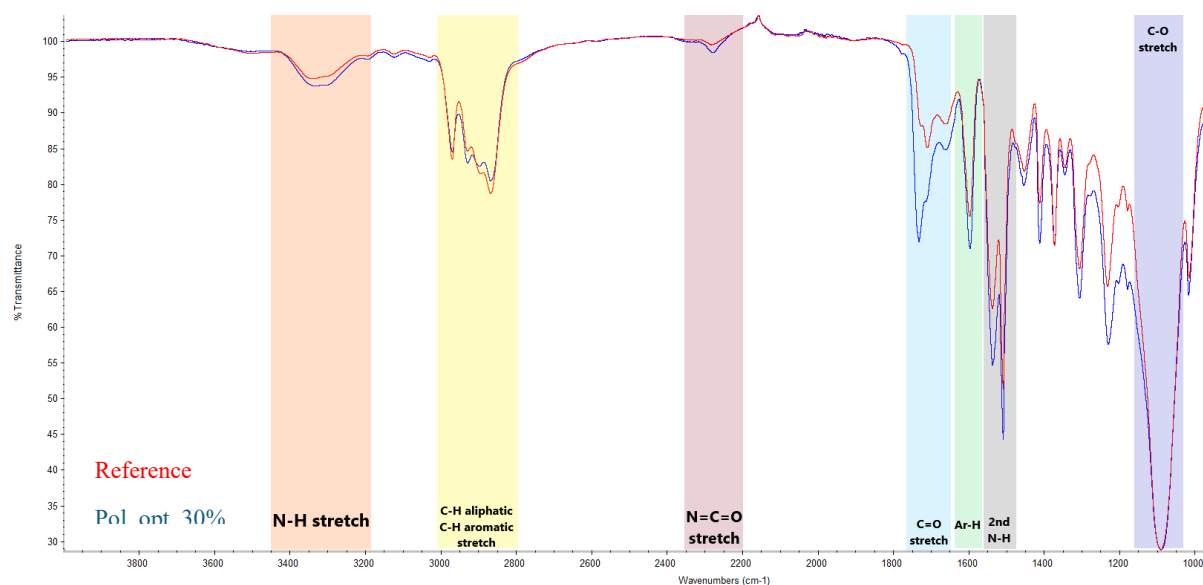


Figure 8.16 FT-IR spectra of the reference and the optimized lignin base polyol's foam

All the other foams present similar spectra with respect to the one showed in the figure, no particular deviation can be assessed.





# Conclusion

The main objective of this thesis work is the synthesis of bio-polyols through the liquefaction of lignin for production of flexible polyurethane foams. The parameters of the liquefaction process were optimized to obtain polyols with characteristics suitable for foam production; special attention was paid to the liquefaction solvent and catalysis. Initially, a screening was done on the various types of lignin to see which one was best suited for the liquefaction process. Then the effect of solvent on the liquefaction process catalyzed by 3% sulfuric acid was investigated. Two renewably sourced polyols (i.e., azelaic acid, commercially known as EMEROX®), which differ in hydroxyl number, molecular weight and viscosity, were used; the efficiency of the reaction was evaluated in terms of yield and hydroxyl number.

The effect of glycerin content of the liquefaction solvent on the reaction yield was also studied. It was found that by adding 0% to 30% glycerin content to the solvent, the liquefaction yield increases. Therefore, two solvent blends were identified to achieve good yield and polyols with optimal characteristics: EMEROX®14511/glycerol 90/10 blend and EMEROX®14511/glycerol 100/0 blend.

The effect of the catalyst during liquefaction was also evaluated; the aim was to decrease the acidity of the polyols obtained when 3 wt% sulfuric acid is used. Therefore, two possibilities were tried: decrease the acid concentration to 1% by weight and change the catalysis to a basic compound, namely sodium hydroxide. A common problem arose in both the solution proposed, i.e., a very low yield and a quite high hydroxyl number, which is detrimental for the production of the flexible foams. Having gathered all this preliminary information, it was possible to set up a design of experiment (DoE) to optimize, specifically minimize, the hydroxyl number starting from the two previously chosen solvents.

Finally, the optimal bio-polyols prepared by liquefaction were used in the synthesis of flexible polyurethane foams. Problems were encountered related to the strong acidity of the bio-based recycled polyols, so the foam formulation had to be modified with special attention to catalysis choice.

The foams properties were compared with those of foam produced from fossil source. The comparison was made considering compressive strength, compression set, thermal conductivity, thermal stability, and fire behaviour. Once the flexible polyurethane foam with the best properties was defined, it was decided to fill it with different biochars to look for further improvements of its performance.

It was found that the introduction of lignin-based bio-polyols within flexible polyurethane foams generally increase compressive strength, improves the fire reaction as well as thermal stability; however, a reduction in the flexibility, assessed by the compression set results, has been also detected; this could be due to the higher aromatic content of the polymeric chains because of the presence of lignin . The addition of biochars again increases the mechanical strength, lowers its glass transition temperature, and increases the thermal stability in the 400-500°C temperature range; better results were obtained by addition of biochar based on rice husks. In addition, from cone calorimeter analysis, the reduction of heat release rate and the total amount of smoke produced are denoted. These characteristics have also been confirmed at the morphological level: in fact, the filled foams exhibit a more regular and uniform char structure.

Therefore, it can be concluded that the liquefaction of lignin should be considered as a possible and viable option for its recycling. The production of flexible polyurethane foams with good performance, comparable to those from fossil sources, is a proof of this. The introduction of polyols derived from renewable sources also makes the production process of polyurethane foams greener. Further research is needed to improve the morphology and mechanical properties of foams to ensure the sustainability of lignin recycling over time.



# Bibliography

1. Hodlur RM, Rabinal MK. Self assembled graphene layers on polyurethane foam as a highly pressure sensitive conducting composite. *Compos Sci Technol*. 2014 Jan 10;90:160–5.
2. Kang SM, Kwon SH, Park JH, Kim BK. Carbon nanotube reinforced shape memory polyurethane foam. *Polymer Bulletin* [Internet]. 2013;70(3):885–93. Available from: <https://doi.org/10.1007/s00289-013-0905-4>
3. Singhal P, Small W, Cosgriff-Hernandez E, Maitland DJ, Wilson TS. Low density biodegradable shape memory polyurethane foams for embolic biomedical applications. *Acta Biomater*. 2014 Jan 1;10(1):67–76.
4. Levchik S V, Weil ED. Thermal decomposition, combustion and fire-retardancy of polyurethanes—a review of the recent literature. *Polym Int*. 53:1585–610.
5. Chattopadhyay DK, Webster D. Thermal stability and flame retardancy of polyurethanes. *Prog Polym Sci*. 34:1068–133.
6. Randall D, Lee S. *The Polyurethanes Book*. Wiley & Sons Ltd;
7. Haq I, Mazumder P, Kalamdhad AS. Recent advances in removal of lignin from paper industry wastewater and its industrial applications – A review. *Bioresour Technol*. 2020 Sep 1;312:123636.
8. Cazacu G, Capraru M, Popa V. *Advances in Natural Polymers* [Internet]. Thomas S, Visakh PM, Mathew AjiP, editors. *Advances in Natural Polymers*. Berlin, Heidelberg: Springer Berlin Heidelberg; 2013. (Advanced Structured Materials; vol. 18). Available from: <https://link.springer.com/10.1007/978-3-642-20940-6>
9. Vanholme R, Demedts B, Morreel K, Ralph J, Boerjan W. Lignin Biosynthesis and Structure. *Plant Physiol* [Internet]. 2010 Jul 1;153(3):895–905. Available from: <https://academic.oup.com/plphys/article/153/3/895/6109625>
10. Ralph J, Lundquist K, Brunow G, Lu F, Kim H, Schatz PF, et al. Lignins: Natural polymers from oxidative coupling of 4-hydroxyphenyl- propanoids. *Phytochemistry Reviews*. 2004 Jan;3(1–2):29–60.
11. Vanholme R, Demedts B, Morreel K, Ralph J, Boerjan W. Lignin Biosynthesis and Structure. *Plant Physiol*. 2010 Jul 1;153(3):895–905.

12. Hatakeyama H, Hatakeyama T. Lignin Structure, Properties, and Applications. In 2009. p. 1–63.
13. Hatfield R, Vermerris W. Lignin Formation in Plants. The Dilemma of Linkage Specificity. *Plant Physiol.* 2001 Aug 1;126(4):1351–7.
14. Chung H, Washburn NR. Chemistry of lignin-based materials. *Green Mater.* 1:137–60.
15. Mohd Noor N. Comparison of Adipic Versus Renewable Azelaic Acid Polyester Polyols as Building Blocks in Soft Thermoplastic Polyurethanes. *JAOCS, J Am Oil Chem Soc.* 93:1529–40.
16. Oleochemicals Emery. Recycled Content Polyols [Internet]. Brochure. 2016 [cited 2024 Oct 13]. Available from: [https://www.emeryoleo.com/sites/default/files/2019-11/Emery\\_EP\\_Brochure\\_Web.pdf](https://www.emeryoleo.com/sites/default/files/2019-11/Emery_EP_Brochure_Web.pdf)
17. Nüchter M, Ondruschka B, Bonrath W, Gum A. Microwave assisted synthesis – a critical technology overview. *Green Chem.* 6:128–41.
18. Falciglia PP. A review on the microwave heating as a sustainable technique for environmental remediation/detoxification applications. *Renew Sustain Energy Rev.* 95:147–70.
19. Sun J, Wang W, Yue Q. Review on microwave-matter interaction fundamentals and efficient microwave-associated heating strategies. *Materials (Basel).* 9.
20. Gabriel C, Gabriel SG, Halsad EH, J. S, Michael DP, Grant EH, et al. Dielectric parameters relevant to microwave dielectric heating. *Chem Soc Rev.* 27:213–23.
21. Kappe CO, Dallinger D. Controlled microwave heating in modern organic synthesis: Highlights from the 2004-2008 literature. *Mol Divers.* 13:71–193.
22. Chemat F, Esveld E. Microwave super-heated boiling of organic liquids: origin, effect and application. *Chem Eng Technol.* 24:735–44.
23. Perreux L, Loupy A. A tentative rationalization of microwave effects in organic synthesis according to the reaction medium, and mechanistic considerations. *Tetrahedron.* 57:9199–223.
24. Kuhnert N. Microwave-Assisted Reactions in Organic Synthesis—Are There Any Nonthermal Microwave Effects? Highlights 1863–1866.
25. Leonelli C, Veronesi P. Production of Biofuels and Chemicals with Microwave. *Springer Sci.* 3.

26. Favretto L. Milestone's microwave labstation. *Mol Divers.* 7:287–91.
27. Gosz K, Kosmela P, Hejna A, Gajowiec G, Piszczyk Ł. Biopolyols obtained via microwave-assisted liquefaction of lignin: structure, rheological, physical and thermal properties. *Wood Sci Technol.* 52:599–617.
28. Mahmood N, Yuan Z, Schmidt J, Xu C. Depolymerization of lignins and their applications for the preparation of polyols and rigid polyurethane foams: A review. *Renew Sustain Energy Rev.* 60:317–29.
29. Hu S, Luo X, Li Y. Polyols and polyurethanes from the liquefaction of lignocellulosic biomass. *ChemSusChem.* 7:66–72.
30. Niu M, Zhao G jie, Alma MH. Polycondensation reaction and its mechanism during lignocellulosic liquefaction by an acid catalyst: A review. *For Stud China.* 13:71–9.
31. Liu HM, Liu YL. Characterization of milled solid residue from cypress liquefaction in sub- and super ethanol. *Bioresour Technol.* 151:424–7.
32. Lin L, Nakagame S, Yao Y, Yoshioka M, Shiraishi N. Liquefaction Mechanism of b -O-4 Lignin Model Compound in the Presence of Phenol under Acid Catalysis Part 1 Identification of the Reaction Products. *Holzforschung.* 55:625–30.
33. Lin L, Nakagame S, Yao Y, Yoshioka M, Shiraishi N. Liquefaction Mechanism of b -O-4 Lignin Model Compound in the Presence of Phenol under Acid Catalysis Part 2 Reaction behavior and pathways. *Holzforschung.* 55:625–30.
34. Jasiukaitytė-Grojzdek E, Kunaver M, Crestini C. Lignin Structural Changes During Liquefaction in Acidified Ethylene Glycol. *J Wood Chem Technol.* 32:342–60.
35. Shi Y. Solvolysis kinetics of three components of biomass using polyhydric alcohols as solvents. *Bioresour Technol.* 221:102–10.
36. Yan Y, Hu M, Wang Z. Kinetic study on the liquefaction of cornstalk in polyhydric alcohols. *Ind Crops Prod.* 32:349–52.
37. Palle I, Hori N, Iwata T, Takemura A. Optimization of polyol production via liquefaction from *Acacia mangium* and analysis of the polyols by traditional methods and two-dimensional correlation spectroscopy. *Holzforschung.* 72:451–8.
38. Zhao Y, Yan N, Feng M. Polyurethane Foams Derived from Liquefied Mountain Pine Beetle-Infested Barks. *Wiley Online Libr*;
39. Jin Y, Ruan X, Cheng X, Lü Q. Liquefaction of lignin by polyethyleneglycol and glycerol. *Bioresour Technol.* 102:3581–3.

40. Hassan EM, Shukry N. Polyhydric alcohol liquefaction of some lignocellulosic agricultural residues. Elsevier. 7:33–8.
41. Alma MH, Shiraishi N. Preparation of polyurethane-like foams from NaOH-catalyzed liquefied wood. Holz Als Roh-Und Werkst. 56:245–6.
42. Xue BL, Wen JL, Sun RC. Producing lignin-based polyols through microwave-assisted liquefaction for rigid polyurethane foam production. Materials (Basel. 8:586–99.
43. Sequeiros A, Serrano L, Briones R, Labidi J. Lignin liquefaction under microwave heating. J Appl Polym Sci. 130:3292–8.
44. Kiliaris P, Papaspyrides CD. Polymer/layered silicate (clay) nanocomposites: An overview of flame retardancy. Prog Polym Sci. 35:902–58.
45. Lorenzetti A. Sintesi di polimeri espansi modificati: valutazione di espandenti alternativi in relazione alle caratteristiche termoisolanti e di comportamento al fuoco. Università degli Studi di Padova;
46. Modesti M. Dispense del corso di “Ingegneria dei Polimeri.” Università di Padova;
47. Sengupta R, Bhattacharya M, Bandyopadhyay S, Bhowmick AK. A review on the mechanical and electrical properties of graphite and modified graphite reinforced polymer composites. Prog Polym Sci. 36:638–70.
48. Santarpia L. Dispense del corso di “Sistemi e Impianti Antincendio.” Università di Roma “La Sapienza”;
49. Hrelja D. Studio ed ottimizzazione di sistemi polimerici nanocompositi con migliorata reazione al fuoco. DPCI, Università degli Studi di Padova;
50. PETER D. Sulfonation of lignins [Internet]. US: WESTVACO CORP; 1991. Available from: <https://lens.org/015-164-393-066-129>
51. Beauchet R, Monteil-Rivera F, Lavoie JM. Conversion of lignin to aromatic-based chemicals (L-chems) and biofuels (L-fuels). Bioresour Technol. 2012 Oct 1;121:328–34.
52. Guo H, Bian K, Cai H, Zhang H, Li H, Chen X, et al. Investigation on the Liquefaction Performances, Mechanism and Kinetics of Wheat Straw in Different Solvents. Waste Biomass Valorization. 2024 Mar 18;15(3):1519–31.
53. da Silva SHF, dos Santos PSB, Thomas da Silva D, Briones R, Gatto DA, Labidi J. Kraft Lignin-Based Polyols by Microwave: Optimizing Reaction Conditions. Journal of Wood Chemistry and Technology. 2017 Sep 3;37(5):343–58.

54. Schuerch C. Solvent Properties of Liquids : Relation to Fractionation of Lignin 5061 The Solvent Properties of Liquids and Their Relation to the Solubility, Swelling, Isolation and Fractionation of Lignin [Internet]. 1952. Available from: <https://pubs.acs.org/sharingguidelines>
55. Tang Q, Sun Y, Du L, Zhou M, Yang D. Preparation and performance of 10 wt% of chlorantraniliprole Nano-suspension concentrate (SC) using polyether amine-bridged sulfonated alkali lignin (PSAL) as a dispersant. *Ind Crops Prod.* 2024 Aug;214:118539.
56. Kane S, Hodge DB, Saulnier B, Bécsy-Jakab VE, Dülger DN, Ryan C. Role of sodium sulfate in electrical conductivity and structure of lignin-derived carbons. *J Anal Appl Pyrolysis.* 2024 Aug;181:106600.
57. Huang J, Fu S, Gan L, editors. *Lignin Chemistry and Applications.* Elsevier; 2019.